ISSN 1814-9758

UKRAINICA BIOORGANICA ACTA

2020, Vol. 15, N 1

Scientific journal • Established in 2004

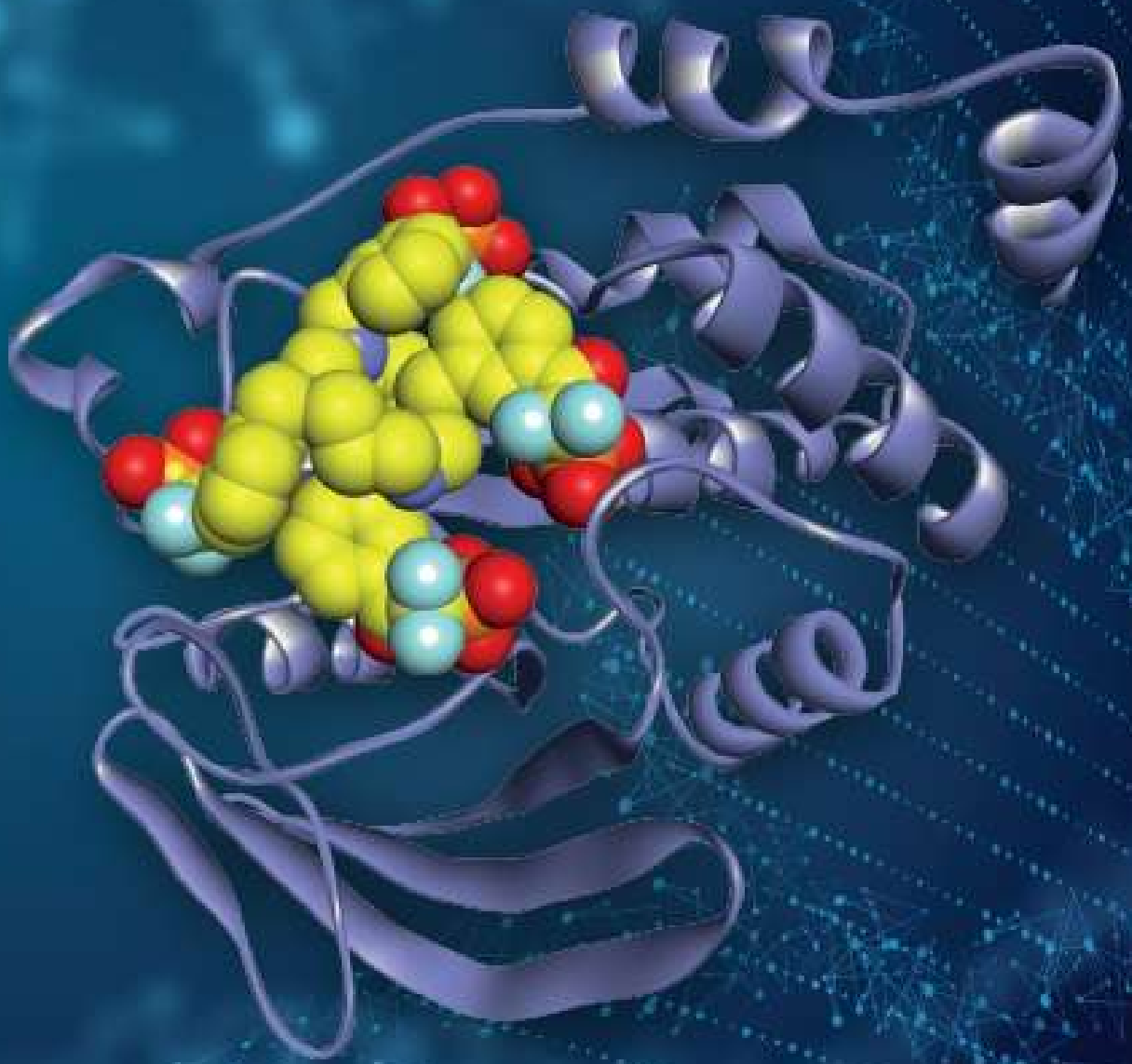

National Academy of Sciences of Ukraine

V.P. KUKHAR INSTITUTE OF BIOORGANIC CHEMISTRY AND PETROCHEMISTRY
INSTITUTE OF MOLECULAR BIOLOGY AND GENETICS

UBA

UKRAINICA BIOORGANICA ACTA

Vol. 15, N 1, 2020

Scientific journal | *Established in 2004* | *Issued twice a year*

Founders/Publishers: Institute of Molecular Biology and Genetics of the NAS of Ukraine
V.P. Kukhar Institute of Bioorganic Chemistry and Petrochemistry of the NAS of Ukraine

Editorial address: V.P. Kukhar Institute of Bioorganic Chemistry and Petrochemistry of the NAS of Ukraine,
1 Murmanska St.,
Kyiv, Ukraine, 02094

Tel.: +38044-5585388;
E-mail: uba@bioorganica.org.ua
www.bioorganica.org.ua

The state registration certificate for print media: series KV No 24164-14004 PR, 01.10.2019

Editors: N.V. Lyutenko, L.V. Pletnova

Page layout: V.V. Shvadchak, E.V. Vilchynska

Signed for printing 30.06.2020. Format 210 x 297. Coated paper 115 g/m².
Fonts: Times New Roman. Publishing sheets: 7. Edition 100 copies. Order 420/20.
Original layout design: E.V. Vilchynska, Enamine Ltd.
Print: LLC "SPE "Interservice", Kyiv, Boryspilska St. 9, tel.: +38044 3628307. Lic. DK 3534, 24.07.2009

NATIONAL ACADEMY OF SCIENCES OF UKRAINE
V.P. KUKHAR INSTITUTE OF BIOORGANIC CHEMISTRY AND PETROCHEMISTRY
INSTITUTE OF MOLECULAR BIOLOGY AND GENETICS

UKRAINICA BIOORGANICA ACTA

Volume 15, N 1, June, 2020 **Kyiv**

hpps://doi.org/10.15407/bioorganica2020.01

C O N T E N T S

З М І С Т

ISSN 1814-9758. Ukr. Bioorg. Acta, 2020, Vol. 15, N 1
UDC 547.789+615.277.3
DOI: hpps://doi.org/10.15407/bioorganica2020.01.002

Ukrainica Bioorganica Acta
www.bioorganica.org.ua

UBA

RESEARCH ARTICLE

Anticancer evaluation of di- and trifunctional substituted 1,3-thiazoles

Kostyantyn V. Turov, Oleg P. Mitiukhin, Svitlana A. Chumachenko, Vladimir S. Zyabrev, Volodymyr S. Brovarets*

V. P. Kukhar Institute of Bioorganic Chemistry and Petrochemistry of the NAS of Ukraine, 1 Murmanska St., Kyiv, 02094, Ukraine

Abstract: Anticancer activity of a series of polyfunctional substituted 1,3-thiazoles has been studied within the international scientific program "NCI-60 Human Tumor Cell Lines Screen". Screening was performed *in vitro* on 60 cell lines of lungs, kidneys, CNS, ovaries, prostate, and breast cancer, epithelial cancer, leukemia, and melanoma. The most effective compounds were those with a piperazine substituent at C^2 of the 1,3-thiazole cycle: 1-(4-((4-methylphenyl)sulfonyl)-2-phenyl-1,3-thiazol-5-yl)piperazine (average lg GI_{50} = -5.87, lg TGI = -5.54, lg LC_{50} = -5.21), 1-(2-(3,5-dimethyl-1*H*-pyrazol-1-yl)-4-((4-methylphenyl)sulfonyl)-1,3-thiazol-5-yl)piperazine (average lg GI_{50} = -5.66, lg TGI = -5.26, lg LC_{50} = -4.83), and 1-(2,4-bis((4-methylphenyl)sulfonyl)-1,3-thiazol-5-yl)piperazine (average lg GI_{50} = -5.67, lg TGI = -5.21, lg LC_{50} = -4.67).

Keywords: 1,3-thiazole; anticancer activity; growth inhibitor; cytostatic activity; cytotoxic activity.

Introduction

Derivatives of 1,3-thiazoles play an important role in basic and applied research. It has been demonstrated that 1,3-thiazoles are widely used for creation of dyes, insecticides, herbicides, and pharmaceuticals. Di- and tri-substituted 1,3-thiazole are effective anti-inflammatory, anthelmintic, antiviral, and bactericidal agents [1-6]. The nature of the chemical groups in the heterocycle can significantly affect their pharmacological properties. Despite of wide range of thiazole libraries, many of trisubstituted thiazoles stays unavailable due to multistep and complicated pathways for its synthesis.

The purpose of this work was to synthesize and evaluate the antitumor activity of di- and tri- substituted 1,3-thiazole. S_NAr reactions were convenient for direct introduction of substituents into proper positions of heterocycle. Well known that substitution of halogen atom in C^4 or C^5 position demands high temperatures and Pd catalysis. Present of EWG makes liable of halogen atom in position 5 of thiazole ring. That allows to modify one by introducing different O, N and substituents. Such reactions pass in mild conditions and with high level of regioselectivity, that's why yields of desired products was pretty fine.

Received: 20.03.2020
Revised: 03.04.2020
Accepted: 10.04.2020
Published online: 30.06.2020

* Corresponding author. Tel.: +380-44-573-2596;
e-mail: brovarets@bpci.kiev.ua (V. S. Brovarets)
ORCID: 0000-0001-6668-3412

Results and Discussion

Chemistry

Syntheses of compounds **1-23** are presented in Schemes 1 and 2. 1-*R*-3-Tosyl-1,4,4-trichloro-2-aza-1,3-butadienes **I** and 1-tosyl-2,2-dichloroethenylisothiocyanate **II** were used as starting compounds. Imidoyl chlorides **I** react with thiourea to give 2-*R*-4-tosyl-5-chloro-1,3-thiazoles **1, 10**. 5-Chloro-1,3-thiazole **1** reacts with *N*-, *O*- and *S*-nucleophiles to eliminate the chlorine anion and form the corresponding 1,3-thiazole derivatives **2-7**. Heating of compound **3** with hydrogen peroxide in acetic acid followed by the reaction of the obtained product with morpholine or benzylamine yields 4-aminosubstituted 5-((4-chlorophenyl) sulfanyl)-2-phenyl-1,3-thiazoles **8, 9**.

1-Tosyl-2,2-dichloroethenylisothiocyanate **II** was used for the synthesis of trifunctionally substituted 1,3-thiazoles **11-23**. Compound **II** was treated with thiophenols or alkyl mercaptans in the presence of pyridine. A cyclization took place to form intermediate 2-aryl(alkyl)sulfanyl-4-tosyl-5-

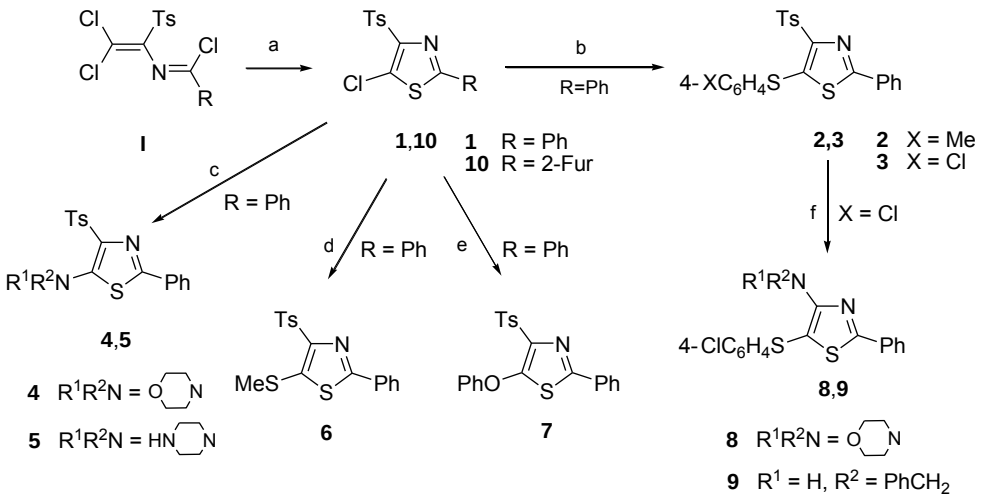

Scheme 1. Synthesis of 4,5-difunctional substituted 1,3-thiazoles **1-10**. Reagents and conditions: (a) $(H_2N)_2C=S$ (excess), MeCN, reflux, 2 h; (b) 4-MeC_6H_4SH or 4-ClC_6H_4SH, Et_3N, MeCN, reflux, 2 h; (c) morpholine or piperazine (excess), dioxane, 100 °C, 24 h; (d) NaSH (excess), THF, 60 °C, 3 h; MeI, MeONa, MeOH, 20 °C, 5 h; (e) PhONa, THF, 20 °C, 24 h; (f) H_2O_2 (excess), CF_3CO_2H, reflux, 3 h; morpholine or $PhCH_2NH_2$ (excess), dioxane, 100 °C, 24 h.

chloro-1,3-thiazoles, which were oxidized with hydrogen peroxide to 1,3-thiazoles **III** containing at position C^2 an arylsulfonyl or an alkylsulfonyl and at position C^4 the tosyl group. Substitution of the chlorine atom at position C^5 of compounds **III** with 4-chlorothiophenol followed by the oxidation of the sulfanyl group under the action of hydrogen peroxide in trifluoroacetic acid yields 1,3-thiazole derivatives **IV** with three different sulfonyl groups. 1,3-Thiazoles **11-16** were obtained under the treatment of compounds **IV** by *N*- and *O*-nucleophiles. The reaction of 1,3-thiazoles **IV** with dimethylamine, benzylamine, or ammonia in a molar ratio of 1:2 at 20 °C yields 2-amino-1,3-thiazole derivatives **11-13** as a result of replacing a sulfonyl group at position C^2. Treatment of thiazoles **IV** with the excess of an amine or sodium 4-chlorophenolate, leads to the substitution of the two arylsulfonyl groups yielding compounds **14-16**. 1,3-Thiazole **17** was obtained from reagent **II**, hydrazine hydrate, and acetylacetone. It gives when heated with morpholine or piperazine, the corresponding 5-amino-2-pyrazolyl-4-tosyl-1,3-thiazoles **18, 19** and, when treated with sodium hydrogen sulfide followed by propyl iodide, 1,3- thiazole **20**.

5-Piperazino-substituted 1,3-thiazoles **21, 22** were prepared by the nucleophilic substitution of the chlorine atom in compounds **III** for piperazine in boiling ethanol. 1,3-Thiazole **23** was obtained from isothiocyanate **II**, methyl mercaptan, piperazine, and hydrochloric acid.

Structures of synthesized compounds shown in Table 1 were confirmed by ^1H NMR spectra and elemental analysis.

Biological Evaluation

Anticancer activity of the synthesized compounds was studied within an international scientific program of the US National Institutes of Health. The screening was performed *in vitro* on 60 cell lines of lungs, kidneys, CNS, ovaries, prostate, and breast cancer, epithelial cancer, leukemia, and melanoma at a substance concentration of 10^{-5} M. Growth percentage (GP) of cancer cells compared to the control (in the absence of a chemical substance, 100%) was determined [7-10]. Synthesized 1,3-thiazole derivatives have been shown to be active against several types of cancer cells (Table 1).

For example, 2-phenyl-4-tosyl-5-chloro-1,3-thiazole (**1**) considerably inhibits growth of cells of leukemia (K-562, GP = 30.07% and SR, GP = 13.60%), lung cancer (NCI-H522, GP = 44.91%), melanoma (M14, GP = 37.06% and MDA-MB-435, GP = 1.37%), and breast cancer (MDA-MB-468, GP = 0.73%).

The replacement of the chlorine atom in compound **1** with p-tolylsulfanyl group (compound **2**) results in a significant 70% reduction of the inhibitory activity towards leukemia and lung cancer cells and in the full extinction of the activity towards melanoma cells MDA-MB-435 (GP = 106.38%) and M14 (GP = 102.19%).

The substitution of the chlorine atom by methylsulfanyl group (compound **6**) results in a uniform decrease of the inhibitory activity towards leukemia and lung cancer cells and does not change melanoma and breast cancer cells inhibition. The substitution of the chlorine atom in compound **1** with morpholine (compound **4**) as well as phenoxy group (compound **7**) also does not change leukemia and melanoma cells growth inhibition. In summary, any replacement of the chlorine atom results in a decrease of inhibitory activity in relation to parent compound **1**.

1,3-Thiazoles **8, 9** containing the 4-chlorophenylsulfonyl group at position C^5 and a substituted amino group at position C^4 are somewhat more active than compound **4** with the morpholino group at position C^5. Thus, 1,3-thiazole

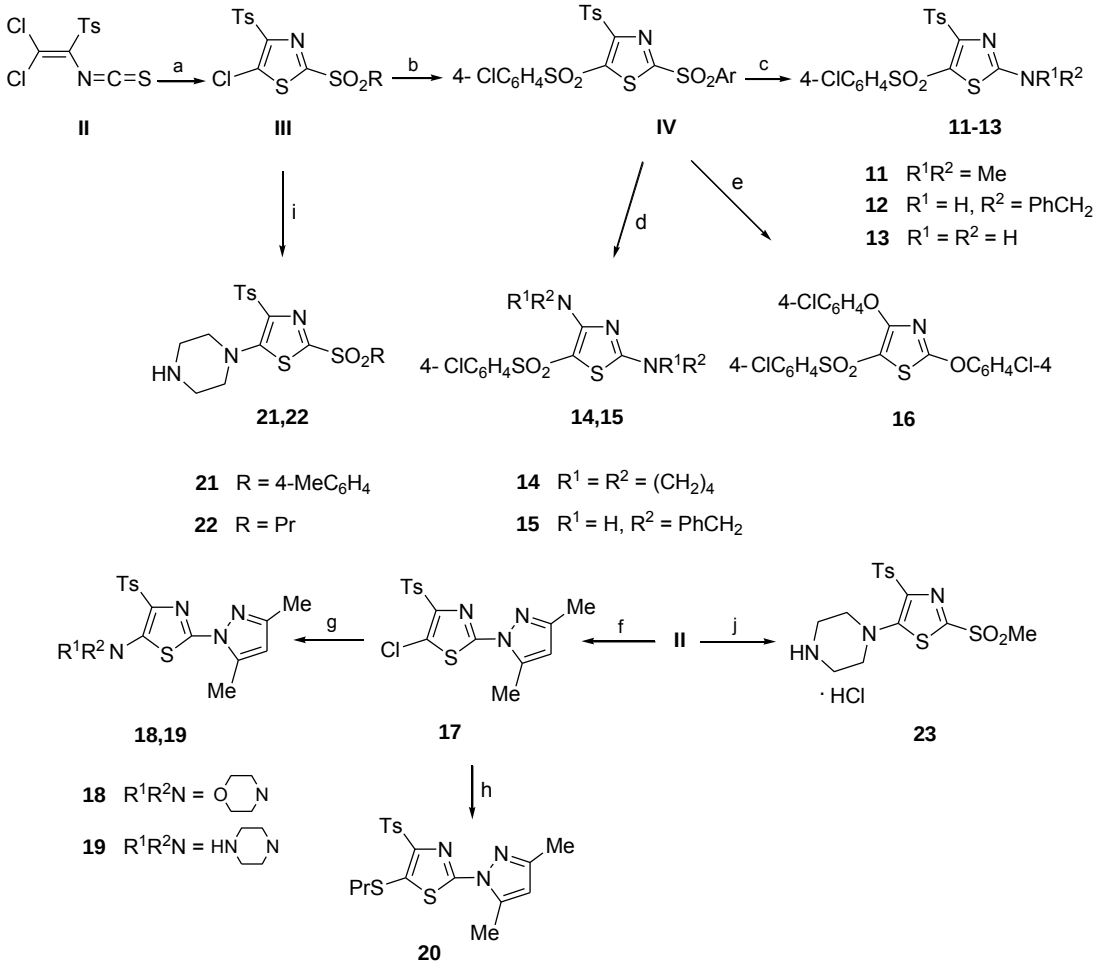

Scheme 2. Synthesis of 2,4,5-trifunctional substituted 1,3-thiazoles **11**-**23**. Reagents and conditions: (a) ArSH or PrSH, Py, benzene, 15 °C, 8 h; H_2O_2 (excess), AcOH, reflux, 4 h; (b) 4-ClC_6H_4SH, Et_3N, THF, 5 °C, 30 h; H_2O_2 (excess), CF_3CO_2H, reflux 4 h; (c) Me_2NH or $PhCH_2NH_2$, or NH_3, THF, 20 °C, 24 h; (d) piperidine or $PhCH_2NH_2$ (excess), THF, 60 °C, 48 h; (e) 4-ClC_6H_4ONa (excess), THF, 20 °C, 24 h; (f) NH_2NH_2 H_2O (excess), THF, 20 °C, 5 h; Ac_2CH_2 (excess), AcOH, reflux, 10 h; (g) morpholine or piperazine (excess), BuOH, reflux, 20 h; (h) NaSH (excess), MeOH, 20-25 °C, 20 h; PrI, MeONa, MeOH, reflux, 3 h; (i) piperazine (excess), EtOH, reflux, 1 h; (j) MeSH, Py, benzene, 20-25 °C, 5 h; H_2O_2 (excess), AcOH, reflux, 4 h; piperazine (excess), EtOH, reflux, 2 h; HCl (excess), 4 °C, 24 h.

8 was active against leukemia HL-60(TB) (GI = 49.92% and K-562 (GP = 72.30%) as well as breast cancer MDA-MB-468 (GP = 72.05%) cells. Compound **9** showed appreciable inhibitory activity only against lung cancer cells NCI-H522 (GI = 59.56%).

1,3-Thiazole **17** which bears a pyrazole ring instead of the benzene one at C^2 showed lower inhibitory activity compared with that of the parent compound **1**. It showed only minor activity towards breast cancer cells BT-549 (GP = 84.33%). On the other hand, the substitution of the chlorine atom in compound **17** with the propylsulfanyl group results in compound **20**, which inhibitory activity towards lung cancer cells HOP-92 is significantly higher (GP = 20.91%). The activity of compound **20** against the other cancer types remains at the level of compound **17**. The replacement of the chlorine atom in compound **17** with the morpholine cycle does not increase the inhibitory activity. Compound **18** proved to be practically inactive towards all types of cancer cells.

Entering a furan cycle in position C^2 of the 1,3-thiazole leads to a significant increase in the anticancer activity. Thus, synthesized 5-chloro-2-(furan-2-yl)-4-tosyl-1,3-thiazole (**10**) was active against leukemia (K-562, GP = 18.83% and SR, GP = 8.28%), lung cancer (NCI-H522, GP = 18.49%), melanoma (M14, GP = 32.33% and MDA-BM-435, GP = 4.90%), and breast cancer (MDA-MB-468, GP = -22.87%).

The most active were 1,3-thiazoles containing a piperazine ring in position C^5. Thus, compound **19** was active against epithelial cancer cells HCC-2998 (GP = -88.55%) and HT29 (GP = -33.93%), almost all melanoma lines (MALME-3M, GP = -55.98%; M14, GP = -89.83%; MDA-MB-435, GP = -2,08%; SK-MEL-28, GP = -83.71%; SK-MEL-5, GP = 80.68%; UACC-257, GP = -79.19%; UACC-62, GP = 72.05%), and breast cancer as well (T-47D, GP = -29.33%; MDA-MB-468, GP = -55.79%).

1,3-Thiazole **21** with two tosyl groups and C^5 linked piperazine also showed high anticancer activity (average GP = -5.77%). The most effect was observed on leukemia HL-60 (TB) (GP = -45.35%), lung cancer NCI-H522 (GP = -44.16%) and NCI-H460 (GP = -38.88%), colon cancer COLO 205 (GP = -32.92%), CNS cancer SF-539

(GP = -15.93%), melanoma LOX IMVI (GP = -41.57%), M14 (GP = -49.08%) and MDA-MB-435 (GP = -43.55%), prostate cancer DU-145 (GP = -35.29%), breast cancer HS 578T (GP = -21.17%) and MDA-MB-468 (GP = -21.44%) cells.

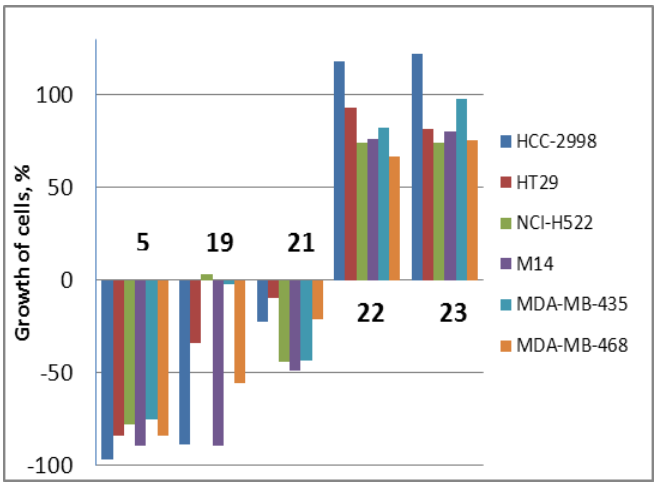

Figure 1. Antitumor activity of 5-(piperazin-1-yl)-4-tosyl-1,3-thiazoles **5, 19, 21-23**.

2-Phenyl-5-(piperazin-1-yl)-4-tosyl-1,3-thiazole (**5**) has been a prominent anticancer agent. It significantly decreased the growth of ovarian cancer cells (IGROV-1, GP = 31.39% and OVCAR, GP = 49.75%), and destroyed, with the average GP of -70%, almost all cell lines of leukemia, melanoma, and colon, CNS, kidney, and breast cancer. The most significant are the data reflecting the almost complete destruction of the following cell lines: colon cancer HCC2998 (GP = -96.68%), CNS U251 (GP = -91.74%), melanoma SK-MEL-28 (GP = -97.03%) and SK-MEL-5 (GP = -98.77%), kidney cancer TK-10 (GP = -88.46%), breast cancer MCF7 (GP = -84.29%) and MDA-MB-468 (GP = -84.34%).

Advanced *in vitro* study of compounds **5, 19, 21** at five concentrations of the 10-fold dilution (10^{-4}-10^{-8} M) was also performed towards 60 human cancer cell lines, the set of which was identical to that for the pre-screening stage (Table 2). High antitumor potential of compound **21** has been confirmed by a significant level of inhibition (average lg GI_{50} = -5.67), as well as cytostatic (average lg TGI = -5.21) and cytotoxic (average lg LC_{50} = -4.67) effects. The highest data were found for compound **5**: average lg GI_{50} = -5.87, lg TGI = -5.54, and lg LC_{50} = -5.21.

It is of interest that among the 5-piperazino-substituted 1,3-thiazoles **5, 19, 21-23** compounds **22, 23** containing a C^2 linked alkylsulfonyl group exhibit the lowest level of antitumor activity. This is readily illustrated by Figure 1 with some selected cell lines. The average activity value of compounds **22** and **23** was 95.48% and 98.61%, respectively (Table 1).

Conclusions

The study of the antitumor activity of di- and trifunctionally substituted 1,3-thiazoles towards the NCI 60 human cancer cell lines revealed "leader compounds" – 5-(piperazin-1-yl)-4-tosyl-1,3-thiazoles. Therein, the nature of the substituent at C^2 of the 1,3-thiazole cycle critically affects the level of activity. Most preferred is the presence of phenyl, tosyl or 3,5-dimethyl-1*H*-pyrazol-1-yl substituent in this position.

Table 1. Mitotic activity of the 1,3-thiazole derivatives towards NCI 60 cell lines at the 10^{-5} M concentration.

Compd	Structure	Average GP	The most sensitive cell lines (GP)
1	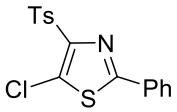	85.92	*leukemia* K-562 (30.07), SR (13.60); *lung cancer* NCI-H522 (44.91); *melanoma* M-14 (37.06), MDA-MB-435 (1.37); *breast cancer* MDA-MB-468 (0.73)
2	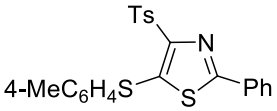	97.48	*leukemia* K-562 (90.20), SR (88.33); *lung cancer* NCI-H522 (83.67); *melanoma* M-14 (109.28), MDA-MB-435 (119.03); *kidney cancer* CAKI-1 (71.89)
4	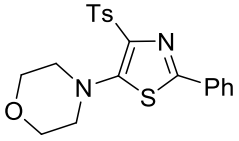	100.29	*leukemia* K-562 (103.76), SR (88.33); *lung cancer* NCI-H522 (75.91); *melanoma* MDA-MB-435 (106.38); *breast cancer* T-47D (70.39)
5	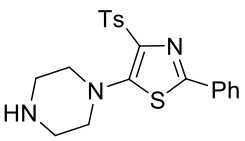	-52.89	*colon cancer* HCC-2998 (-96.68); *melanoma* SK-MEL-5 (-98.77); *CNS cancer* U251 (-91.74); *breast cancer* MDA-MB-468 (-84.34)

Table 1. (*Contd.*)

Compd	Structure	Average GP	The most sensitive cell lines (GP)
6	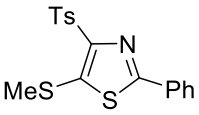	89.71	*leukemia* K-562 (58.49), SR (49.84); *lung cancer* NCI-H522 (74.11); *melanoma* M-14 (94.70), MDA-MB-435 (36.78); *breast cancer* MDA-MB-468 (65.56)
7	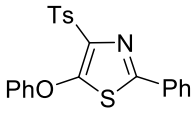	90.45	*leukemia* SR (95.44); *lung cancer* NCI-H522 (85.13); *melanoma* M-14 (101.29), MDA-MB-435 (107.97); *breast cancer* T-47D (54.11)
8	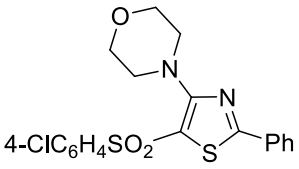	94.46	*leukemia* HL-60(TB) (49.92), SR (92.70); *lung cancer* NCI-H522 (83.12); *melanoma* M-14 (101.29), MDA-MB-435 (107.63); *breast cancer* MDA-MB-468 (72.05)
9	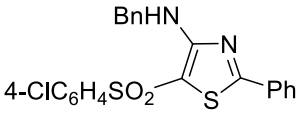	92.98	*leukemia* K-562 (88.04), SR (77.65); *lung cancer* NCI-H522 (59.56); *melanoma* M-14 (100.66), MDA-MB-435 (107.82); *breast cancer* MDA-MB-468 (96.90)
10	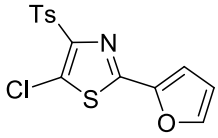	71.98	*leukemia* K-562 (18.83), SR (8.28); *lung cancer* NCI-H522 (18.49); *melanoma* M-14 (32.33), MDA-MB-435 (4.90); *breast cancer* MDA-MB-468 (-22.87)
11	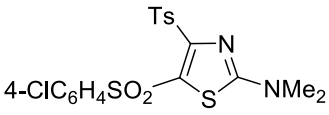	84.17	*leukemia* HL-60(TB) (52.69); *lung cancer* A549/ATCC (56.18); *melanoma* UACC62 (59.80); *breast cancer* MDA-MB-468 (66.25)
12	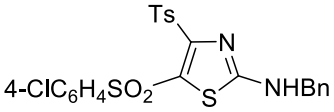	107.47	*CNS cancer* SNB-75 (64.32); *melanoma* UACC-62 (79.75)
13	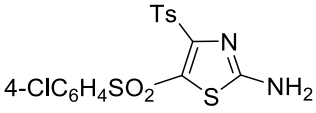	91.75	*leukemia* CCRF-CEM (72.45), HL-60(TB) (72.65), K-562 (73.24), MOLT (64.64); *lung cancer* HOP-92 (47.03)
14	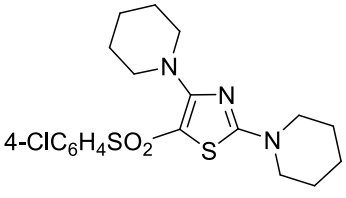	100.46	*leukemia* K-562 (114.19), SR (100.78); *lung cancer* NCI-H522 (91.60); *melanoma* M-14 (106.27); *breast cancer* MDA-MB-468 (94.07); *CNS cancer* SNB-75 (73.04)
15	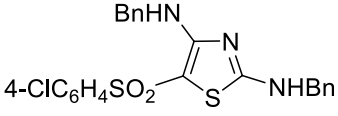	84.40	*leukemia* HL-60(TB) (81.31), K-562 (85.08); *lung cancer* A549/ATCC (44.72), NCI-H522 (49.57); *melanoma* M-14 (77.99), MDA-MB-435 (114.47); *breast cancer* MDA-MB-231/ATCC (42.35)

Table 1. (*Contd.*)

Compd	Structure	Average GP	The most sensitive cell lines (GP)
16	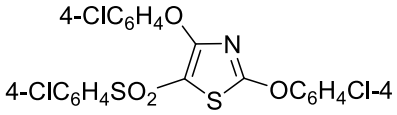	98.55	*leukemia* HL-60(TB) (71.46), K-562 (96.63), SR (43.24); *lung cancer* NCI-H522 (88.25); *melanoma* M-14 (99.61), MDA-MB-435 (96.32); *breast cancer* MCF7 (76.99)
17	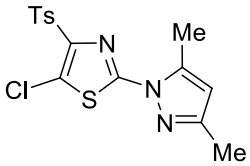	102.42	*leukemia* K-562 (92.44); *lung cancer* NCI-H522 (89.59); *melanoma* M-14 (111.85), MDA-MB-435 (107.95); *breast cancer* BT-549 (84.33)
18	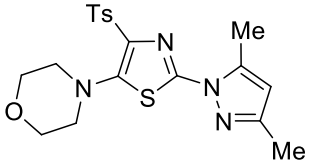	89.56	*leukemia* MOLT-4 (81.01), K-562 (81.84); *lung cancer* HOP-92 (20.91), NCI-H522 (78.32); *CNS cancer* SNB-19 (77.87); *breast cancer* MDA-MB-231/ATCC (68.26)
19	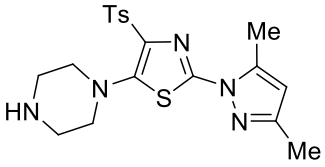	23.20	*leukemia* SR (-8.89); *colon cancer* HCC-2998 (-88.55); *melanoma* SK-MEL-28 (-83.71); *breast cancer* MDA-MB-468 (-55.79)
20	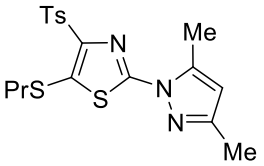	89.56	*leukemia* MOLT-4 (81.01), K-562 (92.44); *lung cancer* HOP-92 (20.91), NCI-H322M (88.60); *CNS cancer* SNB-19 (98.94); *breast cancer* MDA-MB-468 (117.20)
21	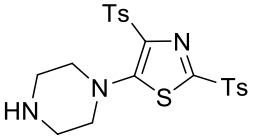	-5.77	*leukemia* HL-60(TB) (-45.35); *lung cancer* NCI-H522 (-44.16); *melanoma* M-14 (-49.08); *ovarian cancer* OVCAR-3 (-40.27); *prostate cancer* DV-145 (-35.29)
22	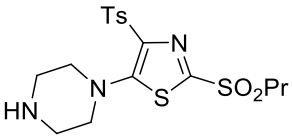	95.48	*leukemia* SR (64.37); *colon cancer* SW-620 (134.85); *melanoma* M-14 (76.23); *ovarian cancer* OVCAR-3 (136.53); *breast cancer* MDA-MB-468 (66.81)
23	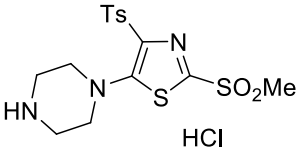	98.61	*colon cancer* HCC-2998 (-88.55); *CNS cancer* SNB-19 (98.94); *renal cancer* RXF-393 (115.77); *breast cancer* MCF-7 (82.11), MDA-MB-468 (75.35)

Table 2. Parameter values (lg) of the anticancer activity of compounds **5, 19, 21** against the NCI 60 human cancer cell lines (five-dose assay).

Cell Line	Compd								
	5			**19**			**21**		
	GI_{50}	TGI	LC_{50}	GI_{50}	TGI	LC_{50}	GI_{50}	TGI	LC_{50}
					Leukemia				
CCRF-CEM	-5.73	-5.28	-4.23	-5.57	-4.96	-4.21	-5.63	-5.05	-4.35
HL-60(TB)	-5.72	-5.43	-5.14	-5.62	-5.35	-5.07	-5.64	-5.32	-5.00
K-562	-6.26	-5.62	-5.11	-5.81	-5.39	-4.91	NT	NT	NT
MOLT-4	-5.74	-5.39	-5.03	-5.65	-5.31	-4.88	-5.52	-5.23	-4.53
RPMI-8226	NT	NT	NT	NT	NT	NT	-5.94	-5.01	-4.19
SR	-5.87	-5.47	-5.08	-5.64	-5.24	-4.49	-5.63	-5.31	-4.38
					Non-small cell lung cancer				
A549/ATCC	-5.74	-5.47	-5.20	-5.44	-4.89	-4.38	-5.64	-5.10	-4.48
EKVX	-5.87	-5.52	-5.16	-5.63	-4.90	-4.39	-5.49	-4.91	-4.40
HOP-62	-5.77	-5.51	-5.26	-5.71	-5.39	-5.07	-5.92	-5.39	-4.70
HOP-92	-6.46	-5.79	-5.37	-6.21	-5.50	-4.83	-5.45	-5.12	-4.57
NCI-H226	-5.79	-5.51	-5.23	-5.57	-5.00	-4.38	-5.67	-5.37	-5.06
NCI-H23	-5.84	-5.53	-5.23	-5.29	-4.71	-4.34	-5.63	-5.17	-4.55
NCI-H322M	NT	NT	NT	NT	NT	NT	NT	NT	NT
NCI-H460	-5.79	-5.52	-5.24	-5.74	-5.45	-5.16	-5.64	-5.20	-4.55
NCI-H522	-5.74	-5.46	-5.18	-5.67	-5.39	-5.10	NT	NT	NT
					Colon cancer				
COLO 205	-6.68	-6.33	-5.95	-5.78	-5.52	-5.25	-5.78	-5.45	-5.12
HCC-2998	-6.28	5.76	-5.34	-5.81	-5.52	-5.22	-5.59	5.22	-4.66
HCT-116	-5.93	-5.61	-5.29	-5.79	-5.49	-5.18	-5.75	-5.39	-5.04
HCT-15	-5.84	-5.54	-5.24	-5.67	-5.31	-4.86	-5.70	-5.07	-4.47
HT29	-6.12	-5.65	-5.24	-5.82	-5.40	-4.95	-5.56	-4.98	-4.30
KM12	-5.79	-5.51	-5.24	-5.74	-5.48	-5.22	-5.61	-5.18	-4.50
SW-620	-5.82	-5.54	-5.26	-5.77	-5.48	-5.19	-5.79	-5.44	-5.09
					CNS cancer				
SF-268	-5.80	-5.50	-5.20	-5.48	-4.92	-4.43	-5.58	-5.09	-4.46
SF-295	-5.77	-5.49	-5.21	-5.73	-5.43	-5.14	-5.60	-5.19	-4.59
SF-539	-5.81	-5.53	-5.24	-5.77	-5.46	-5.14	-5.56	-5.25	-4.83
SNB-19	-5.75	-5.36	-4.88	-5.16	-4.68	-4.30	-5.51	-4.95	-4.45
SNB-75	-5.97	-5.62	-5.27	-5.85	-5.39	-4.87	-5.59	-5.09	-4.54
U251	NT	NT	NT	NT	NT	NT	-5.55	-5.01	-4.45
					Melanoma				
LOX IMVI	-5.88	-5.57	-5.26	-5.75	-5.45	-5.15	-5.82	-5.39	-4.86
MALME-3M	-5.77	-5.50	-5.22	-5.33	-4.79	-4.36	-5.61	-5.34	-5.06
M14	-5.76	-5.47	-5.19	-5.67	-5.41	-5.16	-5.80	-5.48	-5.15
MDA-MB-435	-5.87	-5.55	-5.24	-5.75	-5.45	-5.16	-6.23	-5.65	-5.17
SK-MEL-2	-5.69	-5.42	-5.15	-5.65	-5.40	-5.15	NT	NT	NT
SK-MEL-28	-5.81	-5.54	-5.27	-5.76	-5.50	-5.24	-5.74	-5.44	-5.14
SK-MEL-5	-5.82	-5.55	-5.27	-5.78	-5.52	-5.26	-5.84	-5.55	-5.27
UACC-257	-5.80	-5.50	-5.19	-5.77	-5.48	-5.20	-5.79	-5.48	-5.17
UACC-62	-5.80	-5.53	-5.26	-5.77	-5.49	-5.22	-5.79	-5.28	-4.68
					Ovarian cancer				
IGROV1	-5.75	-5.44	-5.14	-5.74	-5.45	-5.17	-5.60	-5.13	-4.37
OVCAR-3	-5.77	-5.50	-5.23	-5.59	-5.15	-4.59	-5.61	-5.28	-4.83
OVCAR-4	-5.76	-5.46	-5.16	-5.38	-4.81	-4.40	-5.56	-4.92	-4.39
OVCAR-5	-5.80	-5.51	-5.22	-5.50	-4.95	-4.46	-5.44	-5.05	-4.51
OVCAR-8	-5.75	-5.46	-5.17	-5.64	-5.22	-4.47	-5.65	-4.99	-4.35
NCI/ADR-RES	-5.81	-5.49	-5.17	-5.50	-4.84	-4.32	-5.55	-4.92	-4.34
SK-OV-3	-5.76	-5.49	-5.23	-5.53	-5.11	-4.57	-5.50	-4.97	-4.43

Table 2. (*Contd.*)

Cell Line	Compd								
	5			**19**			**21**		
	GI_{50}	TGI	LC_{50}	GI_{50}	TGI	LC_{50}	GI_{50}	TGI	LC_{50}
				Renal cancer					
786-0	-5.79	-5.48	-5.17	-5.66	-5.29	-4.77	-5.65	-5.37	-5.08
A498	-5.00	-5.66	-5.33	-5.91	-5.50	-5.08	-5.74	-5.34	-4.84
ACHN	-5.78	-5.50	-5.21	-5.46	-4.92	-4.45	-5.41	-4.91	-4.44
CAKI-1	-5.82	-5.50	-5.18	-5.68	-5.23	-4.65	-5.66	-5.34	-5.03
RXF 393	-5.90	-5.59	-5.29	-5.77	-5.45	-5.12	-5.80	-5.52	-5.24
SN12C	-5.80	-5.51	-5.23	-5.63	-5.15	-4.54	-5.57	-4.99	-4.47
TK-10	-5.76	-5.48	-5.20	-5.58	-5.19	-4.66	-5.42	-4.99	-4.46
UO-31	-5.94	-5.61	-5.29	-5.88	-5.54	-5.20	-5.49	-5.00	-4.45
				Prostate cancer					
PC-3	-5.81	-5.48	-5.15	-5.52	-4.99	-4.46	-5.51	-4.88	-4.41
DU-145	-5.79	-5.52	-5.25	-5.43	-4.88	-4.44	-5.66	-5.28	-4.76
				Breast cancer					
MCF7	-5.84	-5.55	-5.26	-5.76	-5.43	-5.10	-5.78	-5.21	-4.44
MDA-MB-231/ATCC	-5.83	-5.54	-5.25	-5.74	-5.44	-5.13	-5.54	-5.16	-4.62
HS 578T	-5.81	-5.45	-5.09	-5.68	-5.24	-4.25	-5.61	-5.14	-4.00
BT-549	-5.78	5.51	5.23	-5.47	-4.91	-4.43	-5.52	5.11	4.57
T-47D	-5.80	-5.50	-5.19	-5.76	-5.46	-5.16	-6.29	-5.18	-4.43
MDA-MB-468	-6.56	-6.01	-5.44	-5.92	-5.61	-5.30	-6.43	-5.77	-5.23

Experimental section

Chemistry

^{1}H NMR spectra were obtained on a Bruker Avance DRX 500 spectrometer. The melting points were estimated on a Fisher-Johns apparatus. The reaction progress was monitored by the TLC method on silica gel $60F_{254}$ Merck plates. All reagents and solvents were purchased from Aldrich and used without additional purification.

*5-Substituted 4-[(4-methylphenyl)sulfonyl]-2-phenyl-1,3-*thiazoles **1-4, 6-9** [11], *5-Chloro-2-(furan-2-yl)-4-((4-methylphenyl)sulfonyl)-1,3-thiazole* (**10**) [12], *2,4-Di-substituted 5-(4-chlorophenyl)sulfonyl-1,3-thiazoles* **11-16** [13], *2-(3,5-Dimethyl-1H-pyrazol-1-yl)-4-((4-methylphenyl)sulfonyl)-1,3-thiazoles* **17, 18** [14] were synthesized following the procedures described in the corresponding sources cited.

*1-(4-((4-Methylphenyl)sulfonyl)-2-phenyl-1,3-thiazol-5-yl)piperazine (**5**)* was synthesized similarly to compound **4**.

Yield 67%, mp 112-113 °C (EtOH). ^{1}H NMR (500 MHz, $CDCl_3$) δ 2.45 (s, 3H, CH_3), 3.20-3.35 (m, 4H, $2CH_2$), 3.82-3.94 (m, 4H, $2CH_2$), 7.33-7.45 (m, 5H, Ar), 7.78 (d, *J* 7.5 Hz, 2H, Ar), 8.05 (d, *J* 7.5 Hz, 2H, Ar). Anal. Calcd. for $C_{20}H_{21}N_3O_2S_2$: C, 60.12; H, 5.30; N, 10.52; S, 16.05. Found: C, 59.98; H, 5.15; N, 10.32; S, 15.98.

*1-(2-(3,5-Dimethyl-1H-pyrazol-1-yl)-4-((4-methylphenyl)sulfonyl)-1,3-thiazol-5-yl)piperazine (**19**)* was synthesized similarly to compound **18**.

Yield 62%, mp 98-99 °C (EtOH). ^{1}H NMR (500 MHz, $CDCl_3$) δ 2.17 (s, 3H, CH_3), 2.40 (s, 3H, CH_3), 2.44 (s, 3H, CH_3), 3.79-3.88 (m, 4H, $2CH_2$), 4.12-4.23 (m, 4H, $2CH_2$), 6.00 (s, 1H, CH), 7.38 (d, *J* 7.9 Hz, 2H, Ar), 7.82 (d, *J* 7.9 Hz, 2H, Ar). Anal. Calcd. for $C_{19}H_{23}N_5O_2S_2$: C, 54.65; H, 5.55; N, 16.77; S, 15.36. Found: C, 54.48; H, 5.49; N, 16.54; S, 15.12.

*2-(3,5-Dimethyl-1H-pyrazol-1-yl)-4-((4-methylphenyl)-sulfonyl)-5-(propylsulfanyl)-1,3-thiazole (**20**).*

To a suspension of 0.00015 mol of compound **17** in 10 ml of methanol, 0.00075 mol of sodium hydrosulfide was added. The mixture was stirred for 20 h at 20 °C, the precipitate was filtered off, and the filtrate was evaporated in vacuo. To the residue, 5 ml of water followed by 1 ml of concd hydrochloric acid was added to precipitate a solid, which was filtered off. To a suspension of this solid in 5 ml of methanol, 0.00015 mol of sodium methylate followed by 0.0002 mol of propyl bromide was added. The mixture was refluxed for 3 h then cooled to 20 °C, the precipitate was filtered off and recrystallized from ethanol. Yield 65%, mp 142-144 °C (EtOH). Anal. Calcd. for $C_{18}H_{21}N_3O_2S_3$: C, 53.04; H, 5.19; N, 10.31; S, 23.60. Found: C, 52.91; H, 5.00; N, 10.18; S, 23.54.

*General procedure for preparation of compounds (**21, 22**).*

To a solution of 0.08 mol of compound **II** [15] in 150 ml of benzene cooled to 0 °C, 0.08 mol of 4-methylbenzenethiol or propanethiol followed by 0.08 mol of pyridine was added. The mixture was stirred for 8 h at 15 °C, the solvent was removed in vacuo, the residue was

washed with water, and dissolved in 200 ml of acetic acid. To this solution, 30 ml of a 30% aqueous hydrogen peroxide solution was added, the reaction mixture was boiled for 4 h then cooled to 10 °C. The precipitate was filtered off and dissolved in 50 ml of ethanol. To this solution, 0.25 mol of piperazine was added, the reaction mixture was boiled for 1 h then evaporated in vacuo. To the residue, 20 ml of water was added to precipitate a solid, which was filtered off and recrystallized from ethanol.

*1-(2,4-Bis((4-methylphenyl)sulfonyl)-1,3-thiazol-5-yl)-piperazine (**21**).*

Yield 72%, mp 132-133 °C (EtOH). ^{1}H NMR (500 MHz, $CDCl_3$) δ 2.43 (s, 3H, CH_3), 2.47 (s, 3H, CH_3), 3.80-3.89 (m, 4H, $2CH_2$), 4.15-4.30 (m, 4H, $2CH_2$), 7.29 (d, *J* 7.6 Hz, 2H, Ar), 7.35 (d, *J* 7.9 Hz, 2H, Ar), 7.38 (d, *J* 7.6 Hz, 2H, Ar), 7.86 (d, *J* 7.9 Hz, 2H, Ar). Anal. Calcd. for $C_{21}H_{23}N_3O_4S_3$: C, 52.70; H, 4.78; N, 8.80; S, 20.14. Found: C, 52.81; H, 4.85; N, 8.63; S, 20.04.

*1-(4-((4-Methylphenyl)sulfonyl)-2-(propylsulfonyl)-1,3-thiazol-5-yl)piperazine (**22**).*

Yield 68%, mp 131-132 °C (EtOH). ^{1}H NMR (500 MHz, $CDCl_3$) δ 0.91 (t, *J* 7.4 Hz, 3H, CH_3), 1.55-1.68 (m, 2H, CH_2), 2.45 (s, 3H, CH_3), 3.02-3.18 (m, 4H, $2CH_2$), 3.19-3.31 (m, 4H, $2CH_2$), 3.33-3.45 (m, 4H, $2CH_2$), 7.34 (d, *J* 7.5 Hz, 2H, Ar), 7.89 (d, *J* 7.5 Hz, 2H, Ar). Anal. Calcd. for $C_{17}H_{23}N_3O_4S_3$: C, 47.53; H, 5.03; N, 9.78; S, 22.39. Found: C, 47.45; H, 4.93; N, 9.65; S, 22.10.

*1-(4-((4-Methylphenyl)sulfonyl)-2-(methylsulfonyl)-1,3-thiazol-5-yl)piperazine (**23**).*

To a solution of 0.0026 mol of isothiocyanate **II** [15] and 00078 mol of pyridine in 10 ml of benzene, methanethiol was passed, obtained by the hydrolysis of 0.012 mol of *S*-methyl-isothiouronium sulfate. The mixture was stirred for 5 h, the precipitate was filtered off, and the filtrate was evaporated in vacuo. To the residue, 4 ml of acetic acid followed by 1.5 ml of 30% aqueous hydrogen peroxide solution was added. The reaction mixture was heated under reflux for 1.5 h then cooled to room temperature and the precipitate was separated. To a suspension of this solid in 5 ml of acetonitrile, 0.005 mol of piperazine was added. The mixture was stirred for 20 h and the precipitate was filtered off. To the filtrate, 0.5 ml of concd hydrochloric acid was added, the mixture was kept at 4 °C for 1 day, and the precipitate was separated. Yield 25%, mp 245-247 °C (dec.). ^{1}H NMR (500 MHz, DMSO-d_6) δ 2.39 (s, 3H, CH_3), 3.28 (s, 4H, $2CH_2$), 3.36 (s, 3H, CH_3), 3.56 (s, 4H, $2CH_2$), 7.46 (d, *J* 8.0 Hz, 2H, Ar), 7.86 (d, *J* 8.1 Hz, 2H, Ar), 9.54 (s, 2H, NH, HCl). Anal. Calcd. for $C_{15}H_{20}ClN_3O_4S_3$: C, 41.13; H, 4.60; Cl, 8.09; N, 9.59; S, 21.96. Found: C, 41.24; H, 4.57; Cl, 8.17; N, 9.65; S, 21.85.

Biological tests

Anticancer *in vitro* screening methodology as well as data interpretation rules is described in details at the NCI Development Therapeutics Program site [16].

Notes

Acknowledgements. We would like to thank National Cancer Institute, Bethesda, MD, US for the anticancer activity investigations and Enamine Ltd. for the material and technical support.

References

1. Forlani, L.; Todesco, P. E. In *Thiazole and Its Derivatives, Part 1,* Metzger, J. V., Ed.; *The Chemistry of Heterocyclic Compounds,* Weissberger, A.; Taylor, E. C., Eds.; Wiley: New York, USA, 1979; Vol. 34, pp 567-571.
2. *Medicines,* Mashkovsky, M. D., Ed., New Wave: Moscow, 2005.
3. Ji, K.; Choi, K.; Lee, S.; Park, S.; Khim, J. S.; Jo, E. H.; Choi, K.; Zhang, X.; Giesy, J. P. Effects of sulfathiazole, oxytetracycline and chlortetracycline on steroidogenesis in the human adrenocarcinoma (H295R) cell line and freshwater fish Oryzias latipes. *J. Hazardous Materials* **2010**, *182*, 494-502.
4. Felise, H. B.; Nguyen, H. V.; Pfuetzner, R. A.; Barry, K. C.; Jackson, S. R.; Blanc, M. P.; Bronstein, Ph. A.; Kline, T.; Miller, S. I. An Inhibitor of Gram-Negative Bacterial Virulence Protein Secretion. *Cell Host & Microbe* **2008**, *4*, 325-336.
5. Kovalishyn, V.; Grouleff, J.; Semenyuta, I.; Sinenko, V.; Slivchuk, S.; Hodyna, D.; Brovarets, V.; Blagodatny, V.; Poda, G.; Tetko, I.; Metelytsia, L. Rational design of isonicotinic acid hydrazide derivatives with antitubercular activity: Machine learning, molecular docking, synthesis and biological testing. *Chem. Biol. Drug Des.* **2018**, *92*, 1272-1278.
6. Mak, J. Y. W.; Xu, W.; Fairlie, D. P. In *Peptidomimetics I*, Lubell, W. D., Ed.; Springer, 2015; pp 235-266.
7. Alley, M. C.; Scudiero, D. S.; Monks, P. A.; Hursey, M. L.; Czerwinski, M. J.; Fine, D. L.; Abbott, B. J.; Mayo, J. G.; Shoemaker, R. H.; Boyd, M. R. Feasibility of Drug Screening with Panels of Human Tumor Cell Lines Using a Microculture Tetrazolium Assay. *Cancer Research* **1988**, *48*, 589-601.
8. Grever, M. R.; Schepartz, S. A.; Chabner, B. A. The National Cancer Institute: cancer drug discovery and development program. *Seminars in Oncology* **1992**, *19*, 622-638.
9. Boyd, M. R.; Paull, K. D. Some practical considerations and applications of the national cancer institute in vitro anticancer drug discovery screen. *Drug Development Research* **1995**, *34*, 91-109.
10. Shoemaker, R. H. The NCI60 human tumour cell line anticancer drug screen. *Nature Reviews* **2006**, *6*, 813-823.
11. Turov, K. V.; Vinogradova, T. K.; Brovarets, V. S.; Drach, B. S. Reactions of 4-tosyl-2-phenyl-5-chloro-1, 3-thiazole with *N*-, *O*-, and *S*-nucleophiles. *Russ. J. Gen. Chem.* **2010**, *80*, 825-828.
12. Turov, K. V.; Vinogradova, T. K.; Rusanov, E. B. *et al*. Reaction of 1-tosyl-2,2-dichloroenamines with the Lawesson's reagent. *Russ. J. Gen. Chem.* **2012**, *82*, 848-852.
13. Turov, K. V.; Drach. B. S. Reaction of 1-tosyl-2, 2-dichloroenamines with the Lawesson's reagent. *Russ. J. Gen. Chem.* **2008**, *78*, 629-633.
14. Turov, K. V.; Vinogradova, T. K.; Drach, B. S. Transformations of 5-chloro-2-hydrazino-4-p-tolylsulfonyl-1,3-thiazole. *Russ. J. Gen. Chem.* **2008**, *78*, 2132-2136.
15. Babii, S. B.; Zyabrev, V. S.; Drach, B. S. Cyclocondensation of 1-Tosyl-2,2-dichloroethenyl Isothiocyanate with *O*-, *S*-, *N*-, and *C*-Nucleophiles. *Russ. J. Gen. Chem.* **2002**, *72*, 1730-1735.
16. NCI-60 Human Tumor Cell Lines Screen. DTP Developmental Therapeutics Program, NIH website [Internet]. Available from: https://dtp.cancer.gov/discovery_development/nci-60/default.htm (accessed on March 20, 2020).

Оцінка протиракової активності ди- та трифункціональнозаміщених 1,3-тіазолів

К. В. Туров, О. П. Мітюхін, С. А. Чумаченко, В. С. Зябрєв, В. С. Броварець*

Інститут біоорганічної хімії та нафтохімії ім. В.П. Кухаря НАН України, вул. Мурманська, 1, Київ, 02094,Україна.

Резюме: Синтезовано ряд ди- та трифункціональнозаміщених 1,3-тіазолів з використанням в якості вихідних сполук 1-*R*-3-тозил-1,4,4-трихлоро-2-аза-1,3-бутадієнів або 1-тозил-2,2-дихлороетенілізотіоціанату. Скринінгові дослідження протиракової активності синтезованих сполук проведено *in vitro* на 60 лініях ракових клітин людини: лейкемії (лінії CCRF-CEM, HL-60 (TB), K-562, MOLT-4, RPMI-8226, SR), меланоми (лінії LOX IMVI, MALME-3M, M14, MDA-MB-435, SK-MEL-2, SK-MEL-28, SK-MEL-5 , UACC-257, UACC-62), раку легенів (лінії A549/ATCC, EKVX, HOP-62, HOP-92, NCI-H226, NCI-H23, NCI-H322M, NCI-H460, NCI-H522), товстої кишки (лінії COLO 205, HCC-2998, HCT-116, HCT-15, HT29, KM12, SW-620), мозку (лінії SF-268, SF-295, SF-539, SNB-19, SNB-75, U251), яєчників (лінії IGROV1, OVCAR-3, OVCAR-4, OVCAR-5, OVCAR-8, NCI/ADR-RES, SK-OV-3), нирок (лінії 786-0, A498, ACHN, CAKI-1, RXF 393, SN12C, TK-10, UO-31), простати (лінії PC-3, DU-145) і грудей (лінії MCF7, MDA-MB-231/ATCC, HS 578T, BT-549, T- 47D, MDA-MB-468) при концентрації $1\cdot10^{-5}$ М. В результаті визначено відсоток росту (GP) клітин ліній раку у порівнянні з контролем (контроль – 100%). Поглиблений *in vitro* скринінг сполук полягав у вивченні її протипухлинного ефекту в п`яти концентраціях при 10-кратному розведенні (10^{-4}-10^{-8} М). У результаті експерименту розраховано 3 дозозалежні параметри (GI_{50}, TGI, LC_{50}). Серед даних сполук 1-(4-((4-метилфеніл)сульфоніл)-2-феніл-1,3-тіазол-5-іл)піперазин (середні значення lg GI_{50} = -5.87, lg TGI = -5.54, lg LC_{50} = -5.21), 1-(2-(3,5-диметил)-1*H*-піразол-1-іл)-4-((4-метилфеніл)сульфоніл)-1,3-тіазол-5-іл)піперазин (середні значення lg GI_{50} = -5.66, lg TGI = -5.26, lg LC_{50} = -4.83) та 1-(2,4-біс((4-метилфеніл)сульфоніл)-1,3-тіазол-5-іл)піперазин (середні значення lg GI_{50} = -5.67, lg TGI = -5.21, lg LC_{50} = -4.67) виявили найвищу інгібуючу активність. Отримані результати свідчать про перспективність пошуку серед ди- та трифункціональнозаміщених похідних 1,3-тіазолу нових протиракових препаратів.

Ключові слова: 1,3-тіазол; протиракова активність; інгібітори росту; цитостатична активність; цитотоксична активність.

ISSN 1814-9758. Ukr. Bioorg. Acta, 2020, Vol. 15, N 1
UDC 544.182.32+547.31.39+547.787.1+547.874.8
DOI: hpps://doi.org/10.15407/bioorganica2020.01.012

Ukrainica Bioorganica Acta
www.bioorganica.org.ua

UBA

RESEARCH ARTICLE

In silico binding affinity studies of phenyl-substituted 1,3-oxazoles with protein molecules

Maryna Yu. Zhuravlova[1], Nataliya V. Obernikhina[2]*, Stepan G. Pilyo[3], Maryna V. Kachaeva[3], Oleksiy D. Kachkovsky[3], Volodymyr S. Brovarets[3]

[1]*National University of "Kyiv-Mohyla Academy", 2 Skovoroda St., Kyiv, 04070, Ukraine*
[2]*O. O. Bogomolets National Medical University, 13 Shevchenko Blvd., Kyiv, 01601, Ukraine*
[3]*V. P. Kukhar Institute of Bioorganic Chemistry and Petrochemistry of the NAS of Ukraine, 1 Murmanska St., Kyiv, 02094, Ukraine*

Abstract: The new model approach of interaction between the pharmacophores with bio-molecules, fragment-to-fragment, is presented. It is a new step of the molecular modeling that takes correctly into consideration not only the spatial complementarity of the interacted molecules but also the contribution of the stacking π-π-electron interaction and hydrogen bonds. As an example, the correct analysis of the interaction of the biological active phenyl-substituted 1,3-oxazoles with protein fragments is performed. It was shown that the length and energy of the hydrogen bond uniquely depend on the chemical constitution of both components in the created complex [*Pharmacophore*(Oxazole)-*Biomolecule* (H-X)]. The binding energy decreases in the series X → O, S, NH (fragments of the corresponding biomolecules). It should be pointed out that introduction of the conjugated phenyl groups at positions 2 and 5 of oxazoles increase the stability of the generated complex *Pharmacophore-Biomolecule* [*Pharm-BioM*] with fragments of the corresponding biomolecules along the core of oxazole by 0.2 and 0.5 kcal/mole. At the same time, modeling of the generated complex [*Pharm-BioM*] by phenyl substituents at position 2 and 5 of 1,3-oxazole with phenylalanine as a fragment of protein molecules additionally stabilizes complex by 2.5 kcal/mole by π-stacking mechanism. The observed biological activity of the phenyl substituted 1,3-oxazole is rather connected with ability to generate the stable complex due to the formation of additional bonds with other fragments (conjugated phenyl core). The calculations demonstrated that such substituents do not cause spatial hindrances with the polypeptide chain.

Keywords: biological affinity, 1,3-oxazoles, quantum chemical calculations, [*Pharm-BioM*] complex, π-stacking interaction, hydrogen bonds.

Introduction

The oxazole-based five-membered heterocycles exhibit various pharmacologically interesting properties that have recently been reported in several reviews [1-2]. It enabled the wide introduction of novel pharmacological drugs into medicine. The 1,3-oxazoles with branched conjugated systems demonstrated high biological activity, including antibacterial and antiviral activities [3-4], and multiple drug resistance pump inhibition [5-6]. The substituted 1,3-oxazoles with branched π-conjugated systems also were studied *in vitro* at the National Cancer Institute in the USA, as part of a therapeutic program for the development of DTP. It was found that these compounds are promising component in the development of new biologically active substances exhibiting antitumor activity which is strongly dependent on the nature of the substituents in heterocyclic core [7-10]. That leads to additional research activity toward developing new pharmaceuticals [11-12].

The QSAR models for a wide range of 1,3-oxazole derivatives showed an inhibitory effect on several cancer cell lines. A good correlation between many descriptors and biological activity was established [8]. Therefore, the planar oxazole core can be regarded as an applicable biologically active fragment. Its lone electron pair (LEP) at the two-coordinated nitrogen atom can promote the additional stabilization of [*Pharm-BioM*] complex by hydrogen bonds.

Received: 20.03.2020
Revised: 03.04.2020
Accepted: 10.04.2020
Published online: 30.06.2020

* Corresponding author. Tel.: +380-96-225-7764;
e-mail: nataliya.obernikhina@nmu.ua (N. V .Obernikhina)
ORCID: 0000-0003-1143-8924

At the same time, the introduction of substituents with a conjugated π-electron system in the 1,3-oxazole ring increases the stabilization of resulted complex [*Pharm-BioM*] by π-stacking interaction. The presence of the phenyl substituent in 1,3-oxazole substrate increases biological activity, particularly, the inhibitory effect on the cancerous tumors [9-10]. These molecular fragments can generate an additional complementary structure with many biopolymers, which is considered an important condition for increasing selectivity for potential targets.

This paper presents the results of the *in silico* investigations of the connection between biological properties and electronic structure of phenyl substituted 1,3-oxazoles, including the steric features as well as additional stabilization of the model [*Pharm-BioM*] complex by stacking interaction and by generation hydrogen bonds.

Materials

The 4-cyano substituted 1,3-oxazole derivatives were investigated (Figure 1) as biologically active compounds for interaction with protein fragments. Typically, electron accepting groups at the 4th position of 1,3-oxazoles increase the stability of the 5-membered electron-rich oxazole cycle. Moreover, oxazole derivatives containing similar substituents have demonstrated high biological activity [9].

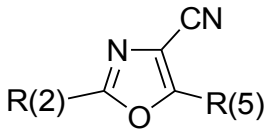

Compd	$R_{(2)}$	$R_{(5)}$
1	Me	Me
2	Ph	Me
3	Me	Ph
4	Ph	Ph

Figure 1. Structures of compounds **1-4**.

The dimethyl substituted oxazole **1** was chosen as a reference molecule; the one- and two-phenyl substituted derivatives **2-4** were compared to oxazole **1**. Compounds **1-4** were evaluated at the National Cancer Institute (NCI) for anticancer activity *in vitro*. Primary *in vitro* one dose anticancer assay was performed in full NCI 60 cell panel representing leukemia, melanoma, and cancers of lung, colon, brain, breast, ovary, kidney, and prostate in accordance with the protocol of the NCI, USA [9].

The main characteristics of the electron structure (optimized molecular geometry, charge distribution, energies and shapes of molecular orbitals) were calculated by DFT computation utilizing wB97XD function and 6-31G(d,p) basis set as implemented in GAUSSIAN 03 program [13].

Binding affinity by fragment-to-fragment approach

Typically, the biological affinity of pharmacophores evaluated by their ability to effectively interact with biological molecules. The pharmacophore (*Pharm*) and biomolecule (*BioM*) should form a stable complex, namely [*Pharm-BioM*]. The stability of such complex depends on the geometrical characteristics of both complex components. The complex can be additionally stabilized by creating hydrogen bonds and stacking interactions with phenyl substituents. The oxazole and its conjugated substituted derivatives are planar molecules and, hence, should be attracted to protein fragments. The amino acids with the aromatic groups as part of its structural characteristics can create a π-complex [*Pharm-BioM*] with oxazole derivatives **1-5**. Therefore the ability to form the π-complex can be considered as a π-electron affinity component. Similarly, the ability to form a complex by hydrogen bonds can be considered as an [H-B] affinity component. As a result, the oxazole π-electron cycle can manifest the π-affinity whereas the two-coordinated nitrogen atom of the oxazole ring can manifest its [H-B]-affinity. These properties can be evaluated by a direct quantum-chemical modeling.

Many events of the [*Pharm-BioM*] interactions can be modeled by elementary interactions between the pharmacophore fragments (1,3-oxazoles) and some fragments of the complex biological molecules by taking into consideration the complementarity of the complex components. We will call this approach a fragment-to-fragment approach.

Results and Discussion

Molecular geometry of substituted 1,3-oxazoles and charge distribution

The 1,3-oxazoles are conjugated planar molecules. The optimization of the molecular geometry of phenyl substituted oxazoles **2-4** with variable substituents in positions 2 and 5 confirmed planar configuration. According to the complementarity rule such compounds should predominantly form complexes [*Pharm-BioM*] with protein fragments that contain conjugated aromatic amino acids (phenylalanine, tyrosine, tryptophan, histidine). These complexes are additionally stabilized by stacking interaction between π-electron systems of both complex components.

Earlier, we have demonstrated that the binding energy of the complex [Pharm-Fullerene] depends on the nature of the substituent in the oxazole ring [14]. We hypothesized that the binding energy of complex [*Pharm-BioM*] formation depends on the nature of the substituent at the 2- and 5-positions of 1,3-oxazoles **1-4**. This dependence should be similar for all types of donor/acceptor characteristics of these biomolecules. The complex formation of 1,3-oxazole

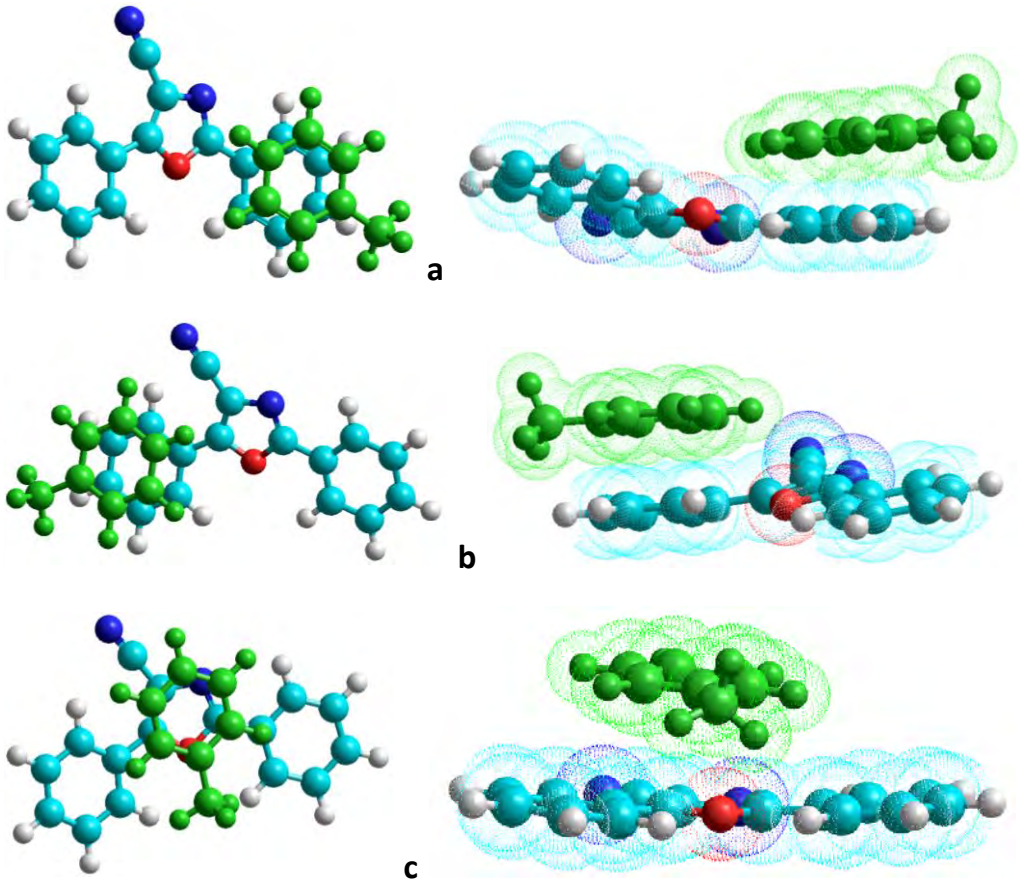

Figure 2. Optimized molecular geometry of three possible complexes of 1,3-oxazole **4** with a model phenylalanine (toluene): a) π-stacking by phenyl group at position 2; b) π-stacking by phenyl group at position 5; v) π-stacking by 1,3-oxazole cycle.

4 with phenylalanine [oxazole-Phe] was examined. Phenylalanine in a polypeptide chain was modeled by toluene, i.e. only conjugated system was taken into consideration. The geometrical characteristics of phenyl group of toluene is similar to the fragments of the phenyl-substituted 1,3-oxazole **4**. As a result, we calculated different possible versions of the generated complex: (i) when the central heterocycle is oriented to model phenylalanine or (ii) when one of the phenyl-group of oxazole **4** is oriented toward model phenylalanine. Three possible complexes of diphenyl substituted oxazole with toluene are presented in Figure 2.

It is noteworthy that the thickness of π-electron systems is 3.4 Å, the distance between the components in the studied complex [*Pharm-BioM*] (i.e., between 1,3-oxazole cycle, phenyl substitutes in the 2- and 5-positions of 1,3-oxazole **4** and model phenylalanine – toluene) is 3.4 Å. Similar founding was reported for deoxyribonucleic acid helix [16] and for polymethine dyes aggregates [17].

*Positions of the frontier orbitals of compounds **1-4** and its donor/acceptor properties*

We assumed that biological activity is connected to the position of frontier orbitals as it was reported previously [15]. The oxazole ligand produces complex with peptide fragments by protein-ligand complex binding [*Pharm-BioM*] [18]. These results indicates the stacking interaction between the π-systems of both complex components: A (*Pharmacophore*) and B (*Biomolecule*). According to the perturbation theory [19], a similar interaction depends on the relative positions of the molecular orbitals of both molecules as well as the overlapping of their π-systems and can be calculated by Equation 1:

$$\Delta E \approx \sum_{\mu}^{A}\sum_{i}^{A}\sum_{\nu}^{B}\sum_{j}^{B}\left[\frac{C_{i\mu}C_{j\nu}}{\varepsilon_i - \varepsilon_j}\right] \qquad (1)$$

where ε_i and ε_j are MO energies; $C_{i\mu}$ and $C_{j\nu}$ are MO coefficients; indices i, μ is energy system A; indices j, ν is energy system B.

The main contributions to the frontier molecular orbitals (MO) are made by the highest occupied MO (HOMO) and the lowest unoccupied MO (LUMO). The geometry of the frontier molecular orbitals contribute to the donor and acceptor ability of the conjugated molecules. The influence of the phenyl groups on the energy level of both HOMO and LUMO are presented in Table 1.

Table 1. Energies of frontier MO of substituted 1,3-oxazoles **1-4**.

Compd	$R_{(2)}$	$R_{(5)}$	ε(MO), eV		Δ, eV	φ_0[a]
			HOMO	LUMO		
1	Me	Me	-8.822	1.137	9.958	0.472
2	Ph	Me	-8.307	0.386	8.694	0.454
3	Me	Ph	-8.228	0.049	8.277	0.436
4	Ph	Ph	-8.004	-0.173	7.830	0.433

[a] φ_0 calculated by Equation 2.

The introduction of the phenyl groups in position 2 or 5 of oxazole ring are accompanied by converging of the frontier orbitals so that energy gap (difference between the energy of highest occupied orbital and lowest vacant orbital) decreases. Phenyl group in position 5 causes the greater effect (1.68 eV) compared to the phenyl substituent in position 2 (1.26 eV). There is no additive effect found upon simultaneous introduction of two phenyl groups to positions 2 and 5 (2.12 eV).

It was proposed [20] to calculate the donor/acceptor ability of the molecules as a relative position of the frontier orbitals by the following Equation 2:

$$\varphi_0 = (\varepsilon_{LUMO} - (\varepsilon_F)/(\varepsilon_{LUMO} - (\varepsilon_{HOMO}) \quad (2)$$

Where ε_{LUMO} is an energy of the lowest unoccupied MO, ε_{HOMO} is an energy of the highest occupied MO, ε_F (α) is an energy of non-bonding MO (α = -3.561 eV) [21].

The calculated values φ_0 for studied compounds are presented in Table 1. The data shows that this parameter is slightly sensitive to introduction of phenyl groups. The phenyl substituent generates the equal number of occupied and unoccupied MO, which symmetrically positioned from the non-bonding MO (Fermi level α) [21]. The acceptor property ($\varphi_0 < 0.5$) is caused by cyano group (-CN) in position 4, although the oxazole *per se* is molecule with donor properties as an electron rich system [18].

Binding energies of π-complex [Pharm-BioM]

In the first approximation, the binding energy $E_{binding}$ can be calculated as the difference of the total energy of the complex [*Pharm-BioM*] and the energies of both its components (Eq. 3):

$$E_{binding} = E_{[Pharm\text{-}BioM]} - E_{Pharm} - E_{BioM} \quad (3)$$

where $E_{[Pharm-BioM]}$ is the energy of optimized complex, while E_{Pharm} and E_{BioM} are energies of optimized components.

This work focuses on the protein fragment in the form of model phenylalanine (Phe-CH_3), which can create a π-complex. The calculations of the donor/acceptor parameter φ_0 of the phenylalanine amino acid gives φ_0 = 0.52; while this parameter of the model fragment, Phe-CH_3, is equal to φ_0 = 0.53. We are investigating the influence of the phenyl substitution in positions 2 and 5 that resulted in change of a π-contribution as well as total affinity of the oxazoles **1-4** in a model complex [Oxazole:Phe-CH_3].

Figure 2 depicted three possible geometries of both components in the model complex. The optimization showed that the distance between components in the stable complex is approximately 3.4 Å. The calculated binding energies of the optimized complexes [Oxazole:Phe-CH_3] are presented in Table 2.

As it can be seen (Table 2 and Figure 2c) that one phenyl group (compounds **2** and **3**) increases the complex stability by orienting the phenyl group to the heterocyclic fragment; in the complex that is formed from di-phenyl-substituted 1,3-oxazole **4**, the binding energy is less than in the complex with the reference molecule **1**.

The stabilization energy of the complex **2c** [Oxazole:Phe-CH_3] is significantly lower compared to other complexes' geometries (Figure 2, Table 2). It is noteworthy that the stabilization energy of the complex that is formed from two phenyl substituted oxazole is minimum among all possible complexes. However, the preferential formation of

Table 2. Binding energies of complexes [Oxazole:Phe-CH_3], where oxazole corresponds to compounds **1-4**.

Figure	Complex	$R_{(2)}$	$R_{(5)}$	Energy (E)[a], a.u.		ΔE[b], kcal/mole
				Oxazole	Complex	
2c	[Oxazole **1**:Phe-CH_3]	Me	Me	-416.825544294	-688.327544051	-12.18
2c	[Oxazole **2**:Phe-CH_3]	Ph	Me	-608.502926733	-880.005254882	-12.38
2a	[Oxazole **2**:Phe-CH_3]	Ph	Me		-880.002988419	-10.96
2c	[Oxazole **3**:Phe-CH_3]	Me	Ph	-608.502469135	-880.005254882	-12.67
2b	[Oxazole **3**:Phe-CH_3]	Me	Ph		-880.000764847	-9.85
2c	[Oxazole **4**:Phe-CH_3]	Ph	Ph	-800.180950747	-1071.68207547	-11.63
2a	[Oxazole **4**:Phe-CH_3]	Ph	Ph		-1071.67606230	-7.86
2b	[Oxazole **4**:Phe-CH_3]	Ph	Ph		-1071.67528637	-7.37
	Phe-CH_3			-271.482591603		

[a] E is total energy.
[b] ΔE is binding energy increases only the stability of the formed complex.

various complexes with the orientation at the heterocycle (Figure 2c) will be difficult because of spatial hindrances with the polypeptide chain.

The formation of hydrogen bonding in [H-B] complex

The oxazole cycle contains a coordinated nitrogen atom (with the lone electron pair – LEP) in position 3. It can be considered as an acceptor center for the formation of hydrogen bonds, while the hydrogen atom of the amino group of some acids (lysine, arginine, histidine, etc.) or groups containing hydrogen (-NH, -OH and -SH) can provide the required proton, i.e. the hydrogen bonds can be formed during complex's formation. This interaction should result in the additional stabilization energy of complexes [Oxazole:H-X] that are formed between oxazole molecules and suitable fragments of biomolecules, where X is a N, O, S atoms.

In our study, the donor centers were modeled by the simplest molecules: methanol HO-CH_3, methylamine H_2N-CH_3 and methanethiol HS-CH_3. Possible complexes of the model bio-fragments with the 1,3-oxazoles **1-4** are shown in Figure 3.

The model peptide fragment and oxazole cycle are positioned perpendicularly. Moreover, the formation of hydrogen bond should depends on the charge at the nitrogen atom as well as on the relative position of the LEP (*n*-MO). Calculation revealed that the *n*-MO is localized near the nitrogen atom, and it actively interacts with the σ-orbital, as it presented in Figure 4. *n*-MO is located directly below of the frontier orbitals: HOMO-1. In the case of phenyl derivatives, the local orbital (MOs localized only on phenyl molecular fragment) are situated between the delocalized HOMO and the *n*-MO. Nevertheless, the energy level of *n*-MOs remains practically the same after every change in the reference oxazole cycle. The calculated atomic charges and *n*-MO energies are presented in Table 3.

Table 3. Charge at nitrogen atom (z) and *n*-MO energy (ε) of substituted oxazoles **1-4**.

Compd	$R_{(2)}$	$R_{(5)}$	z, e.u.	*n*-MO	
				number	ε, eV
1	Me	Me	-0.457	HOMO-1	-10.63
2	Ph	Me	-0.454	HOMO-3	-10.69
3	Me	Ph	-0.491	HOMO-3	-10.70
4	Ph	Ph	-0.458	HOMO-5	-10.77

Table 3 shows that introducing of phenyl group in position 2 slightly decreases a negative charge at the nitrogen atom whereas the phenyl in position 5 causes the opposite effect.

The energy of three complexes of the reference molecule **1** with three model compounds H-X-CH_3 where X is a N, O, S atoms as well as three complexes of one model bio-fragment, H_2N-CH_3, with substituted 1,3-oxazoles **2-4** were calculated and presented in Table 4.

It was found that the length of the hydrogen bond and the binding energy depends on the chemical structure of both components in the generated [Oxazole:H-X] complex. Thus, the change of heteroatoms in a model bio-fragment [H-B(X)] decreases the binding energy and, therefore, the stabilization of the corresponding complex in series: X → O, S, NH. The length of a hydrogen bond is shorter during the interaction with –OH group, whereas the lengths of a hydrogen bond with $–NH_2$ and –SH groups are essentially the same.

The introduction of the phenyl substituents does not change the length of hydrogen bonds in the corresponding complex: $l_{N^-\ldots H} \approx 2.01\pm 0.01$ Å. Moreover, the binding energy is considerably more sensitive to position of the introduced phenyl groups as well as to the number of

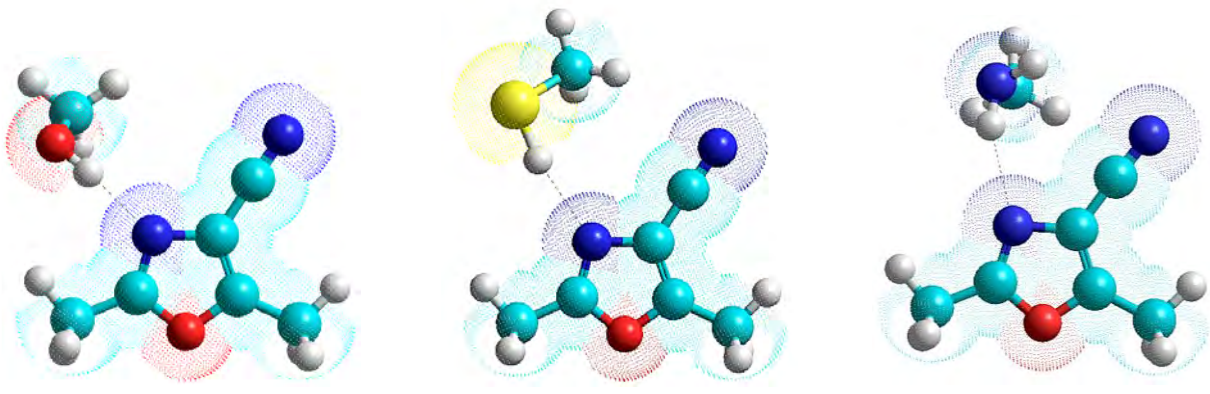

a **b** **c**

Figure 3. Calculated geometry of 1,3-oxazole molecule **1-4** and model fragments of biomolecules: a) methanol; b) methanethiol; c) methylamine.

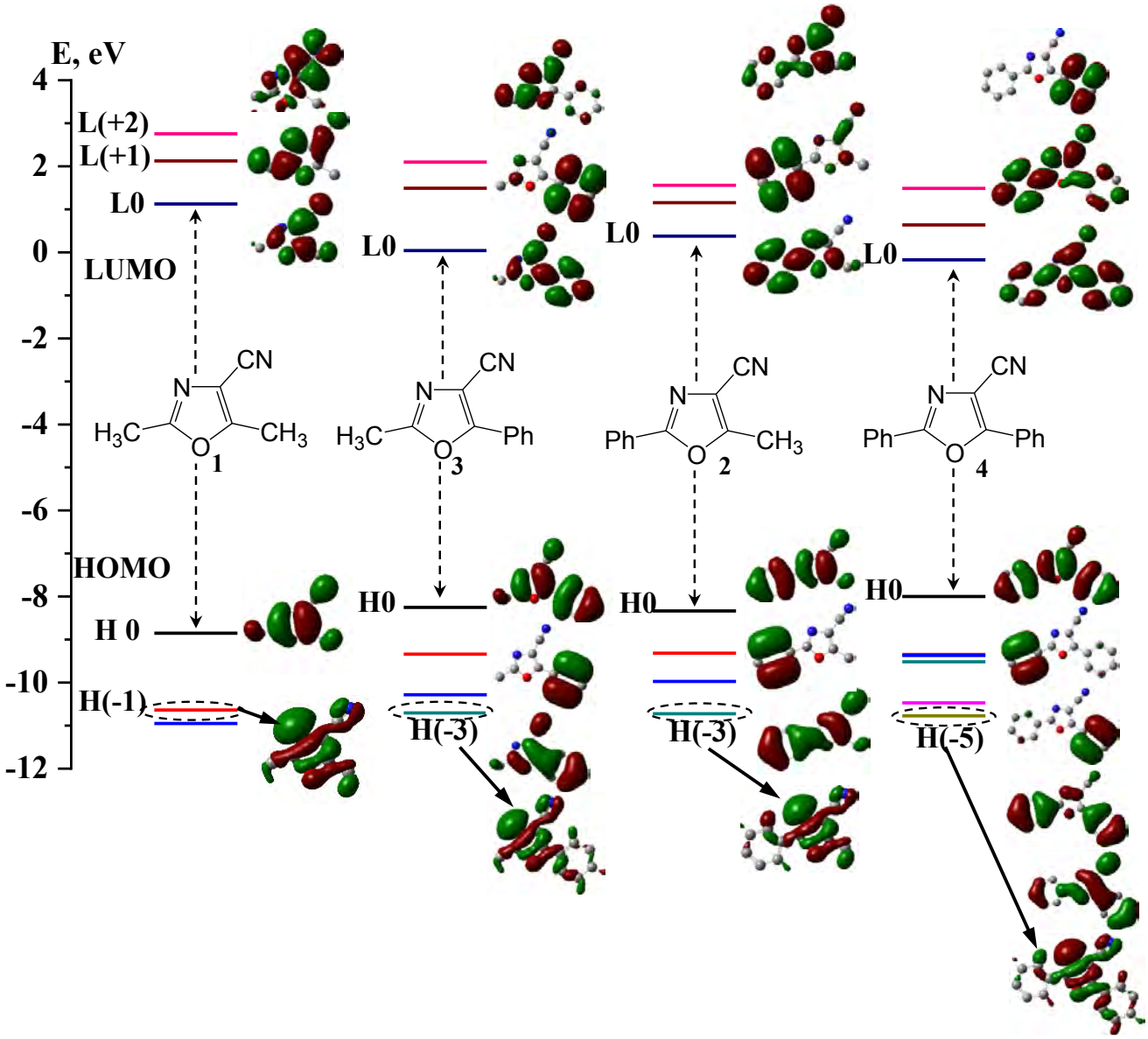

Figure 4. Position and shape of frontier and nearest MOs in 1,3-oxazoles **1-4**.

Table 4. Hydrogen bond energy of complex [Oxazole:H-X] with model methanol, methylamine, and methanethiol.

Complex	$R_{(2)}$	$R_{(5)}$	X	$l_{N\text{-}\ldots H}$[a], Å	Energy (E), a.u.		$\Delta E_{binding}$[b], kcal/mole
					Oxazole	Complex	
[Oxazole **1**:H-X]	Me	Me	-O	1.838	-416.82554429	-532.52885310	-11.47
[Oxazole **1**:H-X]	Me	Me	-HN	2.252	-416.82554429	-512.66886008	-7.68
[Oxazole **1**:H-X]	Me	Me	-S	2.232	-416.82554429	-855.50852371	-9.11
[Oxazole **2**:H-X]	Ph	Me	-O	1.989	-608.50292673	-724.20719212	-12.08
[Oxazole **3**:H-X]	Me	Ph	-O	2.018	-608.50246913	-724.20876140	-13.34
[Oxazole **4**:H-X]	Ph	Ph	-O	1.996	-800.18095074	-915.88462187	-11.70
H-O-CH_3						-115.68502789	
H-HN-CH_3						-95.831078854	
H-S-CH_3						-438.66846361	

[a]$l_{N\text{-}\ldots H}$ is hydrogen bond length.
[b]$\Delta E_{binding}$ is binding energy.

Table 5. Anticancer activity of synthesized compounds [22] model 1,3-oxazoles **2-4**, and their theoretical characteristics.

Compd	$R_{(2)}$	$R_{(5)}$	φ_0	π-stack interaction	H-bond interaction	Anti-Cancer Activity [22], %	
				E, kcal/mol		Leukemia (RPMI-8226)	Non-Small Cell Lung Cancer (EKVX)
1	Me	Me	0.472	-12.18	-9.11	-	-
2	Ph	Me	0.454	-12.4[a]/10.9[b]	-12.08	99.2	73.1
3	Me	Ph	0.436	-12.7[a]/9.9[c]	-13.34	79.3	94.3
4	Ph	Ph	0.433	-11.6[a]/-7.9[b]/-7.4[c]	-11.70	75.0	85.3

[a]π-stack interaction according to Figure 2c. [b]π-stack interaction according to Figure 2a. [c]π-stack interaction according to Figure b.

substituents. The maximum stabilization energy of complex [Oxazole:H-X] (Table 4) reached when the 1,3-oxazole contains phenyl group in position 2 (compound **2**). The introduction of second phenyl group (compound **4**) decreases binding energy so that two phenyl substituents in positions 2 and 5 do not change the stability of the [Oxazole:H-X] complex, in compare with the reference molecule **1** ($R_1 = R_2 = CH_3$).

*The tendency of the quantum-chemical approaches and the anticancer activity of oxazole derivatives **1-4**.*

The synthesized compounds **1-4** were screened for anticancer activity in the 60 cell panel in accordance with the protocol of the NCI, USA, under the Developmental Therapeutic Program DTP [22]. Table 5 presents data from anticancer activity of synthesized compounds [9, 22] and their theoretical characteristics from quantum-chemical model fragment-to-fragment approach.

As can be seen from Table 5, the oxazole derivatives **2-4** inhibits of cell line EKVX (Non-Small Cell Lung Cancer) growth due to the formation of hydrogen bonds and stable [*Pharm-BioM*] complexes with regulatory proteins, which on the outer sphere have free residues of proton donor amino acids.

The growth's inhibition of cell line RPMI-8226 (Leukemia) happened due to the interaction with regulatory proteins that occurs by π-stack interaction of oxazole derivatives **2-4** with regulatory proteins that have open aromatic amino acid residues.

Conclusions

The theoretical analysis of the interaction of biologically active phenyl-substituted 1,3-oxazoles in the framework of the fragment-to-fragment approach (beside the spatial complementarity of the interacted molecules, the contribution of the stacking π-π-electron interaction and hydrogen bonds is taken into consideration) reviled that introduction of conjugated phenyl groups into main heterocyclic platform will not increase the stability of generated complexes. The observed biological activity of substituted 1,3-oxazoles **2-4** can be explained by the formation of additional bonds with other fragments (conjugated phenyl core) during complex formation, so as they do not cause the stearic hindrances with the polypeptide chain.

Notes

The authors declare no conflict of interest.

Author contributions. **M. Yu. Zh.**: provision of study materials, computing resources, or other analysis tools. **N. V. O.**: formulation or evolution of overarching research goals and aims, application of statistical, mathematical, computational, or other formal techniques to analyze study data. **S. G. P.**: development and design of methodology; creation of models, provision of study materials, computing resources, or other analysis tools. **M. V. K.**: preparation, creation and presentation of the published work, specifically visualization. **O. D. K.**: ideas; formulation or evolution of overarching research goals and aims, development or design of methodology; creation of models. **V. S. B.** ideas; formulation or development of common goals and objectives of the research, verification of results, responsibility for managing and coordinating the planning and implementation of research activities.

References

1. Kakkar, S.; Narasimhan, B. A comprehensive review on biological activities of oxazole derivatives. *BMC Chem.* **2019**, *13*, 171-195.
2. Zhang, H. Z.; Zhao, Z. L.; Zhou, C. H. Recent advance in oxazole-based medicinal chemistry. *Eur. J. Med. Chem.* **2018**, *144*, 444-492.
3. Cameron, D. M.; Thompson, J.; March, P. E.; Dahlberg, A. E. Initiation factor IF2, thiostrepton and micrococcin prevent the binding of elongation factor G to the Escherichia coli ribosome. *J. Mol. Biol.* **2002**, *319*, 27-35.
4. Rodnina, M. V.; Savelsbergh, A.; Matassova, N. B.; Katunin, V. I.; Semenkov, Yu. P.; Wintermeyer, W. Thiostrepton inhibits the turnover but not the GTPase of elongation factor G on the ribosome. *Proc. Natl. Acad. Sci. U.S.A.* **1999**, *96*, 9586-9590.
5. Lawrence, D. S.; Copper, J. E.; Smith, C. D. Structure-Activity Studies of Substituted Quinoxalinones as Multiple-Drug-Resistance Antagonists. *J. Med. Chem.* **2001**, *44*, 594-601.
6. Borst, P. Multidrug resistance: A solvable problem? *Ann. Oncol.* **1999**, *10*, 162-164.
7. Nolt, M. B.; Smiley, M. A.; Varga, S. L.; McClain, R. T.; Wolkenberg, S. E.; Lindsley, C. W. Convenient preparation of substituted 5-aminooxazoles via a microwave-assisted Cornforth rearrangement. *Tetrahedron* **2006**, *62*, 4698-4704.

8. Fennell, K. A.; Miller, M. J. Syntheses of Amamistatin Fragments and Determination of Their HDAC and Antitumor Activity. *Org. Lett.* **2007**, *9*, 1683-1685.
9. Kachaeva, M. V.; Hodyna, D. M.; Obernikhina, N. V.; Pilyo, S. G.; Kovalenko, Y. S.; Prokopenko, V. M.; Kachkovsky, O. D.; Brovarets, V. S. Dependence of the anticancer activity of 1,3-oxazole derivatives on the donor/acceptor nature of his substitues. *J. Heterocycl. Chem.* **2019**, *56*, 3122-3134.
10. Liu, X.; Bai, L.; Pan, C.; Song, B.; Zhu, H. Novel 5-Methyl-2-[(un)substituted phenyl]-4-{4,5-dihydro- 3-[(un)substituted phenyl]-5-(1,2,3,4-tetrahydroisoquinoline-2-yl)pyrazol-1-yl}-oxazole Derivatives: Synthesis and Anticancer Activity. *Chin. J. Chem*. **2009**, *27*, 1957-1961.
11. Fennell, K. A.; Miller, M. J. Syntheses of Amamistatin Fragments and Determination of Their HDAC and Antitumor Activity. *Org. Lett*. **2007**, *9*, 1683-1685.
12. Marquez, B. L.; Watts, K. S.; Yokochi, A.; Roberts, M. A.; Verdier-Pinard, P.; Jimenez, J. I.; Hamel, E.; Scheuer, P. J.; Gerwick, W. H. Structure and Absolute Stereochemistry of Hectochlorin, a Potent Stimulator of Actin Assembly. *J. Nat. Prod.* **2002**, *65*, 866-871.
13. Kachaeva, M. V.; Hodyna, D. M.; Semenyuta, I. V.; Pilyo, S. G.; Prokopenko, V. M.; Kovalishyn, V. V.; Metelytsia, L. O.; Brovarets, V. S. Design, synthesis and evaluation of novel sulfonamides as potential anticancer agents. *Comput. Biol. Chem.* **2018**, *74*, 294-303.
14. Frisch, M.; Trucks, G.; Schlegel, H.; Scuseria, G.; Robb, M.; Cheeseman, J.; Montgomery Jr, J.; Vreven, T.; Kudin, K.; Burant, J. and Millam, J. *Gaussian 03, Revision B. 05*, Gaussian Inc.: Pittsburgh, PA, Ringraziamenti, 2003.
15. Obernikhina, N.; Zhuravlova, M.; Kachkovsky, O.; Kobzar, O.; Brovarets, V.; Pavlenko, O.; Kulish, M.; Dmytrenko, O. Stability of fullerene complexes with oxazoles as biologically active compounds. *Appl. Nanosci.* **2020**, *10*, 1345-1353.
16. Zaenger, W. *Principles of Nucleic Acid Structure.* Springer-Verlag: New-York, Berlin, Heidelberg, Tokyo, 1984.
17. Shapiro, B. I. Molecular assemblies of polymethine dyes. *Russ. Chem. Rev.* **2006**, *75*, 433-456.
18. Dahlqvist, A.; Leffler, H.; Nilsson, U. J. C1-Galactopyranosyl Heterocycle Structure Guides Selectivity: Triazoles Prefer Galectin-1 and Oxazoles Prefer Galectin-3. *ACS Omega* **2019**, *4*, 7047-7053.
19. Dewar, M. J. S. *The molecular orbital theory of organic chemistry*. New York: McGraw Hill, 1969.
20. Obernikhina, N.; Kachaeva M.; Shchodryi, V.; Prostota, Ya.; Kachkovsky, O.; Brovarets, V.; Tkachuk, Z. Topological Index of Conjugated Heterocyclic Compounds as Their Donor/Acceptor Parameter. *Polycycl. Aromat. Comp.* **2019**, *39*, 1-14.
21. Obernikhina, N.; Pavlenko, O.; Kachkovsky, A.; Brovarets, V. Quantum-Chemical and Experimental Estimation of Non-Bonding Level (Fermi Level) and π-Electron Affinity of Conjugated Systems. *Polycycl. Aromat. Comp.* **2020**, *40*, 1-10.
22. Kachaeva, M. V.; Pilyo, S. G.; Zhirnov, V. V.; Brovarets, V. S. Synthesis, characterization, and in vitro anticancer evaluation of 2-substituted 5-arylsulfonyl-1,3-oxazole-4-carbonitriles. *Med. Chem. Res.* **2019**, *28*, 71-80.

In silico дослідження афінності зв'язування фенілзаміщенних 1,3-оксазолів з молекулами білків

М. Ю. Журавльова[1], Н. В. Оберніхіна[2]*, С. Г. Пільо[3], М. В. Качаєва[3], О. Д. Качковський[3], В. С. Броварець[3]

[1]*Національний університет "Києво-Могилянська академія", вул. Г. Сковороди, 2, Київ, 04070, Україна.*
[2]*Національний медичний університет імені О. О. Богомольця, бульв. Т. Шевченка, 13, Київ, 01601, Україна.*
[3]*Інститут біоорганічної хімії та нафтохімії ім. В. П. Кухаря НАН України, вул. Мурманська, 1, Київ, 02094, Україна.*

Резюме: Представлений новий пофрагментний підхід моделювання взаємодії фармакофорів з біомолекулами. Це новий, наступний крок молекулярного моделювання, який враховує не тільки просторову відповідну комплементарність взаємодіючих молекул, але й внесок π-електронів при стекінговій взаємодії та *n*-електронів при формуванні водневих зв'язків. Як приклад, проведено повний аналіз взаємодії біологічно активних феніл-заміщених 1,3-оксазолів з білковими молекулами. Було показано, що довжина та енергія водневого зв'язку однозначно залежать від хімічної конституції обох компонентів в утвореному комплексі [*Фармакофор(оксазол)-Біомолекула(H-X)*]. Енергія зв'язку регулярно зменшується у ряді X → O, S, NH (фрагменти відповідних біомолекул). Введення спряжених фенільних груп в положення 2 та 5 оксазолу збільшує стабільність згенерованого комплексу *Фармакофор-Біомолекула* [*Фарм-БіоМ*] з фрагментами відповідних біомолекул по ядру оксазола на 0.2 ккал/моль та 0.5 ккал/моль. При моделюванні утворення комплексу [*Фарм-БіоМ*] по фенільних замісниках 1,3-оксазолу в положенні 2 та 5 з фенілаланіном як фрагментом білкових молекул спостерігається додаткова його стабілізація на 2.5 ккал/моль за механізмом π-стекінгової взаємодії. Скоріш за все, біологічна активність феніл- заміщених 1,3-оксазолів, яка спостерігається, пов'язана з можливістю генерувати стійкий комплекс [*Фарм-БіоМ*] за рахунок утворення додаткових π-зв'язків з іншими фрагментами, що мають кон'юговане ядро. Розрахунки показують, що такі замісники не викликають просторових утруднень з поліпептидними молекулами.

Ключові слова: біологічна афінність, 1,3-оксазоли, квантово-хімічні розрахунки, комплекс [*Фарм-БіоМ*], π-стекінгова взаємодія, водневі зв'язки.

ISSN 1814-9758. Ukr. Bioorg. Acta, 2020, Vol. 15, N 1
UDC 547.78+577.152
DOI: hpps://doi.org/10.15407/bioorganica2020.01.020

Ukrainica Bioorganica Acta
www.bioorganica.org.ua

UBA

RESEARCH ARTICLE

5-Substituted *N*-(9*H*-purin-6-yl)-1,2-oxazole-3-carboxamides as xanthine oxidase inhibitors

Oksana V. Muzychka, Oleksandr L. Kobzar, Oleh V. Shablykin, Volodymyr S. Brovarets, Andriy I. Vovk*

V.P. Kukhar Institute of Bioorganic Chemistry and Petrochemistry of the NAS of Ukraine, 1 Murmanska St., Kyiv, 02094, Ukraine

Abstract: Synthetic 6-substituted purine derivatives are known to exhibit diverse bioactivity. In this paper, a series of *N*-(9*H*-purin-6-yl)-1,2-oxazole-3-carboxamide derivatives were synthesized and evaluated *in vitro* against xanthine oxidase, an enzyme of purine catabolism. The introduction of aryl substituent at position 5 of the oxazole ring was found to increase the inhibition efficiency. Some of the inhibitors containing 5-substituted isoxazole and purine moieties were characterized by IC_{50} values in the nanomolar range. According to the kinetic data, the most active *N*-(9*H*-purin-6-yl)-5-(5,6,7,8-tetrahydronaphthalen-2-yl)-1,2-oxazole-3-carboxamide demonstrated a competitive type of inhibition with respect to the enzyme-substrate. Molecular docking was carried out to elucidate the mechanism of enzyme-inhibitor complex formation. The data obtained indicate that xanthine oxidase may be one of the possible targets for the bioactive purine carboxamides.

Keywords: *N*-(9*H*-purin-6-yl)-1,2-oxazole-3-carboxamides, synthesis, bioactivity, xanthine oxidase.

Introduction

Purine derivatives are known to possess a range of biological properties as inhibitors of kinases, sulfotransferases, phosphodiesterases, and other enzymes as well as ligands of some proteins [1]. It was reported that derivatives of 6-(*N*-benzoylamino)purine can be potent inhibitors of bromodomain-containing protein 4 (BRD4), which control the expression of genes related to inflammation, apoptosis, and cell proliferation [2-3]. Structural analogs of this compound with bulky biaryl substituent were found to be potential inhibitors of the cytosolic 5'-nucleotidase II, which regulates intracellular nucleotide pools and has been recognized as a therapeutic target for hematological cancers [4]. At the same time, 6-(*N*-benzoylamino)purine was described as an inhibitor of the purine catabolizing enzyme, xanthine oxidase [5]. This enzyme catalyzes the oxidation of hypoxanthine and xanthine to uric acid with the generation of superoxide radicals. The increased uric acid levels lead to hyperuricemia and gout, and overproduction of superoxide radicals and other reactive oxygen species can promote chronic inflammatory and cardiovascular diseases, cancer, and diabetes [6].

The inhibitors of xanthine oxidase can be represented by two groups, which include purine derivatives [7-8] and non-purine compounds. The purine analog allopurinol is widely used in clinical practice [9]. More effective non-purine inhibitors of xanthine oxidase have also been developed, such as derivatives of imidazole [10], pyrazole [11], isoxazole [12], selenazole [13], and thiazole [14]. Among them, febuxostat, with inhibition constants in the nanomolar range, was approved for the treatment of hyperuricemia and gout [15]. However, allopurinol and febuxostat are known to induce side effects [9, 16], and there is thus interest in new bioactive compounds targeting xanthine oxidase.

Introducing isoxazole fragment into organic molecules is considered as a strategy for designing bioactive compounds with anticancer, antimicrobial, anti-inflammatory, and other

Received: 15.05.2020
Revised: 22.05.2020
Accepted: 25.05.2020
Published online: 30.06.2020

* Corresponding author. Tel.: +380-44-558-5388;
e-mail: vovk@bpci.kiev.ua (A. I. Vovk)
ORCID: 0000-0001-6167-076X

activities [17, 18]. Many of such compounds are represented by 3,5-substituted isoxazoles bearing other heterocyclic rings [19]. As an example, the hybrid molecules containing isoxazole, purine, and coumarin moieties were synthesized and tested *in vitro* as antioxidants and enzyme inhibitors [20]. In this paper, we synthesized substituted isoxazole-purine conjugates structurally similar to bioactive 6-(*N*-benzoylamino)purine. The 5-substituted derivatives of *N*-(9*H*-purin-6-yl)-1,2-oxazole-3-carboxamides were evaluated *in vitro* as inhibitors of xanthine oxidase.

Results and discussion

The synthesis of 5-substituted isoxazole acids was carried out using known synthetic methods [21] by the reaction of commercially available ketones with diethyl oxalate in the presence of sodium ethoxide [22]. The synthetic route included cyclization of ethyl 2,4-dioxobutanoates into ethyl isoxazole-3-carboxylates by the addition of hydroxylamine hydrochloride in ethanol at reflux [23] followed by saponification of the ester function with sodium hydroxide in ethanol. Corresponding acyl chlorides **3a-g** were synthesized in the reaction of the isoxazole acids and thionyl chloride in benzene and used without purification in acylation of adenine (**1**) or 8-aminoquinoline (**2**) (Scheme 1). All compounds were obtained in moderate to good yield. After crystallization of the crude products, the compounds **4a-g** and **5f** were characterized by ^{1}H NMR, IR spectra, and MS.

The inhibition activities of compounds **4a-g** against xanthine oxidase were assayed by monitoring the rate of enzymatic conversion of xanthine to uric acid. The IC_{50} values were defined as the concentration of the tested compound causing 50% inhibition of the enzyme with 50 μM xanthine as a substrate [24]. Allopurinol and 6-(*N*-benzoylamino)purine were used as reference inhibitors. Given the potential interest of the structures containing isoxazole and purine moieties, compound **4f** was also evaluated *in vitro* against purine nucleoside phosphorylase, however, no effect was observed on this enzyme.

Experimental data (Table 1) showed that compounds **4a** with 5-methyl-1,2-oxazole fragment displayed slightly decreased inhibitory activity as compared with 6-(*N*-benzoylamino)purine. The introduction of the aromatic group at 5-position of the isoxazole ring substantially increased the inhibitory potency of compounds **4b** and **4e**. Further increasing of xanthine oxidase inhibition was observed in the case of methyl or methoxy substituent at *para*-position of the phenyl ring of inhibitors **4c** and **4d**, respectively. Modification of the isoxazole ring by tetrahydronaphthalene fragment led to significant enzyme inhibition by compound **4f** with IC_{50} value of 14 nM which is approximately 280-fold more effective than that of allopurinol. Compound **4g** with more hydrophilic benzodioxinyl substituent demonstrated lower inhibitory potency. The importance of the purine part of the hybrid molecules in the inhibition mechanism was supported by compound **5f** which showed no activity.

Table 1. Xanthine oxidase inhibitory activity of *N*-(9*H*-purin-6-yl)-1,2-oxazole-3-carboxamides **4a-g**.

Compound	IC_{50}, μM[a]
6-(*N*-benzoylamino)purine	0.55±0.04
4a	0.75±0.18
4b	0.074±0.011
4c	0.048±0.013
4d	0.037±0.002
4e	0.078±0.011
4f	0.014±0.004
4g	0.044±0.003
Allopurinol	4.03±0.27

[a]IC_{50} values were calculated as the mean of 2-3 assays ± standard deviation.

Kinetic studies were performed for the most active compounds **4f** at different concentrations of substrate and the inhibitor to characterize the mechanism of inhibition. The double reciprocal Lineweaver-Burk plots indicated a competitive type of inhibition (Figure 1). This reveals that the inhibitor interacts with free enzyme competing with the substrate for the binding site. The calculated K_i value for compound **4f** was 7.46 ± 0.36 nM. It is known that allopurinol in complex with xanthine oxidase provides electron transfer to molecular oxygen with a generation of superoxide, but 6-(*N*-benzoylamino)purine does not exhibit such effect [5]. Compound **4f** was also not able to generate superoxide radical that was confirmed by a test with xanthine oxidase and reduced 2,6-dichlorophenolindophenol, controlled by absorbance at 605 nm. This result suggests that the purine part of the inhibitor with bulky 5-substituted isoxazole fragment is located near the molybdopterin center without electron transfer.

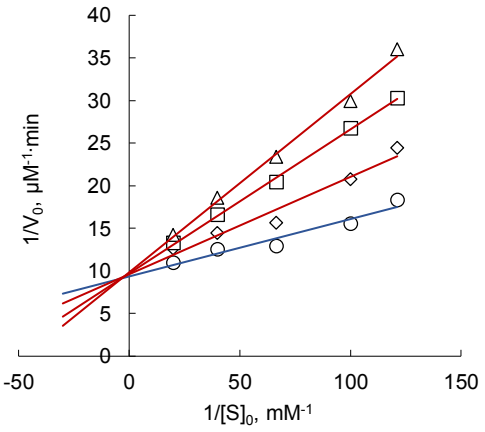

Figure 1. Lineweaver-Burk plots for inhibition of xanthine oxidase by compound **4f**. The inhibitor concentrations were 0 (○), 5 nM (●), 10 nM (□), and 15 nM (Δ).

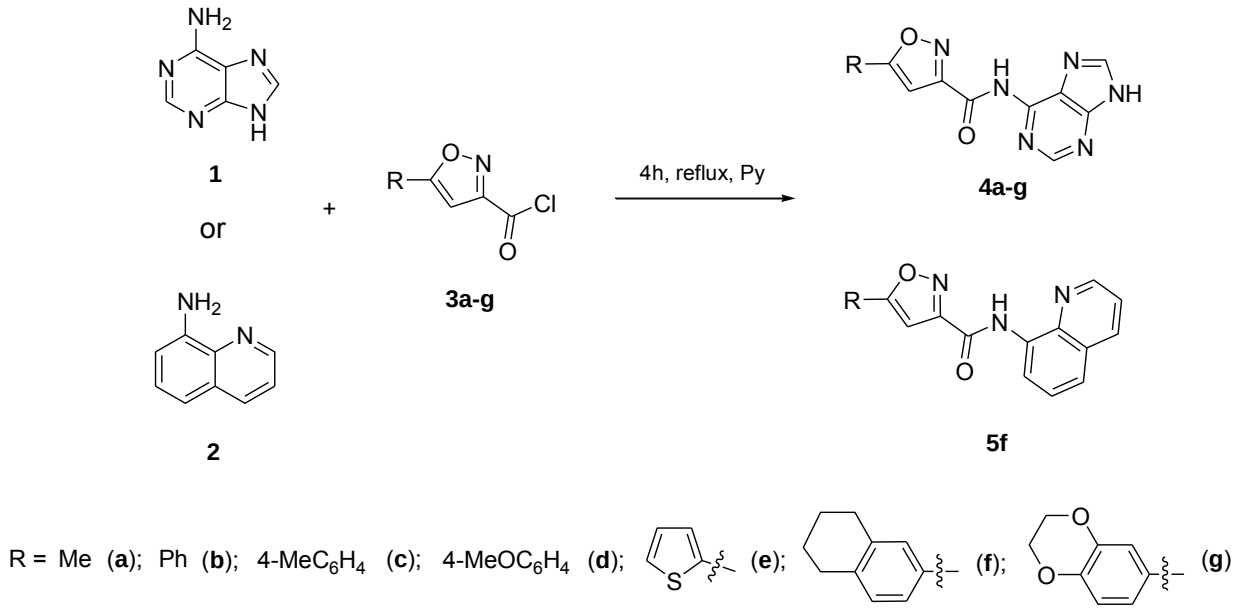

Scheme 1. Synthesis of *N*-(*9H*-purin-6-yl)-1,2-oxazole-3-carboxamides **4a-g** and compound **5f**.

To elucidate the possible mechanism of the enzyme-inhibitor complex formation, computer modeling was performed. Molecular docking calculations using a modified version of Autodock 4.2 [25] showed that the *N*-7-protonated tautomer of purine inhibitor can be preferred for the formation of the enzyme-inhibitor complex. The calculated docking energy for *N*-7- and *N*-9-protonated tautomeric forms of compound **4f** were -9.09 kcal/mol and -8.02 kcal/mol, respectively. The docking results (Figure 2) showed that two NH groups of *N*-7-protonated tautomeric form participate in the formation of hydrogen bonds with carboxylate group of Glu802 which can be involved in protonation of the enzyme-substrate [26, 27]. At the same time, HOH1365 provides the interaction of *N*-9 atom of the purine ring of the inhibitor with Glu1261 which can act as a general base in the enzymatic reaction [28]. Purine fragment of the inhibitor is also stabilized by aromatic-aromatic interaction with Phe914 and Phe1009. The isoxazole ring can form hydrophobic and van der Waals contacts with Leu873 and Val1011. Tetrahydro-naphthalene substituent shows aromatic-sigma interaction with Val1011 as well as hydrophobic and van der Waals contacts with His875 and Phe649 at the site exit.

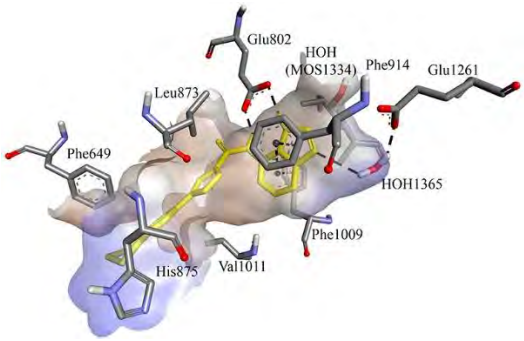

Figure 2. Possible binding mode of inhibitor **4f** in the active site of bovine milk xanthine oxidase.

Conclusions

In the present paper, 5-substituted *N*-(9*H*-purin-6-yl)-1,2-oxazoles were synthesized, and their inhibitory properties were evaluated *in vitro* against xanthine oxidase. The incorporation of a nonpolar bulky substituent at the isoxazole ring provided a better binding affinity to the enzyme active site. The most active compound, *N*-(9*H*-purin-6-yl)-5-(5,6,7,8-tetrahydronaphthalen-2-yl)-1,2-oxazole-3-carboxamide, was a competitive inhibitor of the enzyme with an inhibition constant in the nanomolar range. These data are helpful to consider xanthine oxidase as one of the possible targets for isoxazole-containing purine derivatives with diverse bioactivity.

Experimental section

The xanthine oxidase from bovine milk, bacterial purine nucleoside phosphorylase and xanthine were purchased from Sigma-Aldrich. Spectrophotometric measurements were performed on a Specord M-40. NMR spectra were obtained on a Bruker Avance DRX-500 instrument (^{1}H, 500 MHz) in a solution of DMSO-d_6 relative to internal TMS. The IR spectra were recorded on a Vertex 70 spectrometer from KBr pellets. The melting points were determined on a Fisher-Johns instrument. The LC/MS spectra were recorded on an Agilent 1100 series high-performance liquid chromatograph equipped by a diode matrix with an Agilent LC/MSD SL mass selective detector. The LC/MS parameters were set as follows: column, Zorbax SBC18 1.8 μm, 4.6x15 mm (PN 821975-932); solvents A, acetonitrile-water mixture (95:5), 0.1% trifluoroacetic acid and B, 0.1% aqueous trifluoroacetic acid; eluent flow rate, 3 ml/min; injection volume, 1 μl; UV detection, 215, 254, 265 nm; atmospheric-pressure chemical ionization (APCI) was used; scanning range, m/z 80-1000.

Synthesis

General procedure for the acylation of adenine

A suspension of adenine (**1**) or 8-aminoquinoline (**2**) (7.4 mmol) and corresponding acyl chloride (8 mmol) in pyridine (10 ml) was mixed at room temperature and then heated under reflux for 4 hours. The reaction mixture was cooled and water (20 ml) was added, the precipitate was filtered, washed with ethanol (5 ml). All the products **4a-g** and **5f** were purified by recrystallization from a mixture of DMF and water (1:1).

6-(N-Benzoylamino)purine was synthesized as described previously [29].

Yield 86%, mp 242-242.5 °C [29]. IR (KBr) *ν* 1521, 1552, 1581, 1599, 1621, 1686, 3256, 3369. ^{1}H NMR (500 MHz, DMSO-d$_6$) *δ* 7.56-7.65 (m, 3H), 8.03-8.15 (m, 2H), 8.51 (s, 1H), 8.75 (s, 1H), 11.09 (br s, 0.1H, NH), 11.52 (br s, 0.9H, NH), 12.37 (br s, 0.9H, NH), 13.47 (br s, 0.1H, NH). LC/MS (CI) *m/z* 240,2 (M+H)$^+$. Anal. Calcd. for $C_{12}H_9N_5O$: C, 60.25; H, 3.79; N, 29.27. Found: C, 60.13; H, 3.81; N, 29.19.

5-Methyl-N-(9H-purin-6-yl)-1,2-oxazole-3-carboxamide ***(4a)***.

Yield 60%, mp 270-271 °C. IR (KBr) *ν* 1556, 1597, 1632, 1704, 2900, 3111, 3215. ^{1}H NMR (500 MHz, DMSO-d$_6$) *δ* 2.35 (s, 3H), 7.40 (s, 1H), 8.52 (s, 1H), 8.74 (s, 1H), 11.00-12.25 (br s, 1H, NH), 12.25-14.00 (br s, 1H, NH). LC/MS (CI) *m/z* 245.2 (M+H)$^+$. Anal. Calcd. for $C_{10}H_8N_6O_2$: C, 49.18; H, 3.30; N, 34.41. Found: C, 49.02; H, 3.05; N, 34.23.

3-Phenyl-N-(9H-purin-6-yl)-1,2-oxazole-5-carboxamide ***(4b)***.

Yield 91%, mp 256-257 °C. IR (KBr) *ν* 1526, 1627, 1713, 3341. ^{1}H NMR (500 MHz, DMSO-d$_6$) *δ* 7.50-7.65 (s, 4H), 7.90-8.00 (m, 2H), 8.55 (s, 1H), 8.75 (s, 1H), 10.95-11.40 (br s, 0.2H, NH), 11.40-12.00 (br s, 0.8H, NH), 12.30-12.80 (br s, 0.8H, NH), 13.30-13.90 (br s, 0.2H, NH). LC/MS (CI) *m/z* 307.3 (M+H)$^+$. Anal. Calcd. for $C_{15}H_{10}N_6O_2$: C, 58.82; H, 3.29; N, 27.44. Found: C, 58.64; H, 3.18; N, 27.23.

5-(4-Methylphenyl)-N-(9H-purin-6-yl)-1,2-oxazole-3-carboxamide ***(4c)***.

Yield 86%, mp 255-256 °C. IR (KBr) *ν* 1523, 1559, 1610, 1718, 3354. ^{1}H NMR (500 MHz, DMSO-d$_6$) *δ* 2.37 (s, 3H), 7.37 (d, *J* 7.3, 2H), 7.51 (s, 1H), 7.84 (d, *J* 7.3, 2H), 8.54 (s, 1H), 8.75 (s, 1H), 10.80-12.10 (br s, 1H, NH), 12.10-13.00 (br s, 1H, NH). LC/MS (CI) *m/z* 321.3 (M+H)$^+$. Anal. Calcd. for $C_{16}H_{12}N_6O_2$: C, 60.00; H, 3.78; N, 26.24. Found: C, 60.01; H, 3.54; N, 26.21.

5-(4-Methoxyphenyl)-N-(9H-purin-6-yl)-1,2-oxazole-3-carboxamide ***(4d)***.

Yield 86%, mp 265-266 °C. IR (KBr) *ν* 1468, 1508, 1552, 1610, 1704, 3128, 3366. ^{1}H NMR (500 MHz, DMSO-d$_6$) *δ* 3.83 (s, 3H), 7.11 (d, *J* 7.3, 2H), 7.46 (s, 1H), 7.89 (d, *J* 7.3, 2H), 8.56 (s, 1H), 8.76 (s, 1H), 10.90-11.10 (br s, 0.2H, NH), 11.50-11.80 (br s, 0.8H, NH), 12.40-12.70 (br s, 0.8H, NH), 13.40-13.70 (br s, 0.2H, NH). LC/MS (CI) *m/z* 337.4 (M+H)$^+$. Anal. Calcd. for $C_{16}H_{12}N_6O_3$: C, 57.14; H, 3.60; N, 24.99. Found: C, 57.01; H, 3.34; N, 25.68.

N-(9H-Purin-6-yl)-5-(thiophen-2-yl)-1,2-oxazole-3-carboxamide ***(4e)***.

Yield 86%, mp 252-253 °C. IR (KBr) *ν* 1505, 1524, 1557, 1608, 1628, 1666, 1718, 3107, 3367. ^{1}H NMR (500 MHz, DMSO-d$_6$) *δ* 7.24-7.32 (m, 1H), 7.40 (s, 1H), 7.80-7.86 (m, 1H), 7.86-7.92 (m, 1H), 8.55 (s, 1H), 8.75 (s, 1H), 11.00-11.30 (br s, 0.2H, NH), 11.50-11.90 (br s, 0.8H, NH), 12.35-12.75 (br s, 0.8H, NH), 13.40-13.70 (br s, 1H, NH). LC/MS (CI) *m/z* 312.4 (M+H)$^+$. Anal. Calcd. for $C_{13}H_8N_6O_2S$: C, 50.00; H, 2.58; N, 26.91. Found: C, 49.88; H, 2.13; N, 26.67.

N-(9H-Purin-6-yl)-5-(5,6,7,8-tetrahydronaphthalen-2-yl)-1,2-oxazole-3-carboxamide ***(4f)***.

Yield 86%, mp 229-230 °C. IR (KBr) *ν* 1523, 1621, 1714, 2932, 3359. ^{1}H NMR (500 MHz, DMSO-d$_6$) *δ* 1.65-1.80 (m, 4H), 2.70-2.85 (m, 4H), 7.21 (d, *J* 8.4, 1H), 7.42 (s, 1H), 7.62 (br s, 2H), 8.47 (s, 1H), 8.69 (s, 1H), 10.50-13.50 (br s, 0.5H partially in exchange). LC/MS (CI) *m/z* 361.4 (M+H)$^+$. Anal. Calcd. for $C_{19}H_{16}N_6O_2$: C, 63.33; H, 4.48; N, 23.32. Found: C, 63.17; H, 4.21; N, 23.27.

5-(2,3-Dihydro-1,4-benzodioxin-6-yl)-N-(9H-purin-6-yl)-1,2-oxazole-3-carboxamide ***(4g)***.

Yield 86%, mp 269-270 °C. IR (KBr) *ν* 1506, 1556, 1576, 1624, 1716, 3127, 3356. ^{1}H NMR (500 MHz, DMSO-d$_6$) *δ* 4.27-4.35 (m, 4H), 7.02 (d, *J* 8.1, 1H), 7.40-7.50 (m, 3H), 8.55 (s, 1H), 8.75 (s, 1H), 10.95-11.15 (br s, 0.2H, NH), 11.50-11.75 (br s, 0.8H, NH), 12.40-12.65 (br s, 0.8H, NH), 13.45-13.65 (br s, 0.2H, NH). LC/MS (CI) *m/z* 365.4 (M+H)$^+$. Anal. Calcd. for $C_{17}H_{12}N_6O_4$: C, 56.05; H, 3.32; N, 23.07. Found: C, 56.10; H, 3.11; N, 23.14.

N-(Quinolin-8-yl)-5-(5,6,7,8-tetrahydronaphthalen-2-yl)-1,2-oxazole-3-carboxamide ***(5f)***.

Yield 78%, mp 166-167 °C. IR (KBr) *ν* 1498, 1577, 1615, 1729, 2937, 3129, 3411. ^{1}H NMR (500 MHz, DMSO-d$_6$) *δ* 1.65-1.75 (m, 4H), 2.7-2.85 (m, 4H), 7.18-7.77 (m, 7H), 8.44 (d, *J* 8.4, 1H), 8.71 (d, *J* 7.5, 1H), 8.98 (d, *J* 3.9, 1H), 10.95 (s, 1H, NH). LC/MS (CI) *m/z* 370.3 (M+H)$^+$. Anal. Calcd. for $C_{23}H_{19}N_3O_2$: C, 74.78; H, 5.18; N, 11.37. Found: C, 74.55; H, 5.05; N, 11.13.

Inhibition of xanthine oxidase

The enzymatic reaction was studied in sodium phosphate buffer (50 mM, pH 7.4) at 25 °C. The mixture contained xanthine (50 μM), inhibitor (from 2.5 nM to 50 μM), EDTA (0.1 mM), and 1% DMSO was incubated for 5 min and the reaction was initiated by addition of xanthine oxidase. The enzyme concentration was 0.008 units/mL. The reaction rate was monitored by the change in optical density at 293 nm. The IC_{50} values were calculated from the plot of the inhibition percentage against inhibitor concentrations.

Purine nucleoside phosphorylase test

The reaction mixture contained sodium phosphate buffer (0.1 M, pH 7.4), guanosine (0.1 mM), bacterial purine nucleoside phosphorylase (0.071 units/mL), inhibitor (50 μM), EDTA (0.1 mM) and 0.5% DMSO. The enzymatic reaction was investigated at 25 °C. The reaction rate was monitored by the change in optical density at 258 nm.

Reduction of 2,6-dichlorophenolindophenol

The reaction mixture contained 100 mM sodium phosphate buffer (pH 7.4), 15 μM 2,6-dichlorophenol-indophenol, and 10 μM xanthine or inhibitor. The reaction was initiated by the addition of xanthine oxidase (0.008 units/mL) to the reaction mixture and the absorbance change was monitored at 605 nm.

Molecular docking

The docking simulation was performed to analyze the probable binding mode of inhibitors at the active site of xanthine oxidase by using a modified version of AutoDock 4.2 [25]. The inhibitors were docked into the active site of xanthine oxidase using chain C (PDB code 3B9J) [30]. Before the docking calculations, other chains, ligand (2-hydroxy-6-methylpurine), and water molecules, with the exception of important for catalytic mechanism HOH1365 [31], were removed from the initial structure of the enzyme. The oxygen atom of the molybdopterin cofactor was replaced on a water molecule HOH1334. The structures of inhibitors were converted into three-dimensional ones and optimized in the MMFF94s force field by using program Avogadro [32]. AutoDock Tool (MGLTools 1.5.6) was used to prepare the docking files. The constraint position for the C_8 atom of the purine fragment was added to docking parameter files using the ATPOSCONSTR keyword [25]. A ligand's atom number from PDBQT file and its constrained coordinates (-57.055, -18.200 and 19.928 for x, y, and z, respectively) were included in this parameter with a maximal allowed distance of 3 Å. The Lamarckian genetic algorithm was applied to search for the optimum binding pose of the ligands [33]. The analysis of the binding mode of the inhibitors was performed using Discovery Studio 3.5 visualizer.

Notes

Acknowledgments and finances. The work was financed by the National Academy of Sciences of Ukraine (project CPDF 1-17).

The authors declare no conflict of interest.

Author contributions. **O. V. M**: the investigation of bioactivity, writing. **O. L. K**: molecular docking simulations, analysis of the experimental results, writing. **O. V. S**: synthesis of compounds, writing experimental section. **V. S. B**: synthesis of compounds, conceptualization. **A. I. V**: conceptualization, writing, and editing.

References

1. Legraverend, M.; Grierson, D. S. The Purines: Potent and Versatile Small Molecule Inhibitors and Modulators of Key Biological Targets. *Bioorg. Med. Chem.* **2006**, *14*, 3987-4006.
2. Noguchi-Yachide, T.; Sakai, T.; Hashimoto, Y.; Yamaguchi, T. Discovery and structure-activity relationship studies of N6-benzoyladenine derivatives as novel BRD4 inhibitors. *Bioorg. Med. Chem.* **2015**, *23*, 953-959.
3. Amemiya, S.; Yamaguchi, T.; Sakai, T.; Hashimoto, Y.; Noguchi-Yachide, T. Structure-Activity Relationship Study of N6-Benzoyladenine-Type BRD4 Inhibitors and Their Effects on Cell Differentiation and TNF-α Production. *Chem. Pharm. Bull. (Tokyo)* **2016**, *64*, 1378-1383.
4. Marton, Z.; Guillon, R.; Krimm, I.; Rahimova, R.; Egron, D.; Jordheim, L. P.; Aghajari, N.; Dumontet, C.; Périgaud, C.; Lionne, C.; Peyrottes, S.; Chaloin, L. Identification of Noncompetitive Inhibitors of Cytosolic 5′-Nucleotidase II Using a Fragment-Based Approach. *J. Med. Chem.* **2015**, *58*, 9680-9696.
5. Tamta, H.; Thilagavathi, R.; Chakraborti, A. K.; Mukhopadhyay, A. K. 6-(*N*-benzoylamino)purine as a novel and potent inhibitor of xanthine oxidase: Inhibition mechanism and molecular modeling studies. *J. Enzyme. Inhib. Med. Chem.* **2005**, *20*, 317-324.
6. Brondino, C. D.; Romão, M. J.; Moura, I.; Moura, J. J. Molybdenum and tungsten enzymes: the xanthine oxidase family. *Curr. Opin. Chem. Biol.* **2006**, *10*, 109-114.
7. Nagamatsu, T.; Yamasaki, H.; Fujita, T.; Endo, K.; Machida, H. Novel xanthine oxidase inhibitor studies. Part 2. Synthesis and xanthine oxidase inhibitory activities of 2-substituted 6-alkyl-idenehydrazine- or 6-arylmethylidenehydrazino-7H-purines and 3- and/or 5-substituted 9H-1,2,4-triazolo[3,4-i] purines. *J. Chem. Soc., Perkin Trans. 1* **1999**, *21*, 3117-3125.
8. Hsieh, J.-F.; Wu, S.-H.; Yang, Y.-L.; Choong, K.-F.; Chen, S.-T. The screening and characterization of 6-aminopurine-based xanthine oxidase inhibitors. *Bioorg. Med. Chem.* **2007**, *15*, 3450-3456.
9. Pacher, P.; Nivorozhkin, A.; Szabó, C. Therapeutic Effects of Xanthine Oxidase Inhibitors: Renaissance Half a Century After the Discovery of Allopurinol. *Pharmacol Rev.* **2006**, *58*, 87-114.
10. Zhang, T.; Lv, Y.; Lei, Y.; Liu, D.; Feng, Y.; Zhao, J.; Chen, S.; Meng, F.; Wang, S. Design, synthesis and biological evaluation of 1-hydroxy-2-phenyl-4-pyridyl-1H-imidazole derivatives as xanthine oxidase inhibitors. *Eur. J. Med. Chem.* **2018**, *146*, 668-677.
11. Li, J.; Wu, F.; Liu, X.; Zou, Y.; Chen, H.; Li, Z.; Zhang, L. Synthesis and bioevaluation of 1-phenyl-pyrazole-4-carboxylic acid derivatives as potent xanthine oxidoreductase inhibitors. *Eur. J. Med. Chem.* **2017**, *140*, 20-30
12. Wang, S.; Yan, J.; Wang, J.; Chen, J.; Zhang, T.; Zhao, Y.; Xue, M. Synthesis of some 5-phenylisoxazole-3-carboxylic acid derivatives as potent xanthine oxidase inhibitors. *Eur. J. Med. Chem.* **2010**, *45*, 2663-2670.
13. Guan, Q.; Cheng, Z.; Ma, X.; Wang, L.; Feng, D.; Cui, Y.; Bao, K.; Wu, L.; Zhang, W. Synthesis and bioevaluation of 2-phenyl-4-methyl-1,3-selenazole-5-carboxylic acids as potent xanthine oxidase inhibitors. *Eur. J. Med. Chem.* **2014**, *85*, 508-516.
14. Xu, X.; Deng, L.; Nie, L.; Chen, Y.; Liu, Y.; Xie, R.; Li, Z. Discovery of 2-phenylthiazole-4-carboxylic acid, a novel and potent scaffold as xanthine oxidase inhibitors. *Bioorg. Med. Chem. Lett.* **2019**, *29*, 525-528.
15. Nishino, T.; Okamoto, K. J. Mechanistic insights into xanthine oxidoreductase from development studies of candidate drugs to treat hyperuricemia and gout. *Biol. Inorg. Chem.* **2015**, *20*, 195-207.
16. Voelker, R. Another Warning for Febuxostat. *JAMA* **2019**, *312*, 1245-1245.
17. Zhu, J.; Mo, J.; Lin, H. Z.; Chen, Y.; Sun, H. P. The recent progress of isoxazole in medicinal chemistry. *Bioorg. Med. Chem.* **2018**, *26*, 3065-3075.
18. Sysak, A.; Obmińska-Mrukowicz, B. Isoxazole ring as a useful scaffold in a search for new therapeutic agents. *Eur. J. Med. Chem.* **2017**, *137*, 292-309.
19. Agrawal, N.; Mishra, P. The synthetic and therapeutic expedition of isoxazole and its analogs. *Med. Chem. Res.* **2018**, *27*, 1309-1344.
20. Kallitsakis, M. G.; Carotti, A.; Catto, M.; Peperidou, A.; Hadjipavlou-Litina, D. J.; Litinas, K. E. Synthesis and Biological Evaluation of Novel Hybrid Molecules Containing Purine, Coumarin and Isoxazoline or Isoxazole Moieties. *Open. Med. Chem. J.* **2017**, *11*, 196-211.
21. Tourteau, A.; Andrzejak, V.; Body-Malapel, M.; Lemaire, L.; Lemoine, A.; Mansouri, R.; Djouina, M.; Renault, N.; El Bakali, J.;

Desreumaux, P.; Muccioli, G. G.; Lambert, D. M.; Chavatte, P.; Rigo, B.; Leleu-Chavain, N.; Millet, R. 3-Carboxamido-5-aryl-isoxazoles as New CB2 Agonists for the Treatment of Colitis. *Bioorg. Med. Chem.* **2013**, *21*, 5383-5394.

22. Marvel, C. S.; Dreger, E. E. In *Organic Syntheses Collect*; Blatt, A. H., Ed.; Wiley: New York, NY, 1941; Vol. 1, p 238.
23. Andrzejak, V.; Millet, R.; El Bakali, J.; Guelzim, A.; Gluszok, S.; Chavatte, P.; Bonte, J. P.; Vaccher, C.; Lipka, E. Synthesis of 2,3 and 4,5-Dihydro-hydroxy-isoxazoles and Isoxazoles Under Different pH Conditions. *Lett. Org. Chem.* **2010**, *7*, 32-38.
24. Muzychka, O. V.; Kobzar, O. L.; Popova, A. V.; Frasinyuk, M. S.; Vovk, A. I. Carboxylated aurone derivatives as potent inhibitors of xanthine oxidase. *Bioorg. Med. Chem.* **2017**, *25*, 3606-3613.
25. Tanchuk, V. Yu.; Tanin, V. O.; Vovk A. I. *Multithreaded version of AutoDock 4.2 suitable for massive virtual screening of potential biologically active compounds (enzyme inhibitors)*, Third International Conference "High Performance Computing" HPC-UA 2013, Kyiv, Ukraine, **2013**, 399-401.
26. Pauff, J. M.; Cao, H.; Hille, R. J. Substrate Orientation and Catalysis at the Molybdenum Site in Xanthine Oxidase CRYSTAL STRUCTURES IN COMPLEX WITH XANTHINE AND LUMAZINE. *Biol. Chem.* **2009**, *284*, 8760-8767.
27. Cao, H.; Pauff, J. M.; Hille, R. Substrate Orientation and Catalytic Specificity in the Action of Xanthine Oxidase: The Sequential Hydroxylation of Hypoxanthine to Uric Acid. *J. Biol. Chem.* **2010**, *285*, 28044-28053.
28. Okamoto, K.; Matsumoto, K.; Hille, R.; Eger, B. T.; Pai, E. F.; Nishino, T. The crystal structure of xanthine oxidoreductase during catalysis: Implications for reaction mechanism and enzyme inhibition. *Proc. Natl. Acad. Sci. U. S. A.* **2004**, *101*, 7931-7936.
29. Arnold, L.; Pressova, M.; Saman, D.; Vogtherr, M.; Limmer, S. Preparation of 1'-C Deuterated Synthons for RNA Synthesis by H-Phosphonate Method Aiming at Two-Dimensional NMR Secondary Structure Studies. *Collect. Czech. Chem. Commun.* **1996**, *61*, 389-403.
30. Pauff, J. M.; Zhang, J.; Bell, C. E.; Hille, R. Substrate Orientation in Xanthine Oxidase: Crystal Structure of Enzyme in Reaction With 2-hydroxy-6-methylpurine. *J. Biol. Chem.* **2008**, *283*, 4818-4824.
31. Huber, R.; Hof, P.; Duarte, R. O.; Moura, J. J.; Moura, I.; Liu, M. Y.; LeGall, J.; Hille, R.; Archer, M.; Romão, M. J. A structure-based catalytic mechanism for the xanthine oxidase family of molybdenum enzymes. *Proc. Natl. Acad. Sci. U. S. A.* **1996**, *93*, 8846-8851.
32. Hanwell, M. D.; Curtis, D. E.; Lonie, D. C.; Vandermeersch, T.; Zurek, E.; Hutchison, G. R. Avogadro: an advanced semantic chemical editor, visualization, and analysis platform. *J. Cheminform.* **2012**, *4*, 1-17.
33. Morris, G. M.; Goodsell, D. S.; Halliday, R. S.; Huey, R.; Hart, W. E.; Belew, R. K.; Olson, A. J. Automated Docking Using a Lamarckian Genetic Algorithm and Empirical Binding Free Energy Function. *J. Comput. Chem.* **1998**, *19*, 1639-1662.

5-Заміщені *N*-(9*H*-пурин-6-іл)-1,2-оксазол-3-карбоксаміди як інгібітори ксантиноксидази

О. В. Музичка, О. Л. Кобзар, О. В. Шабликін, В. С. Броварець, А. І. Вовк*

Інститут біоорганічної хімії та нафтохімії ім. В.П. Кухаря НАН України, вул. Мурманська, 1, Київ, 02094, Україна

Резюме: У цій роботі нами синтезовано серію похідних *N*-(9*H*-пурин-6-іл)-1,2-оксазол-3-карбоксаміду та оцінено їх інгібувальну здатність щодо ксантиноксидази, ферменту пуринового катаболізму. Синтез 5-заміщених ізоксазолкарбонових кислот здійснено за допомогою відомих синтетичних методів. Для ацилювання аденіну використовували відповідні ацилхлориди, отримані реакцією ізоксазолкарбонових кислот з тіонілхлоридом. За результатами досліджень *in vitro* наявність фенільного замісника в положенні 5 оксазольного кільця підвищує ефективність інгібування ксантиноксидази. Подальше зростання інгібувального впливу спостерігалося при введенні метильної або метокси-групи в *пара*-положення фенільного кільця. Деякі з інгібіторів, що містять 5-заміщені ізоксазолові та пуринові фрагменти, характеризувались наномолярними значеннями IC_{50}. Згідно кінетичних даних, найбільш активний *N*-(9*H*-пурин-6-іл)-5-(5,6,7,8-тетрагідронафтален-2-іл)-1,2-оксазол-3-карбоксамід демонстрував конкурентний тип інгібування щодо субстрату з константою інгібування 7,46 ± 0,36 нМ. Для з'ясування механізму формування комплексу фермент-інгібітор було проведено молекулярний докінг. Результати моделювання показали, що *N*-7-таутомерна форма інгібітора може забезпечувати формування водневих зв'язків, гідрофобних і Ван-дер-Ваальсових контактів та донорно-акцепторних взаємодій. Отримані результати вказують на те, що ксантиноксидаза може бути однією з можливих мішеней для біоактивних карбоксамідних похідних пурину.

Ключові слова: *N*-(9H-пурин-6-іл)-1,2-оксазол-3-карбоксаміди, синтез, біоактивність, ксантиноксидаза.

ISSN 1814-9758. Ukr. Bioorg. Acta, 2020, Vol. 15, N 1
UDC 547.756 + 547.812 + 547.816.8
DOI: hpps://doi.org/10.15407/bioorganica2020.01.026

Ukrainica Bioorganica Acta
www.bioorganica.org.ua

UBA

RESEARCH ARTICLE

Three-component cyclization as an approach to a combinatorial library of 2*H*-spiro-[chromeno[2,3-*c*]pyrrole-1,3'-indoline]-2',3,9-triones

Roman N. Vydzhak[1], Maryna V. Kachaeva[1], Stepan G. Pilyo[1], Viktoriia S. Moskvina[1,2]*, Olga V. Shablykina[1,2], Andriy V. Kozytskiy[3,4] and Volodymyr S. Brovarets[1]

[1] *V. P. Kukhar Institute of Bioorganic Chemistry and Petrochemistry of the NAS of Ukraine, 1 Murmanska St., Kyiv, 02094, Ukraine*
[2] *Taras Shevchenko National University of Kyiv, 60 Volodymyrska St., Kyiv, 01601, Ukraine*
[3] *L. V. Pisarzhevskii Institute of Physical Chemistry of the NAS of Ukraine, 31 Nauky Ave., Kyiv, 03028, Ukraine*
[4] *Enamine Ltd. (www.enamine.net), 78 Chervonotkatska St., Kyiv, 02094, Ukraine*

Abstract: A versatile and efficient three-component cyclization of methyl 4-(o-hydroxyphenyl)-2,4-dioxobutanoates **1**, N-substituted isatins **2,** and primary amines **3** was explored to synthesize of 2H-spiro[chromeno[2,3-c]pyrrole-1,3'-indoline]-2',3,9-triones. We obtained a library of 122 derivatives with an indolin-2-one motif as an important structural fragment in natural alkaloids. This method is a practical and useful strategy for constructing dihydrochromeno[2,3-c]pyrrole-3,9-diones. Most of the obtained products also have functional groups for easy and further diversification by classical reactions.

Keywords: isatin, multicomponent reactions, chromenes, combinatorial library.

Introduction

The synthesis of privileged heterocyclic compounds has become one of the prime areas of research in the field of synthetic and medicinal chemistry as most of the compounds with biological activity are derived from heterocyclic structures [1, 2].

Natural products are important privileged scaffolds that serve as important, biologically pre-validated platforms for the design of compound libraries in the search for new drug candidates [3]. The structural motif of indolin-2-ones is an important scaffold for medicinal chemistry and can be found in many naturally occurring compounds related to indole alkaloids [4]. Spirocyclic indolenines have significant therapeutic potential, and these structural motifs are present in a number of biologically active natural products. Examples of such spiro[indoline-3,2'-pyrroles] are Horsfiline [5], Coerulescine [6], and Elacomine [7] as well as polyfused Spirotryptostatin A [8] and Strychnofoline [9] (Figure 1).

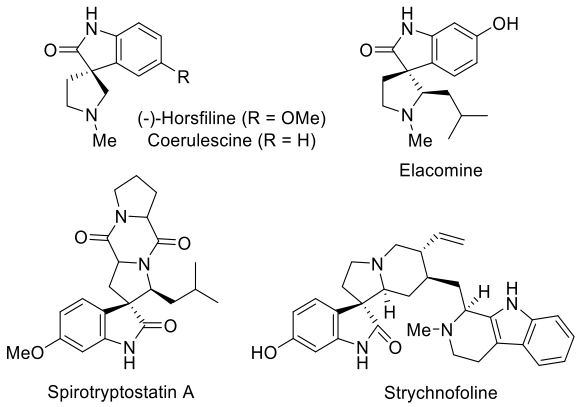

Figure 1. Examples of natural compounds with indolin-2-one motif.

Received: 27.04.2020
Revised: 11.05.2020
Accepted: 16.05.2020
Published online: 30.06.2020

* Corresponding author. Tel.: +380-44-239-3342;
e-mail: v.moskvina@gmail.com (V. S. Moskvina)
ORCID: 0000-0001-5556-9147

The most numerous representatives of polyfused indolin-2-ones are spiro[indoline-3,6'-pyrano[3,4-f]indolizins]. The members of this group differ mostly in the configuration of specific asymmetric centers (like alkaloids Mitraphylline, Formosanine, and Pteropodine, Figure 2) and the presence of substituents in the benzol ring (e.g., mono- and dimethoxy derivativs – Vinerine and Elegantissine (Herboxine) [10].

According to the literature, spiro[indoline-3,6'-pyrano-[3,4-*f*]indolizin] alkaloids are widely represented in plants that have long been used in traditional medicine [11, 12]. It is not surprising therefore that according to the recent data, these and similar structures can find practical use in medicine. For example, Pteropodine has manifested antigenotoxic, antioxidant and lymphocyte induction effects [13], while Mitraphylline has shown anti-inflammatory activity [14]. Several synthetic spiroheterocycles containing both indole and pyran heterocycles possess anticonvulsant and analgesic [15], antimicrobial [16], and herbicidal activities [17].

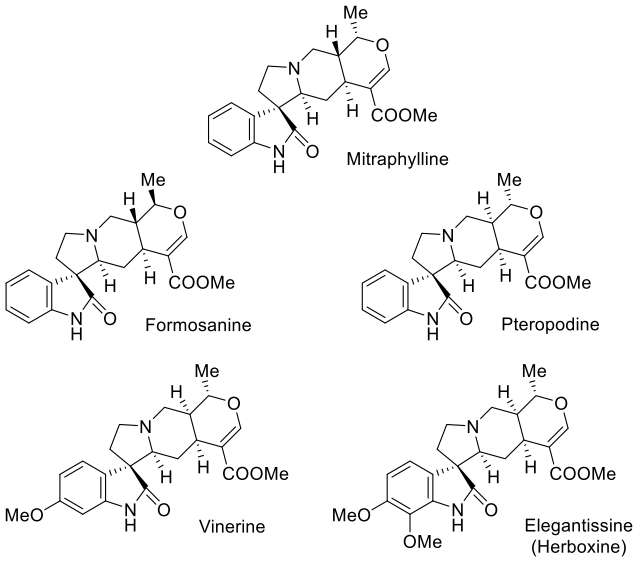

Figure 2. Examples of natural spiro[indoline-3,6'-pyrano[3,4-*f*]-indolizin] alkaloids.

In most cases, the synthesis of these compounds is a challenging task comprising of multiple synthetic steps [18]. One of the main goals of modern synthetic organic chemistry is the rapid construction of target drug-like compound libraries, characterized by several important features, for example, the complexity and variety of molecules, high variability, and easy access from relatively simple and commercially available reagents.

Results and Discussion

In our previous works, several examples of 1,2-dihydrochromeno[2,3-*c*]pyrrole-3,9-diones were obtained in a three-component condensation of methyl 4-(*o*-hydroxy-phenyl)-2,4-dioxobutanoate with aromatic aldehydes and heterocyclic amines [19] or aromatic amines [20], aliphatic amines [21] (Scheme 1). Alternative routes to the synthesis of 2-phenyl-5,6-dihydropyrano[2,3-c]pyrrole-4,7-diones [22] and 1-aryl-2-[2-(dimethylamino)ethyl]-1,2-dihydro-chromeno[2,3-c]pyrrole-3,9-diones [23] were also developed.

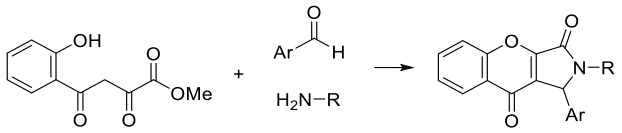

Scheme 1. Synthesis of 1,2-dihydrochromeno[2,3-*c*]pyrrole-3,9-diones (previous work).

Only two examples of 1,2-dihydrochromeno[2,3-*c*]pyrrole-3,9-dione spiro derivatives were obtained in our previous research when *N*-methylisatin was used as the carbonyl component [24].

The goal of the present research was to study a one-pot three-component condensation of methyl 4-(*o*-hydroxy-phenyl)-2,4-dioxobutanoate, *N*-substituted isatins, and primary amines, as well as the applicability of this reaction in the combinatorial synthesis. The utility and scope of this method were tested on a wide range of commercially available substrates.

The substrate scope in this condensation was subsequently explored by employing various methyl 4-(*o*-hydroxyphenyl)-2,4-dioxobutanoates **1**{*1-5*} (5 examples) with *N*-substituted isatins **2**{*1-8*} (8 examples), and primary amines **3**{*1-24*} (24 examples) (Scheme 2). The representative substrates – methyl 4-(*o*-hydroxyphenyl)-2,4-dioxobutanoates (**1**{*1-5*}), *N*-substituted isatins **2**{*1-8*}, and primary amines **3**{*1-24*} are listed in Figure 3.

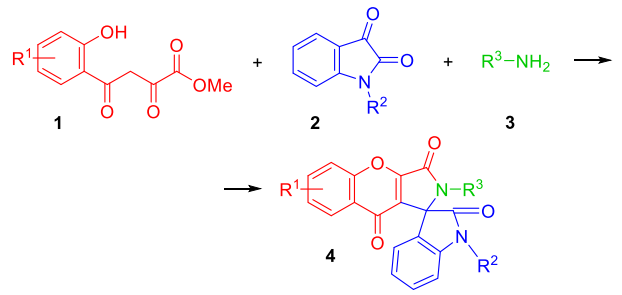

Scheme 2. The 1-aryl-1,2-dihydrochromeno[2,3-*c*]pyrrole-3,9-dione **4** library generation.

First, the compatibility of different *N*-substituted isatins and primary amines in the present transformation was examined. To our delight, a wide range of alkyl groups in the case of *N*-substituted isatins, including methyl, ethyl, propyl, butyl, allyl, and benzyl, were well compatible in this transformation. It should be mentioned that the substituted primary amines were also suitable for the transformation, and synthesis of 2*H*-spiro[chromeno[2,3-*c*]pyrrole-1,3'-indoline]-2',3,9-triones was conducted in MeOH (for **3**{*1-10, 13-15, 24*}), EtOH (for **3**{*11*}), *i*-PrOH (for **3**{*12*}) at 35-40 °C, or acetic acid (for **3**{*16-23*}) under reflux. Methyl 4-(*o*-hydroxyphenyl)-2,4-dioxobutanoates with methyl, chloro, and fluoro substituents were also tolerated in this one-pot three-component procedure. As the

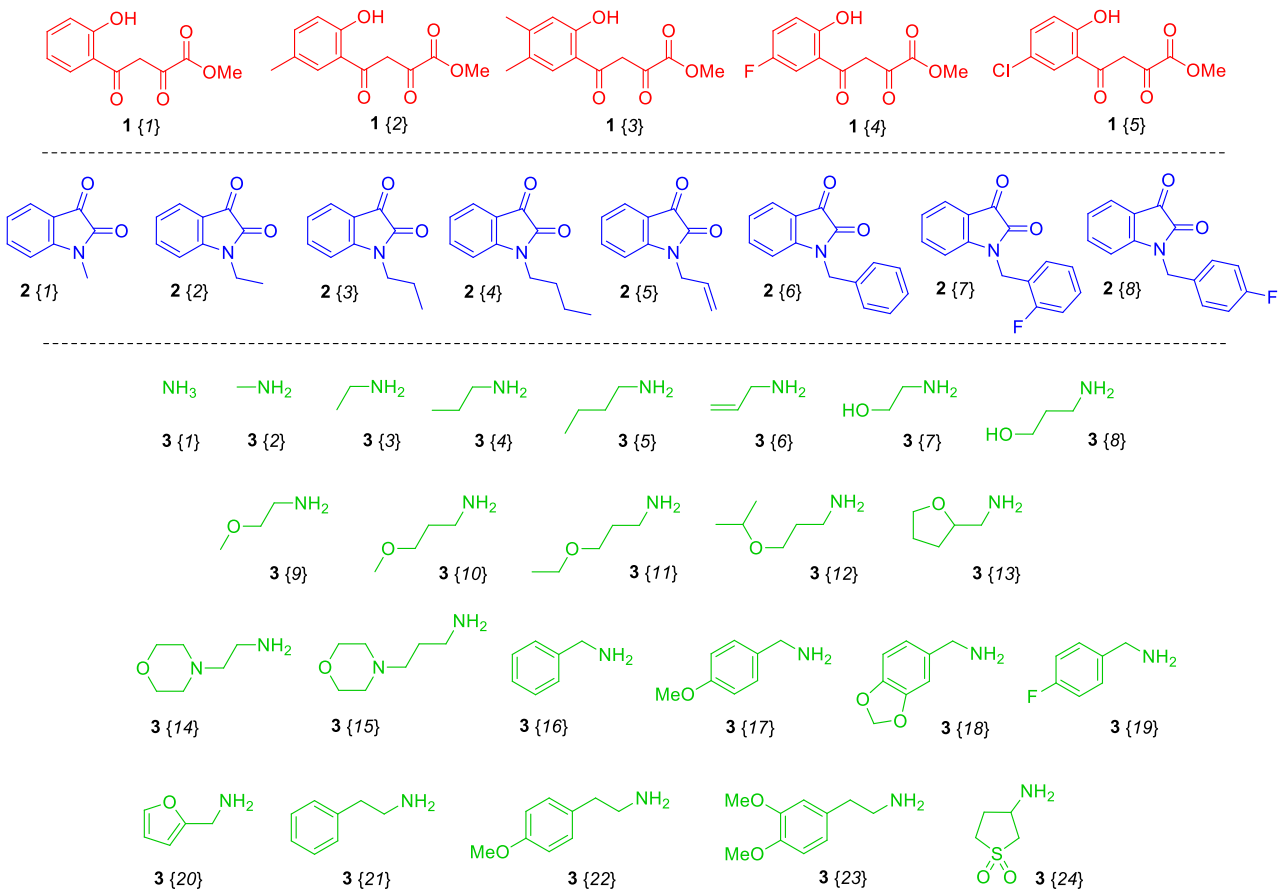

Figure 3. Scope of 4-(2-hydroxyphenyl)-2,4-dioxobutanoates **1**{*1-5*}, isatins **2**{*1-13*} and primary amines **3**{*1-24*}.

result, spiro[chromeno[2,3-*c*]pyrrole-1,3'-indoline]-2',3,9-triones (87% success rate) with good purity (> 95% according MS) (Table 1). In most cases, the yields were in the range of 48-81%, and for more than 50% of the representative set, the yield was over 70%.

^{1}H NMR spectra of products **4** corresponded to the proposed structures. However, because the skeleton of the molecules is complex, ^{13}C NMR spectra were also measured to prove the structure of the compounds, and for several compounds, COSY, HMBS, and HSQC experiments were performed.

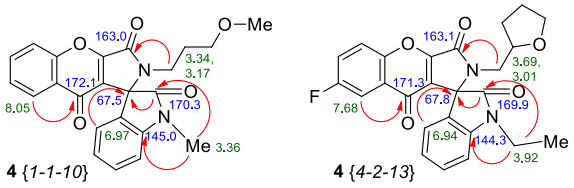

Figure 4. Important HMBC correlations for **4**{*1-1-10*} and **4**{*4-2-13*}.

In ^{13}C NMR spectra of library members **4**{*1-1-10*} and **4**{*4-2-13*}, signals at 163.0-163.1 ppm are attributed to the C-3 atom, signals at 171.3 and 172.1 ppm are attributed to the C-9 atom and signals at 169.9-170.3 ppm are attributed to the C-2' atom. Carbon atom at 67.5, and 67.8 ppm assigned to spirocarbon of pyrrole-1,3'-indoline moiety. Figure 4 shows the assignments and the most important HMBC correlations for **4**{*1-1-10*} and **4**{*4-2-13*} between signals in the ^{13}C NMR spectra (blue) and ^{1}H NMR spectra (green) upon which the assignments were based (red arrow).

The IR spectra of products **4** contain fairly intense absorption bands of carbonyl groups at 1735-1715 cm^{-1} and 1670-1660 cm^{-1}, as well as rather an intensive absorption of the unsaturated fragments conjugated with them, at approximately 1610 cm^{-1}.

Conclusions

In conclusion, we have developed an efficient protocol for the rapid synthesis of 2*H*-spiro[chromeno[2,3-*c*]pyrrole-1,3'-indoline]-2',3,9-triones using *N*-substituted isatins and primary amines in a one-pot three-component cyclo-condensation. This protocol was found to be compatible with a wide range of substituents and paves the way for the practical synthesis of 2*H*-spiro[chromeno[2,3-*c*]pyrrole-1,3'-indoline]-2',3,9-triones with a broad range of substituents under mild conditions.

Table 1. Scope of the products **4**.

4{*1-1-1*}	**4**{*1-1-21*}[a]	**4**{*1-3-5*}	**4**{*1-5-8*}	**4**{*2-1-13*}	**4**{*2-7-10*}	**4**{*3-1-13*}	**4**{*3-5-10*}	**4**{*4-5-9*}
4{*1-1-3*}	**4**{*1-1-22*}	**4**{*1-3-7*}	**4**{*1-5-9*}	**4**{*2-2-13*}	**4**{*2-7-12*}[a]	**4**{*3-2-9*}[a]	**4**{*3-5-12*}	**4**{*4-5-10*}
4{*1-1-4*}	**4**{*1-1-23*}	**4**{*1-3-8*}[a]	**4**{*1-5-10*}	**4**{*2-3-7*}	**4**{*2-7-13*}	**4**{*3-2-10*}	**4**{*3-5-13*}[a]	**4**{*4-5-12*}[a]
4{*1-1-5*}	**4**{*1-2-4*}	**4**{*1-3-9*}	**4**{*1-5-11*}	**4**{*2-3-10*}[a]	**4**{*2-7-17*}	**4**{*3-2-12*}	**4**{*4-1-5*}	**4**{*4-5-21*}
4{*1-1-6*}	**4**{*1-2-5*}	**4**{*1-3-10*}	**4**{*1-5-12*}	**4**{*2-3-9*}	**4**{*2-7-18*}[a]	**4**{*3-2-13*}	**4**{*4-1-10*}	**4**{*5-1-21*}[a]
4{*1-1-7*}	**4**{*1-2-7*}	**4**{*1-3-13*}	**4**{*1-5-13*}	**4**{*2-3-13*}	**4**{*2-7-19*}	**4**{*3-3-7*}[a]	**4**{*4-1-12*}	**4**{*5-2-5*}
4{*1-1-8*}	**4**{*1-2-8*}	**4**{*1-3-11*}	**4**{*1-5-17*}	**4**{*2-3-17*}	**4**{*2-7-20*}[a]	**4**{*3-3-9*}	**4**{*4-2-10*}	**4**{*5-3-17*}[a]
4{*1-1-9*}	**4**{*1-2-9*}	**4**{*1-3-12*}	**4**{*1-6-4*}[a]	**4**{*2-5-7*}	**4**{*2-7-21*}	**4**{*3-3-10*}	**4**{*4-2-12*}	**4**{*5-5-5*}[a]
4{*1-1-10*}[a]	**4**{*1-2-10*}	**4**{*1-3-24*}[a]	**4**{*1-6-11*}	**4**{*2-5-8*}	**4**{*2-7-22*}	**4**{*3-3-12*}	**4**{*4-2-13*}[a]	**4**{*5-5-7*}
4{*1-1-11*}	**4**{*1-2-11*}	**4**{*1-4-11*}	**4**{*1-6-17*}	**4**{*2-5-9*}	**4**{*3-1-7*}	**4**{*3-3-13*}	**4**{*4-3-10*}	**4**{*5-5-19*}
4{*1-1-12*}	**4**{*1-2-12*}	**4**{*1-4-24*}[a]	**4**{*2-1-7*}	**4**{*2-5-10*}	**4**{*3-1-8*}	**4**{*3-3-21*}	**4**{*4-3-12*}	**4**{*5-5-23*}
4{*1-1-13*}	**4**{*1-2-13*}	**4**{*1-5-2*}	**4**{*2-1-8*}	**4**{*2-5-12*}	**4**{*3-1-9*}	**4**{*3-5-8*}	**4**{*4-3-13*}	**4**{*5-6-6*}[a]
4{*1-1-14*}	**4**{*1-2-22*}[a]	**4**{*1-5-5*}	**4**{*2-1-10*}	**4**{*2-5-13*}[a]	**4**{*3-1-10*}[a]	**4**{*3-5-9*}	**4**{*4-3-16*}[a]	**4**{*5-8-10*}[a]
4{*1-1-15*}	**4**{*1-3-4*}	**4**{*1-5-7*}[a]	**4**{*2-1-12*}	**4**{*2-7-9*}				

[a] The method of the synthesis, physicochemical properties, NMR and LCMS spectra are described in the experimental section.

Experimental section

The solvents were purified according to the standard procedures. All starting materials such as substituted methyl 4-(*o*-hydroxyphenyl)-2,4-dioxobutanoates, *N*-substituted isatins, and primary amines were obtained from Enamine, Ltd. All materials were purchased from commercial sources and used without further purification. The success rate was calculated as the number of successful experiments divided by the total number of experiments. ^{1}H NMR spectra were recorded on a Varian VXR-300 spectrometer (300 MHz) or Bruker 170 spectrometer (500 MHz) and ^{13}C NMR spectra were recorded at Bruker 170 spectrometer (125 MHz) spectra in DMSO-d_6 or CF_3CO_2D or $CDCl_3$ solution. Chemical shifts are reported in ppm downfield from TMS as internal standards. Mass spectra were recorded on an LC-MS instrument with chemical ionization (CI). LC-MS data were acquired on an Agilent 1200 HPLC system equipped with DAD/ELSD/LCMS-6120 diode matrix and mass-selective detector. Melting points were measured on a MPA100 OptiMelt automated melting point system. Elemental analyses were performed at the Laboratory of Organic Analysis, Department of Chemistry, Taras Shevchenko National University of Kyiv.

The Experimental Section describes 25 compounds selected in a random manner, which corresponds to generally accepted approaches in combinatorial chemistry (according to ACS standards).

*A representative procedure for the synthesis of 1'-methyl-2-phenethyl-2H-spiro[chromeno[2,3-c]pyrrole-1,3'-indoline]-2',3,9-trione (**4**{1-1-21}).*

To a suspension of 0.01 mol of *N*-methylisatin **2**{*1*} in 15 mL of glacial acetic acid, 0.01 mol of 2-phenylethylamine **3**{*21*} and 0.01 mol of methyl-*o*-hydroxybenzoylpyruvate **1**{*1*} were added. The reaction mixture was refluxed for 1 h, cooled, and evaporated. The residues were purified by crystallization from ethanol. Yield: 335 mg, 77%. ^{1}H NMR (500 MHz, DMSO-d_6) δ 7.98 (d, *J* 7.5 Hz, 1H), 7.92-7.82 (m, 2H), 7.56-7.44 (m, 2H), 7.27-7.10 (m, 5H), 7.07-6.96 (m, 3H), 3.35 (s, 3H), 3.33-3.23 (m, 2H), 2.68 (t, *J* 7.3 Hz, 2H). IR (KBr) ν 3063, 3020, 2934, 1729 (vs), 1715 (vs), 1664 (vs), 1611, 1495, 1457, 1385, 1369, 1341, 1283, 1199, 1184, 1128, 1105, 1085, 938, 888, 751, 699, 690. MS (CI) m/z $(M+H)^+$ 437.

*2-(3-Methoxypropyl)-1'-methyl-2H-spiro[chromeno-[2,3-c]pyrrole-1,3'-indoline]-2',3,9-trione (**4**{1-1-10}).*

Yield: 310 mg, 77%. ^{1}H NMR (500 MHz, DMSO-d_6) δ 7.97 (d, *J* 7.9 Hz, 1H), 7.94-7.83 (m, 2H), 7.54 (t, *J* 6.6 Hz, 1H), 7.47 (t, *J* 7.7 Hz, 1H), 7.25 (t, *J* 6.6 Hz, 2H), 7.07 (t, *J* 7.5 Hz, 1H), 3.32 (s, 3H), 3.29-3.00 (m, 7H), 1.66-1.45 (m, 2H). ^{13}C NMR (125 MHz, $CDCl_3$) δ 172.1, 170.3, 163.0, 156.5, 155.7, 145.0, 134.7, 131.3, 126.2, 125.9, 125.9, 125.4, 123.9, 123.6, 121.7, 119.2, 109.6, 69.7, 67.5, 58.4, 39.2, 28.0, 27.3. IR (KBr) ν 2976, 2931, 2894, 2832, 2808, 1735 (vs), 1712 (vs), 1665 (vs), 1611, 1463, 1374, 1304, 1279, 1200, 1106, 943, 873, 755, 692. MS (CI) m/z $(M+H)^+$ 405.

*1'-Ethyl-2-(4-methoxyphenethyl)-2H-spiro[chromeno-[2,3-c]pyrrole-1,3'-indoline]-2',3,9-trione (**4**{1-2-22}).*

Yield: 360 mg, 75%. ^{1}H NMR (500 MHz, DMSO-d_6) δ 7.99 (d, *J* 7.9 Hz, 1H), 7.95-7.83 (m, 2H), 7.59-7.51 (m, 1H), 7.47 (t, *J* 7.6 Hz, 1H), 7.30 (d, *J* 7.8 Hz, 1H), 7.18 (d, *J* 7.3 Hz, 1H), 7.03 (t, *J* 7.4 Hz, 1H), 6.89 (d, *J* 8.5 Hz, 2H), 6.74 (d, *J* 8.5 Hz, 2H), 3.90 (q, *J* 6.7 Hz, 2H), 3.69 (s, 3H), 3.35-3.09 (m, 2H), 2.59 (t, *J* 7.9 Hz, 2H), 1.31 (t, *J* 7.0 Hz, 3H). IR (KBr) ν 3073, 3046, 2976, 2932, 2840, 1727 (vs), 1664, 1610, 1513, 1492, 1463, 1365, 1307, 1284, 1245, 1187, 1134, 1026, 884, 833, 757, 688. MS (CI) m/z $(M+H)^+$ 480.

*2-(3-Hydroxypropyl)-1'-propyl-2H-spiro[chromeno[2,3-c]-pyrrole-1,3'-indoline]-2',3,9-trione (**4**{1-3-8}).*

Yield: 305 mg, 73%. ^{1}H NMR (500 MHz, DMSO-d_6) δ 7.98 (d, *J* 7.8 Hz, 1H), 7.95-7.83 (m, 2H), 7.59-7.49 (m, 1H), 7.44 (t, *J* 7.7 Hz, 1H), 7.30-7.19 (m, 2H), 7.05 (t, *J* 7.5 Hz, 1H), 4.30 (br s, 1H), 3.86-3.68 (m, 2H), 3.35-2.99 (m, 4H), 1.75 (m, 2H), 1.55-1.38 (m, 2H), 1.00 (t, *J* 7.4 Hz, 3H). IR (KBr) *v* 3512 (vs, br), 3063, 2955, 2934, 2877, 1728 (vs), 1664 (vs), 1610, 1490, 1462, 1361, 1312, 1284, 1191, 1135, 1107, 1069, 942, 871, 759, 690. MS (CI) m/z $(M+H)^+$ 419.

*2-(1,1-Dioxidotetrahydrothiophen-3-yl)-1'-propyl-2H-spiro[chromeno[2,3-c]pyrrole-1,3'-indoline]-2',3,9-trione (**4**{1-3-24}).*

Yield: 349 mg, 73%. ^{1}H NMR (500 MHz, DMSO-d_6) δ 7.97 (d, *J* 7.9 Hz, 1H), 7.94-7.83 (m, 2H), 7.53 (ddd, *J* 8.2, 6.0, 2.3 Hz, 1H), 7.47 (t, *J* 7.8 Hz, 1H), 7.39 (t, *J* 8.2 Hz, 1H), 7.27 (d, *J* 7.9 Hz, 1H), 7.06 (t, *J* 7.5 Hz, 1H), 3.92-3.55 (m, 3.5H), 3.49-3.27 (m, 1.5H), 3.17-2.95 (m, 1.5H), 2.92-2.59 (m, 1.5H), 2.28-2.13 (m, 0.4H), 2.13-1.98 (m, 0.6H), 1.85-1.67 (m, 2H), 1.00 (t, *J* 7.3 Hz, 3H). IR (KBr) *v* 3069, 3036, 2963, 2942, 2875, 1732 (vs), 1718 (vs), 1666 (vs), 1610, 1486, 1463, 1414, 1349, 1320, 1287, 1215, 1192, 1127, 1089, 940, 875, 757, 688, 654, 572. MS (CI) m/z $(M+H)^+$ 479.

*1'-Butyl-2-(1,1-dioxidotetrahydrothiophen-3-yl)-2H-spiro[chromeno[2,3-c]pyrrole-1,3'-indoline]-2',3,9-trione (**4**{1-4-24}).*

Yield: 373 mg, 76%. ^{1}H NMR (500 MHz, DMSO-d_6) δ 7.98 (d, *J* 8.0 Hz, 1H), 7.94-7.83 (m, 2H), 7.54 (ddd, *J* 8.1, 5.8, 2.4 Hz, 1H), 7.47 (t, *J* 7.7 Hz, 1H), 7.43-7.35 (m, 1H), 7.25 (d, *J* 7.9 Hz, 1H), 7.06 (t, *J* 7.5 Hz, 1H), 3.95-3.55 (m, 3.5H), 3.50-3.25 (m, 1.5H), 3.18-2.94 (m, 1.5H), 2.89-2.59 (m, 1.5H), 2.27-2.13 (m, 0.5H), 2.11-1.97 (m, 0.5H), 1.78-1.64 (m, 2H), 1.51-1.35 (m, 2H), 0.97 (t, *J* 7.3 Hz, 3H). IR (KBr) *v* 3100, 3069, 3038, 3020, 2961, 2936, 2875, 1732 (vs), 1667 (vs), 1610, 1488, 1464, 1411, 1351, 1322, 1306, 1288, 1189, 1126, 1106, 1089, 942, 756, 690, 573. MS (CI) m/z $(M+H)^+$ 493.

*1'-Allyl-2-(2-hydroxyethyl)-2H-spiro[chromeno[2,3-c]-pyrrole-1,3'-indoline]-2',3,9-trione (**4**{1-5-7}).*

Yield: 309 mg, 77%. ^{1}H NMR (500 MHz, DMSO-d_6) δ 8.00 (d, *J* 7.8 Hz, 1H), 7.98-7.90 (m, 2H), 7.64-7.54 (m, 1H), 7.46 (t, *J* 7.8 Hz, 1H), 7.36 (d, *J* 7.4 Hz, 1H), 7.17 (d, *J* 7.9 Hz, 1H), 7.08 (t, *J* 7.5 Hz, 1H), 6.00-5.87 (m, 1H), 5.49 (d, *J* 17.4 Hz, 1H), 5.25 (d, *J* 10.4 Hz, 1H), 4.76 (br s, 1H), 4.54 (d, *J* 16.9 Hz, 1H), 4.39 (d, *J* 17.1 Hz, 1H), 3.42-3.07 (m, 4H). IR (KBr) *v* 3477 (s, br), 2966, 2932, 2886, 1725 (vs), 1659 (vs), 1610, 1490, 1459, 1361, 1285, 1178, 1055, 933, 888, 756, 691. MS (CI) m/z $(M+H)^+$ 403.

*1'-Benzyl-2-propyl-2H-spiro[chromeno[2,3-c]pyrrole-1,3'-indoline]-2',3,9-trione (**4**{1-6-4}).*

Yield: 336 mg, 75%. ^{1}H NMR (500 MHz, DMSO-d_6) δ 7.98 (d, *J* 7.6 Hz, 1H), 7.94-7.81 (m, 2H), 7.58-7.49 (m, 1H), 7.45 (t, *J* 7.7 Hz, 1H), 7.30-7.19 (m, 2H), 7.05 (t, *J* 7.4 Hz, 1H), 3.94-3.77 (m, 2H), 3.26-3.10 (m, 1H), 2.98 (dt, *J* 14.1, 7.0 Hz, 1H), 1.40-1.21 (m, 2H), 0.77 (t, *J* 7.3 Hz, 3H). IR (KBr) *v* 3095, 3064, 3042, 2963, 2932, 2875, 1720 (vs), 1666 (vs), 1610, 1488, 1467, 1367, 1342, 1286, 1198, 1152, 1135, 1097, 946, 832, 775, 756, 689. MS (CI) m/z $(M+H)^+$ 451.

*2-(3-Methoxypropyl)-7-methyl-1'-propyl-2H-spiro-[chromeno[2,3-c]pyrrole-1,3'-indoline]-2',3,9-trione (**4**{2-3-10}).*

Yield: 343 mg, 77%. ^{1}H NMR (500 MHz, DMSO-d_6) δ 7.78-7.72 (m, 2H), 7.68 (dd, *J* 8.8, 2.0 Hz, 1H), 7.44 (td, *J* 7.8, 1.1 Hz, 1H), 7.28-7.21 (m, 2H), 7.04 (t, *J* 7.4 Hz, 1H), 3.87-3.69 (m, 2H), 3.28-3.15 (m, 3H), 3.15-2.99 (m, 4H), 2.42 (s, 3H), 1.83-1.66 (m, 2H), 1.65-1.47 (m, 2H), 1.00 (t, *J* 7.4 Hz, 3H). IR (KBr) *v* 3055, 3029, 2980, 2942, 2888, 2878, 2827, 2745, 1721 (vs), 1664 (vs), 1611, 1479, 1469, 1367, 1321, 1281, 1204, 1113, 1095, 1027, 945, 926, 909, 886, 825, 796, 749, 689, 658. MS (CI) m/z $(M+H)^+$ 447.

*1'-Allyl-7-methyl-2-((tetrahydrofuran-2-yl)methyl)-2H-spiro[chromeno[2,3-c]pyrrole-1,3'-indoline]-2',3,9-trione (**4**{2-5-13}).*

Yield: 351 mg, 77%. ^{1}H NMR (500 MHz, DMSO-d_6) δ 7.82 (d, *J* 8.4 Hz, 1H), 7.80-7.71 (m, 2H), 7.43 (t, *J* 7.4 Hz, 1H), 7.29 (t, *J* 7.4 Hz, 1H), 7.15-7.02 (m, 2H), 5.98-5.85 (m, 1H), 5.52 (d, *J* 15.6 Hz, 1H), 5.24 (d, *J* 13.4Hz, 1H), 4.52 (br d, *J* 15.0 Hz), 4.36 (m, 1H), 3.70-3.54 (m, 2H), 5.55-3.37 (m, 2H), 3.00 (dd, *J* 14.4, 4.8 Hz, 0.7H), 2.91 (dd, *J* 14.4, 7.5 Hz, 0.3H), 2.42 (s, 3H), 1.82-1.63 (m, 3H), 1.62-1.35 (m, 1H). IR (KBr) *v* 3075, 3057, 3025, 2981, 2965, 2918, 2869, 1729 (vs), 1664 (vs), 1612, 1479, 1467, 1362, 1282, 1191, 1091, 993, 948, 923, 819, 750, 736. MS (CI) m/z $(M+H)^+$ 457.

*1'-(2-Fluorobenzyl)-2-(3-isopropoxypropyl)-7-methyl-2H-spiro[chromeno[2,3-c]pyrrole-1,3'-indoline]-2',3,9-trione (**4**{2-7-12}).*

Yield: 410 mg, 76%. ^{1}H NMR (500 MHz, DMSO-d_6) δ 7.82-7.74 (m, 2H), 7.70 (dd, *J* 8.7, 1.9 Hz, 1H), 7.55 (t, *J* 7.7 Hz, 1H), 7.43-7.32 (m, 2H), 7.29 (d, *J* 6.9 Hz, 1H), 7.26-7.14 (m, 2H), 7.10-7.01 (m, 2H), 5.14 (d, *J* 16.4 Hz, 1H), 5.04 (d, *J* 16.3 Hz, 1H), 3.44-3.02 (m, 5H), 2.45 (s, 3H), 1.56-1.40 (m, 2H), 0.99 (t, *J* 6.3 Hz, 6H). IR (KBr) *v* 3058, 2972, 2932, 2864, 1732 (vs), 1723 (vs), 1662 (vs), 1614, 1491, 1469, 1409, 1360, 1341, 1311, 1284, 1228, 1201, 1172, 1146, 1099, 943, 921, 828, 816, 758, 748, 690. MS (CI) m/z $(M+H)^+$ 541.

*2-(Benzo[d][1,3]dioxol-5-ylmethyl)-1'-(2-fluorobenzyl)-7-methyl-2H-spiro[chromeno[2,3-c]pyrrole-1,3'-indoline]-2',3,9-trione (**4**{2-7-18}).*

Yield: 430 mg, 75%. ^{1}H NMR (500 MHz, DMSO-d_6) δ 7.82-7.74 (m, 2H), 7.70 (dd, *J* 8.7, 1.9 Hz, 1H), 7.47 (t, *J* 7.7 Hz, 1H), 7.40-7.26 (m, 2H), 7.24-7.08 (m, 3H), 6.99-6.86 (m, 2H), 6.59 (d, *J* 7.9 Hz, 1H), 6.48 (d, *J* 1.4 Hz, 1H), 6.32 (dd, *J* 7.9, 1.4 Hz, 1H), 5.92 (s, 2H), 4.92 (d, *J* 16.6 Hz, 1H), 4.78 (d, *J* 16.5 Hz, 1H), 4.42 (d, *J* 15.1 Hz, 1H), 4.13 (d, *J* 15.1 Hz, 1H), 2.43 (s, 3H). IR (KBr) *v* 3098, 3060, 3027, 2926, 2890, 2782, 1722 (vs), 1663 (vs), 1611, 1491, 1467, 1448, 1367, 1308, 1285, 1253, 1228, 1187,

1099, 1042, 946, 823, 771, 754, 687. MS (CI) m/z $(M+H)^+$ 575.

*1'-(2-Fluorobenzyl)-2-(furan-2-ylmethyl)-7-methyl-2H-spiro[chromeno[2,3-c]pyrrole-1,3'-indoline]-2',3,9-trione (**4**{2-7-20}).*

Yield: 390 mg, 75%. ^{1}H NMR (500 MHz, DMSO-d_6) δ 7.78 (d, *J* 8.5 Hz, 2H), 7.71 (dd, *J* 8.7, 2.0 Hz, 1H), 7.55 (t, *J* 7.2 Hz, 1H), 7.41-7.27 (m, 3H), 7.28-7.13 (m, 3H), 6.98 (t, *J* 7.5 Hz, 1H), 6.92 (d, *J* 7.9 Hz, 1H), 6.17 (dd, *J* 3.0, 1.9 Hz, 1H), 5.87 (d, *J* 3.1 Hz, 1H), 4.96 (d, *J* 16.7 Hz, 1H), 4.81 (d, *J* 16.6 Hz, 1H), 4.62 (d, *J* 15.8 Hz, 1H), 4.20 (d, *J* 15.8 Hz, 1H), 2.44 (s, 3H). IR (KBr) *v* 3048, 2923, 1730 (vs), 1660 (vs), 1612, 1491, 1472, 1424, 1361, 1288, 1229, 1204, 1182, 1146, 1102, 1080, 1010, 942, 828, 767, 753, 733, 689. MS (CI) m/z $(M+H)^+$ 521.

*2-(3-Methoxypropyl)-1',6,7-trimethyl-2H-spiro[chromeno-[2,3-c]pyrrole-1,3'-indoline]-2',3,9-trione (**4**{3-1-10}).*

Yield: 311 mg, 72%. ^{1}H NMR (500 MHz, DMSO-d_6) δ 7.66 (s, 1H), 7.61 (s, 1H), 7.45 (td, *J* 8.7, 1.1 Hz, 1H), 7.22 (d, *J* 8.5 Hz, 2H), 7.06 (t, *J* 7.9 Hz, 1H), 3.32 (s, 3H), 3.29-3.15 (m, 3H), 3.13 (s, 3H), 3.11-2.98 (m, 1H), 2.40 (s, 3H), 2.31 (s, 3H), 1.67-1.44 (m, 2H). IR (KBr) *v* 3061, 3047, 3029, 2973, 2928, 2876, 2834, 1733 (vs), 1719 (vs), 1662 (vs), 1611, 1467, 1414, 1367, 1350, 1284, 1195, 1133, 1113, 1084, 1020, 942, 754, 690. MS (CI) m/z $(M-H)^-$ 430.

*1'-Ethyl-2-(2-methoxyethyl)-6,7-dimethyl-2H-spiro-[chromeno[2,3-c]pyrrole-1,3'-indoline]-2',3,9-trione (**4**{3-2-9}).*

Yield: 320 mg, 74%. ^{1}H NMR (500 MHz, DMSO-d_6) δ 7.68 (s, 1H), 7.62 (s, 1H), 7.43 (td, *J* 7.8, 1.1 Hz, 1H), 7.21 (d, *J* 7.8 Hz, 1H), 7.18 (d, *J* 6.7 Hz, 1H), 7.03 (t, *J* 7.3 Hz, 1H), 3.98-3.70 (m, 2H), 3.50-3.36 (m, 1H), 3.31-3.09 (m, 6H), 3.03 (s, 3H), 2.40 (s, 3H), 2.31 (s, 3H), 1.30 (t, *J* 7.1 Hz, 3H). IR (KBr) *v* 3060, 3031, 2986, 2935, 2886, 2832, 1727 (vs), 1664 (vs), 1611, 1493, 1467, 1414, 1373, 1303, 1194, 1160, 1123, 1093, 1008, 873, 765, 690. MS (CI) m/z $(M+H)^+$ 433.

*2-(2-Hydroxyethyl)-6,7-dimethyl-1'-propyl-2H-spiro-[chromeno[2,3-c]pyrrole-1,3'-indoline]-2',3,9-trione (**4**{3-3-7}).*

Yield: 311 mg, 72%. ^{1}H NMR (500 MHz, CF_3CO_2D) δ 7.98 (s, 1H), 7.64 (s, 2H), 7.37-7.18 (m, 3H), 4.64-4.39 (m, 1H), 4.15-3.90 (m, 3H), 3.90-3.69 (m, 1.5H), 3.63-3.46 (m, 0.5H), 2.55 (s, 3H), 2.45 (s, 3H), 2.08-1.88 (m, 2H), 1.15 (t, *J* 7.2 Hz, 3H). IR (KBr) *v* 3500 (vs, br), 3052, 2966, 2934, 2876, 1726 (vs), 1667 (vs), 1610 (vs), 1489, 1468, 1410, 1367, 1305, 1285, 1193, 1139, 1095, 1054, 943, 852, 763, 690. MS (CI) m/z $(M+H)^+$ 433.

*1'-Allyl-6,7-dimethyl-2-((tetrahydrofuran-2-yl)methyl)-2H-spiro[chromeno[2,3-c]pyrrole-1,3'-indoline]-2',3,9-trione (**4**{3-5-13}).*

Yield: 357 mg, 76%. ^{1}H NMR (500 MHz, CF_3CO_2D) δ 7.98 (s, 1H), 7.73-7.56 (m, 2H), 7.39-7.18 (m, 3H), 6.16-5.93 (m, 1H), 5.58 (dd, *J* 17.3, 4.9 Hz, 1H), 5.47 (d, *J* 10.4 Hz, 1H), 4.82-4.68 (m, 1H), 4.67-4.50 (m, 1H), 4.43-4.32 (m, 0.6H), 4.32-4.21 (m, 0.4H), 4.11-3.89 (m, 2H), 3.82 (dd, *J* 15.1, 5.3 Hz, 0.6H), 3.66-3.34 (m, 1.4H), 2.56 (s, 3H), 2.45 (s, 3H), 2.26-1.98 (m, 3H), 1.97-1.78 (m, 1H). IR (KBr) *v* 3092, 3056, 2971, 2952, 2924, 2854, 1731 (vs), 1662 (vs), 1609, 1489, 1467, 1436, 1408, 1360, 1303, 1275, 1182, 1132, 1067, 941, 864, 825, 764, 692, 675. MS (CI) m/z $(M+H)^+$ 469.

*1'-Ethyl-7-fluoro-2-((tetrahydrofuran-2-yl)methyl)-2H-spiro[chromeno[2,3-c]pyrrole-1,3'-indoline]-2',3,9-trione (**4**{4-2-13}).*

Yield: 363 mg, 81%. ^{1}H NMR (500 MHz, DMSO-d_6) δ 8.07 (dd, *J* 9.3, 4.2 Hz, 1H), 7.91-7.78 (m, 1H), 7.68 (dd, *J* 8.3, 3.1 Hz, 1H), 7.46 (t, *J* 7.8 Hz, 1H), 7.33-7.22 (m, 2H), 7.06 (t, *J* 7.5 Hz, 1H), 3.92-3.71 (m, 2H), 3.71-3.53 (m, 1H), 3.52-3.30 (m, 3H), 3.05 (dd, *J* 14.7, 4.9 Hz, 0.3H), 2.92 (dd, *J* 14.4, 7.4 Hz, 0.7H), 1.85-1.59 (m, 3H), 1.59-1.33 (m, 1H), 1.25 (t, *J* 7.1 Hz, 3H). ^{13}C NMR (125 MHz, $CDCl_3$) δ (as a mixture of two diastereomers (1:2.5), signals of the main isomer) 171.3, 169.9, 163.1, 160.0 (d, $J_{C\text{-}F}$ 249.0 Hz), 155.5, 152.6, 144.4, 131.2, 126.7 (d, $J_{C\text{-}F}$ 7.4 Hz), 125.9, 124.1, 123.1, 122.8 (d, $J_{C\text{-}F}$ 25.4 Hz), 121.4, 121.3 (d, $J_{C\text{-}F}$ 8.2 Hz), 111.07 (d, $J_{C\text{-}F}$ 24.1 Hz), 109.5, 76.6, 67.8, 45.1, 35.9, 29.5, 28.3, 25.2, 12.4. IR (KBr) *v* 3068, 2978, 2949, 2876, 1726 (vs), 1670 (vs), 1609, 1475, 1362, 1282, 1258, 1191, 1140, 1110, 1056, 932, 897, 834, 764, 750, 689. MS (CI) m/z $(M+H)^+$ 449.

*2-Benzyl-7-fluoro-1'-propyl-2H-spiro[chromeno[2,3-c]-pyrrole-1,3'-indoline]-2',3,9-trione (**4**{4-3-16}).*

Yield: 355 mg, 76%. ^{1}H NMR (500 MHz, DMSO-d_6) δ 8.09 (dd, *J* 9.3, 4.2 Hz, 1H), 7.86 (ddd, *J* 9.2, 8.0, 3.2 Hz, 1H), 7.68 (dd, *J* 8.3, 3.1 Hz, 1H), 7.40 (t, *J* 7.7 Hz, 1H), 7.25-7.11 (m, 5H), 7.00-6.88 (m, 3H), 4.49 (d, *J* 15.4 Hz, 1H), 4.17 (d, *J* 15.4 Hz, 1H), 3.52 (t, *J* 6.9 Hz, 2H), 1.66-1.47 (m, 2H), 0.89 (t, *J* 7.4 Hz, 3H). IR (KBr) *v* 3091, 3056, 3043, 2967, 2935, 2919, 2876, 1727 (vs), 1667, 1609, 1580, 1470, 1376, 1354, 1326, 1285, 1256, 1189, 1140, 1086, 940, 883, 832, 735, 704, 687. MS (CI) m/z $(M+H)^+$ 469.

*1'-Allyl-7-fluoro-2-(3-isopropoxypropyl)-2H-spiro[chromeno[2,3-c]pyrrole-1,3'-indoline]-2',3,9-trione (**4**{4-5-12}).*

Yield: 366 mg, 77%. ^{1}H NMR (500 MHz, DMSO-d_6) δ 8.00 (dd, *J* 9.3, 4.2 Hz, 1H), 7.82-7.71 (m, 1H), 7.65 (dd, *J* 8.2, 3.1 Hz, 1H), 7.43 (t, *J* 7.3 Hz, 1H), 7.27 (d, *J* 7.2 Hz, 1H), 7.13 (d, *J* 7.9 Hz, 1H), 7.06 (t, *J* 7.5 Hz, 1H), 5.90 (ddd, *J* 15.1, 10.2, 5.0 Hz, 1H), 5.45 (d, *J* 17.3 Hz, 1H), 5.24 (d, *J* 10.4 Hz, 1H), 4.51 (dd, *J* 16.8, 4.4 Hz, 1H), 4.39 (dd, *J* 16.8, 4.7 Hz, 1H), 3.45-3.01 (m, 5H), 1.60-1.44 (m, 2H), 1.00 (t, *J* 6.2 Hz, 3H). IR (KBr) *v* 3083, 3061, 3044, 3035, 3028, 2974, 2932, 2885, 2843, 1729 (vs), 1660 (vs), 1610, 1471 (vs), 1368, 1335, 1286, 1258, 1189, 1141, 1087, 977, 922, 886, 838, 756, 705, 691, 561. MS (CI) m/z $(M+H)^+$ 477.

*7-Chloro-1'-methyl-2-phenethyl-2H-spiro[chromeno-[2,3-c]pyrrole-1,3'-indoline]-2',3,9-trione (**4**{5-1-21}).*

Yield: 371 mg, 79%. ^{1}H NMR (500 MHz, CF_3CO_2D) δ 8.18 (d, *J* 1.1 Hz, 1H), 7.91 (dd, *J* 9.1, 1.1 Hz, 1H), 7.79 (d,

J 9.1 Hz, 1H), 7.65 (t, *J* 7.8 Hz, 1H), 7.33-7.18 (m, 5H), 7.08-6.97 (m, 3H), 3.74-3.50 (m, 3H), 3.03-2.85 (m, 2H). IR (KBr) *v* 3074, 3024, 2937, 1730 (vs), 1714 (vs), 1665 (vs), 1609, 1494, 1461, 1367, 1349, 1282, 1177, 1114, 1087, 942, 823, 757, 700, 688, 655. MS (CI) m/z $(M+H)^+$ 471.

*7-Chloro-2-(4-methoxybenzyl)-1'-propyl-2H-spiro[chromeno[2,3-c]pyrrole-1,3'-indoline]-2',3,9-trione (**4**{5-3-17}).*

Yield: 386 mg, 75%. ^{1}H NMR (500 MHz, DMSO-d_6) δ 7.99-7.93 (m, 1H), 7.93-7.87 (m, 2H), 7.39 (t, *J* 7.7 Hz, 1H), 7.12 (d, *J* 7.9 Hz, 1H), 7.08 (d, *J* 7.3 Hz, 1H), 6.94 (t, *J* 7.5 Hz, 1H), 6.79 (d, *J* 8.6 Hz, 2H), 6.65 (d, *J* 8.6 Hz, 2H), 4.49 (d, *J* 15.0 Hz, 1H), 4.03 (d, *J* 15.0 Hz, 1H), 3.70 (s, 3H), 3.57-3.38 (m, 2H), 1.69-1.49 (m, 2H), 0.92 (t, *J* 7.4 Hz, 3H). IR (KBr) *v* 3088, 3076, 2958, 2932, 2873, 2841, 1736 (vs), 1725 (vs), 1668 (vs), 1609 (vs), 1512, 1488, 1463, 1436, 1365, 1313, 1281, 1265, 1247, 1201, 1180, 1139, 1111, 1087, 1024, 942, 902, 825, 765, 687, 656. MS (CI) m/z $(M+H)^+$ 515.

*1'-Allyl-2-butyl-7-chloro-2H-spiro[chromeno[2,3-c]-pyrrole-1,3'-indoline]-2',3,9-trione (**4**{5-5-5}).*

Yield: 313 mg, 70%. ^{1}H NMR (500 MHz, CF_3CO_2D) δ 7.98 (s, 1H), 7.69-7.56 (m, 2H), 7.36-7.21 (m, 3H), 6.04 (ddt, *J* 15.9, 10.4, 5.3 Hz, 1H), 5.54 (d, *J* 17.3 Hz, 1H), 5.47 (d, *J* 10.3 Hz, 1H), 4.68 (qd, *J* 16.4, 5.4 Hz, 2H), 3.64-3.45 (m, 1H), 3.45-3.25 (m, 1H), 2.56 (s, 3H), 2.46 (s, 1H), 1.63-1.48 (m, 2H), 1.41-1.23 (m, 2H), 0.87 (t, *J* 7.3 Hz, 3H). IR (KBr) *v* 3058, 3048, 3029, 2960, 2931, 2874, 2860, 1731 (vs), 1718 (vs), 1663 (vs), 1621, 1610, 1487, 1467, 1438, 1410, 1391, 1360, 1306, 1285, 1192, 1136, 1104, 954, 868, 752, 692. MS (CI) m/z $(M+H)^+$ 449.0.

*2-Allyl-1'-benzyl-7-chloro-2H-spiro[chromeno[2,3-c]-pyrrole-1,3'-indoline]-2',3,9-trione (**4**{5-6-6}).*

Yield: 347 mg, 72%. ^{1}H NMR (500 MHz, CF_3CO_2D) δ 8.23 (br s, 1H), 7.94 (br d, *J* 9.1 Hz, 1H), 7.81 (d, *J* 9.1 Hz, 1H), 7.59-7.34 (m, 6H), 7.31-7.18 (m, 3H), 5.76-5.58 (m, 1H), 5.23 (d, *J* 15.4 Hz, 1H), 5.08 (d, *J* 15.4 Hz, 1H), 4.96 (d, *J* 10.1 Hz, 1H), 4.88 (d, *J* 17.0 Hz, 1H), 4.43 (dd, *J* 15.3, 5.4 Hz, 1H), 3.80 (dd, *J* 15.4, 8.0 Hz, 1H). IR (KBr) *v* 3092, 3073, 3025, 2984, 2932, 2907, 1730 (vs), 1661 (vs), 1608, 1489, 1461, 1368, 1350, 1282, 1256, 1200, 1177, 1114, 944, 928, 829, 756, 698, 657. MS (CI) m/z $(M+H)^+$ 483.

*7-Chloro-1'-(4-fluorobenzyl)-2-(3-methoxypropyl)-2H-spiro[chromeno[2,3-c]pyrrole-1,3'-indoline]-2',3,9-trione (**4**{5-8-10}).*

Yield: 372 mg, 70%. ^{1}H NMR (500 MHz, CF_3CO_2D) δ 8.22 (br s, 1H), 7.94 (br d, *J* 9.1 Hz, 1H), 7.81 (d, *J* 9.1 Hz, 1H), 7.62-7.47 (m, 3H), 7.33-7.23 (m, 3H), 7.13 (t, *J* 8.2 Hz, 2H), 5.27 (d, *J* 15.5 Hz, 1H), 5.16 (d, *J* 15.6 Hz, 1H), 3.63 (t, *J* 5.9 Hz, 2H), 3.59-3.42 (m, 5H), 1.98-1.77 (m, 2H). IR (KBr) *v* 3071, 2984, 2929, 2868, 2826, 2805, 1728 (vs), 1667 (vs), 1608, 1509, 1489, 1462, 1374, 1360, 1323, 1287, 1258, 1225, 1202, 1174, 1118, 1095, 944, 907, 839, 826, 763, 687, 676, 663. MS (CI) m/z $(M+H)^+$ 533.

Notes

Acknowledgments. Authors are grateful to ENAMINE Ltd., Kyiv for financial support and for providing NMR spectra.

The authors declare no conflict of interest.

Author contributions. **R. N. V.**: synthesis of compounds, investigation, formal analysis, editing. **M. V. K.**: synthesis of compounds, investigation, formal analysis. **S. G. P.**: synthesis of compounds, investigation, formal analysis, editing. **V. S. M.**: investigation, formal analysis, writing of the most part of the manuscript, editing. **O. V. S.**: formal analysis, writing experimental section, editing. **A. V. K.**: NMR correlation experiment. **V. S. B.** conceptualization, supervision, writing - review & editing.

References

1. Welsch, M. E.; Snyder, S. A.; Stockwell, B. R. Privileged scaffolds for library design and drug discovery. *Curr. Opin. Chem. Biol.* **2010**, *14*, 347-361.
2. Rodrigues, T.; Reker, D.; Schneider, P. Schneider, G. Counting on natural products for drug design. *Nature Chem.* **2016**, *8*, 531-541.
3. Davison, E. K.; Brimble, M. A. Natural product derived privileged scaffolds in drug discovery. *Curr. Opin. Chem. Biol.* **2019**, *52*, 1-8.
4. James, M. J.; O'Brien, P.; Taylor, R. J. K.; Unsworth, W. P. Synthesis of Spirocyclic Indolenines. *Chem. Eur. J.* **2016**, *22*, 2856-2881.
5. Jossang, A.; Jossang, P.; Hadi, H. A.; Sevenet, T.; Bodo, B. Horsfiline, an oxindole alkaloid from Horsfieldia superba. *J. Org. Chem.* **1991**, *56*, 6527-6530.
6. Anderton, N.; Cockrum, P. A.; Colegate, S. M.; Edgar, J. A.; Flower, K.; Vit, I.; Willing, R. I. Oxindoles from Phalaris coerulescens. *Phytochemistry* **1998**, *48*, 437-439.
7. James, M. N. G.; Williams, G. J. B. The Molecular and Crystal Structure of an Oxindole Alkaloid (6-Hydroxy-2′-(2-methylpropyl)-3,3′-spirotetrahydropyrrolidino-oxindole). *Can. J. Chem.* **1972**, *50*, 2407-2412.
8. Edmondson, S.; Danishefsky, S. J.; Sepp-Lorenzino, L.; Rosen, N. Total Synthesis of Spirotryprostatin A, Leading to the Discovery of Some Biologically Promising Analogues. *J. Am. Chem. Soc.* **1999**, *121*, 2147-2155.
9. Ohiri, F. C.; Verpoorte, R.; Svendsen, A. B. The African Strychnos Species and Their Alkaloids: A Review. *J. Ethnopharmacol.* **1983**, *9*, 167-223.
10. *Natural Compounds: Alkaloids. Plant Sources, Structure and Properties*, Azimova, S. S.; Yunusov, M. S., Eds., Springer Science & Business Media: New York, NY, USA, 2013.
11. Gonzales, G.; Valerio, L. Medicinal Plants from Peru: A Review of Plants as Potential Agents Against Cancer. *Anti-Cancer Agents Med. Chem.* **2006**, *6*, 429-444.
12. Krishnaiah, D.; Sarbatly, R.; Nithyanandam, R. A review of the antioxidant potential of medicinal plant species. *Food Bioprod. Process.* **2011**, *89*, 217-233.
13. Paniagua-Pérez, R.; Madrigal-Bujaidar, E.; Molina-Jasso, D.; Reyes-Cadena, S.; Álvarez-González, I.; Sánchez-Chapul, L.; Pérez-Gallaga. Antigenotoxic, Antioxidant and Lymphocyte Induction Effects Produced by Pteropodine. *J. Basic Clin. Pharmacol. Toxicol.* **2009**, *104*, 222-227.
14. Rojas-Duran, R.; González-Aspajo, G.; Ruiz-Martel, C.; Bourdy, G.; Doroteo-Ortega, V. H.; Alban-Castillo, J.; Robert, G.; Auberger, P.; Deharo, E. Anti-inflammatory activity of Mitraphylline isolated from Uncaria tomentosa bark. *J. Ethnopharmacol.* **2012**, *143*, 801-804.
15. Joshi, K. C.; Jain, R.; Sharma, K.; Bhattacharya, S. K.; Goel, R. Studies in Spiro-Heterocycles. Part 12. Synthesis of Some Fluorine Containing Spiro (3H-indole-3, 4′(4H)-pyrano (2, 3-d) pyrimidine)-2, 5′, 7′(1H)-triones as CNS Agents. *J. Indian Chem. Soc.* **1988**, *65*, 202-204.
16. Nandakumar, A.; Thirumurugan, P.; Perumal, P. T.; Vembu, P.; Ponnuswamy, M. N.; Ramesh, P. One-pot multicomponent synthesis and anti-microbial evaluation of 2′-(indol-3-yl)-2-oxospiro(indoline-

3,4′-pyran) derivatives. *Bioorg. Med. Chem. Lett.* **2010**, *20*, 4252-4258.
17. Joshi, K. C.; Jain, R.; Arora, S. Spiro Heterocycles. Part 8. Synthesis, Herbicidal, and Fungicidal Activities of Some New Fluorine-Containing Spiro (3H-indole-3, 4′(1′ H)-pyrano (2, 3-c) pyrazole)-5′-carbonitriles/carboxylic Acid Ethyl Esters. *J. Indian Chem. Soc.* **1988**, *65*, 277-279.
18. Xu, J.; Shao, L.-D.; Shi, X.; Ren, J.; Xia, C.; Zhao, Q.-S. Collective formal synthesis of (±)-rhynchophylline and homologues. *RSC Adv.* **2016**, *6*, 63131-63135.
19. Vydzhak, R. N.; Panchishin, S. Ya.; Bezuglaya, E. M.; Chernega, A. N. A convenient approach to the synthesis of 1H-pyrrolo[3,4-b]chromene-3,9-dione derivatives *Zh. Org. Farm. Khim.* **2005**, *3*, 58-63. (In Rus.)
20. Vydzhak, R. N.; Panchishin, S. Ya. Simple synthesis of 1,2-diaryl-1,2-dihydrochromeno[2,3-c]pyrrole-3,9-diones. *Russ. J. General. Chem.* **2006**, *76*, 1681-1682.
21. Vydzhak, R. N.; Panchishin, S. Ya. Synthesis of 2-alkyl-1-aryl-1,2-dihydrochromeno[2,3-c]pyrrole-3,9-dione derivatives. *Russ. J. General. Chem.* **2008**, *78*, 2391-2397.
22. Vydzhak, R. N.; Panchishin, S. Ya. Synthesis of 2-phenyl-5,6-dihydropyrano[2,3-c]pyrrole-4,7-dione derivatives. *Russ. J. General. Chem.* **2008**, *78*, 1641-1642.
23. Vydzhak, R. N.; Panchishin, S. Ya. Synthesis of 1-aryl-2-[2-(dimethylamino)ethyl]-1,2-dihydrochromeno[2,3-c]pyrrole-3,9-diones and their analogs. *Russ. J. General. Chem.* **2010**, *80*, 323-329.
24. Vydzhak, R. N.; Panchishin, S. Ya. Synthesis of 1,2-dihydro-chromeno[2,3-c]pyrrole-3,9-diones spiro derivatives *Russ. J. General. Chem.* **2011**, *81*, 617-619.

Трикомпонентна циклізація як підхід до створення комбінаторної бібліотеки 2*H*-спіро[хромено[2,3-*c*]пірол-1,3'-індолін]-2',3,9-трионів

Р. Н. Виджак[1], М. В. Качаєва[1], С. Г. Пільо[1], В. С. Москвіна[1,2]*, О. В. Шабликіна[1,2], А. В. Козицький[3,4], В. С. Броварець[1]

[1] *Інститут біоорганічної хімії та нафтохімії ім. В.П. Кухаря НАН України, вул. Мурманська, 1, Київ, 02094, Україна*
[2] *Київський національний університет імені Тараса Шевченка, вул. Володимирська, 60, Київ, 01601, Україна*
[3] *Інститут фізичної хімії ім. Л. В. Пісаржевського НАН України, просп. Науки, 31, Київ, 03028, Україна*
[4] *ТОВ НВП «Єнамін», вул. Червоноткацька, 78, Київ, 02094, Україна*

Резюме: Представлено дослідження трикомпонентної циклізації метилових естерів 4-(*o*-гідроксифеніл)-2,4-діоксобутанових кислот **1**, *N*-заміщених ізатинів **2** та первинних амінів **3**, що веде до утворення 2*H*-спіро[хромено[2,3-*c*]пірол-1,3'-індолін]-2',3,9-трионів. Спіроциклічні індолін-2-они досить широко представлені серед природних біоактивних сполук, зокрема, у складі алкалоїдів, молекули яких містять систему спіро[індолін-3,6'-пірано[3,4-*f*]індолізину]. Зараз є доведеним, що деякі популярні в традиційній медицині лікарські рослини зобов'язані своїм цілющим властивостям саме алкалоїдам цієї групи. Разом із тим, синтез таких похідних досить складний, що обмежує можливості їх використання на практиці. Альтернативною стратегією є високоефективний трикомпонентний одностадійний синтез близьких за будовою структур, зокрема, 2*H*-спіро[хромено[2,3-*c*]пірол-1,3'-індолін]-2',3,9-трионів, з можливістю варіації в широких межах замісників і функціональних груп. В ході досліджень було підтверджено, що вказана трикомпонентна гетероциклізація дійсно є універсальним та ефективним інструментом синтезу 2*H*-спіро[хромено[2,3-*c*]пірол-1,3'-індолін]-2',3,9-трионів. На основі естерів 4-(*o*-гідроксифеніл)-2,4-діоксобутанових кислот, ізатинів із алкільними, алільним та бензильними замісниками в положенні 1, а також широкого набору аліфатичних амінів (в тому числі з активними функціональними групами, ароматичними та гетероциклічними фрагментами) було створено комбінаторну бібліотеку з 122 похідних, причому синтетична ефективність склала 87%, а виходи більш ніж 50% представників бібліотеки перевищували 70%. Синтетична процедура є простою у виконанні, допускає варіацію розчинників і придатна для автоматизації. ЯМР дослідження синтезованих сполук, а саме ^{1}H та ^{13}C спектри ЯМР, а також (для окремих представників) – COSY, HMBS та HSQC, дозволили не лише однозначно підтвердити структуру речовин, але й встановити характеристичні сигнали в спектрах ^{1}H та ^{13}C ЯМР, зокрема сигнал спіроатома карбону – близько 67 м.ч. Сигнали карбонільних груп в ІЧ спектрах виявляються двома широкими та інтенсивними смугами – 1735-1715 та 1670-1660 см$^{-1}$.

Ключові слова: ізатин, трикомпонентна циклізація, 1,2-дигідрохромено[2,3-*c*]пірол-3,9-діони, комбінаторна бібліотека.

ISSN 1814-9758. Ukr. Bioorg. Acta, 2020, Vol. 15, N 1
UDC 547.8:615.277.3
DOI: hpps://doi.org/10.15407/bioorganica2020.01.034

Ukrainica Bioorganica Acta
www.bioorganica.org.ua

UBA

RESEARCH ARTICLE

Cationic carboxamide derivatives of tricyclic heteroaromatic compounds: synthesis and preliminary evaluation of antiproliferative activity

Valentina G. Kostina, Inna V. Alexeeva, Nadia A. Lysenko, Valentina V. Negrutska, Igor Y. Dubey*

Institute of Molecular Biology and Genetics of the NAS of Ukraine, 150 Zabolotnogo St., Kyiv, 03680, Ukraine

Abstract: This research was aimed at the synthesis and study of biological activity of the carboxamides of tricyclic heteroaromatic systems, acridone, phenazine, and thioxanthone, containing the aliphatic and aromatic cationic substituents at amide fragment. These heterocyclic cores are DNA intercalating agents, whereas the introduction of cationic groups provides additional ionic interactions of the ligands with their biological targets, such as DNA and enzymatic complexes of the system of nucleic acids biosynthesis. A convenient way of the introduction of such groups is a modification of heterocyclic carboxamides. A small library of new *N*-substituted cationic amide derivatives of acridone-4-, phenazine-1- and thioxanthone-4-carboxylic acids was obtained. They were synthesized in 37-81% yield by mild and selective quaternization of the nitrogen atoms at *N,N*-dimethylaminoalkyl (alkyl = ethyl, propyl) and pyridylmethyl fragments of the neutral *N*-functionalized carboxamides with methyl iodide. Tricyclic heteroaromatic cores were not affected. Convenient protocol for the synthesis of thioxanthone-4-carboxylic acid (TCA) based on the reaction of 2-mercaptobenzoic and 2-iodobenzoic acids followed by cyclization of the intermediate was developed (yield 79%). A series of new *N*-functionalized neutral amides of TCA, the precursors of corresponding cationic carboxamide, were also obtained via the reaction of acyl chloride with amines. Preliminary *in vitro* testing of four compounds as potential antitumor agents in U87MG tumor cell culture (human malignant glioma) demonstrated their significant antiproliferative activity at low micromolar concentrations, with growth inhibition values GI_{50} in the range 1.7-11 μM. These results suggest that cationic carboxamides of tricyclic heteroaromatic systems are promising scaffolds for the design of new antitumor drugs.

Keywords: acridone; phenazine; thioxanthone; carboxamides; antitumor agents.

Introduction

Condensed tricyclic heteroaromatic systems are privileged scaffolds for the design of therapeutic agents for the treatment of various diseases [1-5]. In particular, a broad variety of antitumor, antibacterial, and antiviral drugs belong to this class of compounds, including the derivatives of acridine, phenazine, and thioxanthone. In most cases, such compounds target the cellular enzymatic systems of nucleic acids biosynthesis. Small molecules based on condensed tricyclic heterocycles were reported as efficient inhibitors of a number of enzymes involved in nucleic acids metabolism, including e.g. DNA and RNA polymerases [6], topoisomerases [7-19], and telomerase [20-25].

The majority of non-nucleoside inhibitors of the enzymes of nucleic acid biosynthesis are based on heteroaromatic polycyclic scaffolds. Their effect is usually associated with interaction with DNA (duplex and quadruplex structures) via intercalation or groove binding, or with DNA-enzyme complexes [26-31]. It should be noted that the planar aromatic systems of acridines and acridones, phenazines, thioxanthones, and similar molecules allow efficient intercalation into DNA via the π-π-stacking with electronic systems of nucleic base pairs [11, 12, 32, 33].

Easily available functionalized tricyclic heteroaromatic carboxamides containing *N*-alkyl and *N*-aryl substituents have been extensively studied as potential anticancer, antibacterial, and antiviral drugs [8-10, 16, 18, 20, 24]. Important factors influencing their biological activity are

Received: 20.05.2020
Revised: 29.05.2020
Accepted: 12.06.2020
Published online: 30.06.2020

* Corresponding author. Tel.: +380-44-200-0379;
e-mail: dubey@imbg.org.ua (I. Y. Dubey)
ORCID: 0000-0003-4023-4293

Important factors influencing their biological activity are the structure of heterocycle, the nature of amide substituent, and the position of the carboxamide group in the core molecule [10, 16].

Biological activity of carboxamide derivatives of acridine and phenazine has been investigated for several decades. Carboxamides containing the $NHCH_2CH_2NMe_2$ pharmacophore, such as *N*-[2-(dimethylamino)-ethyl] carboxamide derivatives of phenazine [34], acridine (DACA) [8] and 9-aminoacridine [35] were identified as efficient antitumor agents and topoisomerase inhibitors. *N*-arylamides of acridone-4-carboxylic acid are active against hepatitis C virus infection inhibiting the transcription and RNA replication [36]. *N*-pyridyl derivatives of acridone carboxamides were found to inhibit NS3 helicase [36, 37], telomerase [24], and topoisomerase I [38]. *N*-aryl(hetaryl)-substituted amides of phenazine-1-carboxylic acid appeared to be efficient antimicrobial agents, including the compounds active against drug-resistant *Mycobacterium tuberculosis* strains [39, 40].

Much less attention has been paid to the studies of bioactivity of compounds based on thioxanthone, a close acridone analogue. Among thioxanthone derivatives, antitumor agents have been reported [41-43], although we were unable to find have not found in the literature data on the activity of thioxanthone carboxamides.

We have previously obtained a series of carboxamides of acridone and phenazine whose amide groups were functionalized with *N,N*-dimethylaminoalkyl and pyridyl fragments [38]. The introduced basic functions can be protonated under physiological conditions to form cationic moieties. Structure design was based on the fact that the attachment of basic/cationic substituents to DNA-intercalating ligands could enhance their binding to DNA or enzymatic complexes formed by the enzymes of nucleic acids biosynthesis (topoisomerase, telomerase, DNA, and RNA polymerases, etc.) by additional interactions with either anionic DNA phosphates or acidic groups within the enzymes. At the same time, the aromatic pyridyl residues could also interact with nucleic acids bases or aromatic amino acids via the hydrophobic mechanism further enhancing the binding of ligands to their molecular targets. Phenazine and acridone derivatives containing aromatic pyridyl fragments were found to inhibit the topoisomerase I at 100 μM concentration, whereas their analogues with aliphatic basic substituents at carboxamide fragment were less efficient [38]. At the same time, the free core heterocycles and their non-substituted carboxamides are inactive against topoisomerase [38] and telomerase [24].

Thus, the introduction of protonable basic substituents significantly increased the biological activity of tricyclic carboxamides, and we could expect that the modification of core heterocycles with cationic fragments would result in even more efficient inhibitors with potential antitumor and/or antibacterial properties. In this work, we have significantly extended the range of *N*-substituted tricyclic carboxamides as potential antitumor agents.

Results and discussion

Before we have synthesized a set of neutral carboxamide derivatives of acridone **1a-e** and phenazine **2a-e**

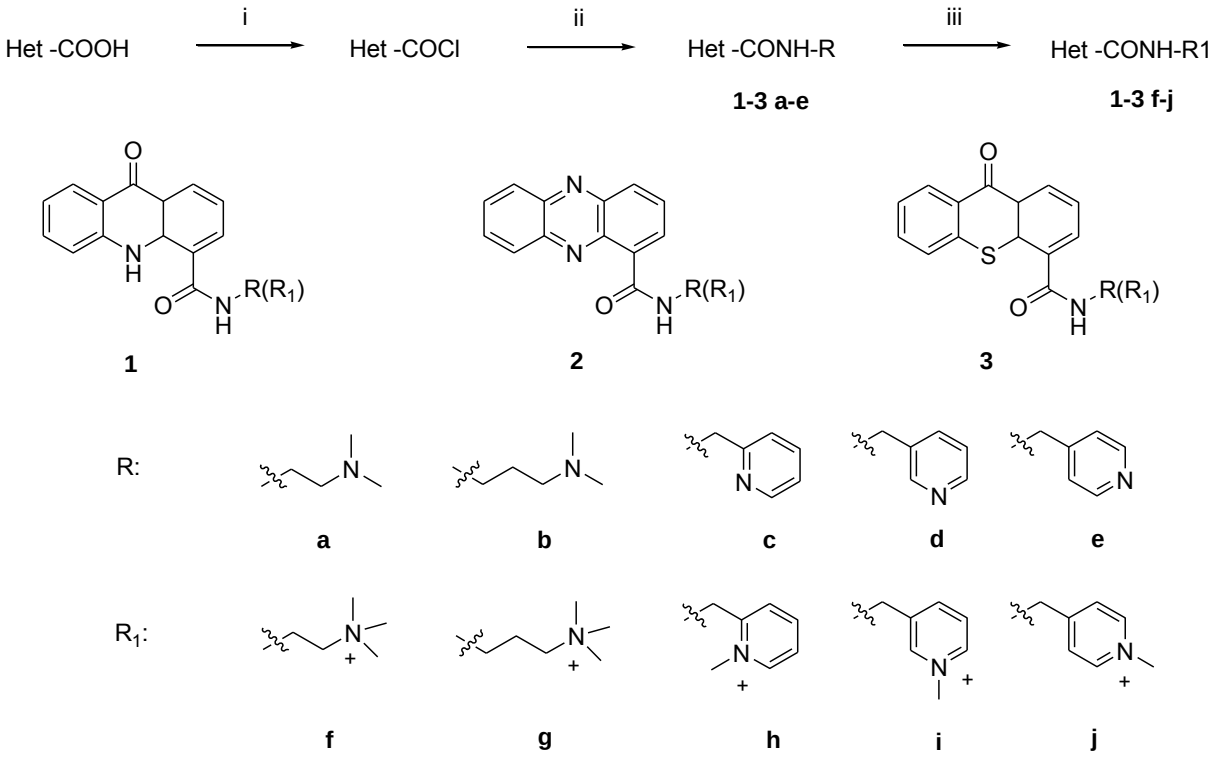

Scheme 1. Synthesis of neutral (**a-e**) and cationic (**f-j**) derivatives of tricyclic carboxamides. (i). $SOCl_2$, toluene, Py, Δ; (ii). R-NH_2, triethylamine, rt; (iii) methyl iodide, MeOH or CH_3CN, 20-50 °C, 37-81%.

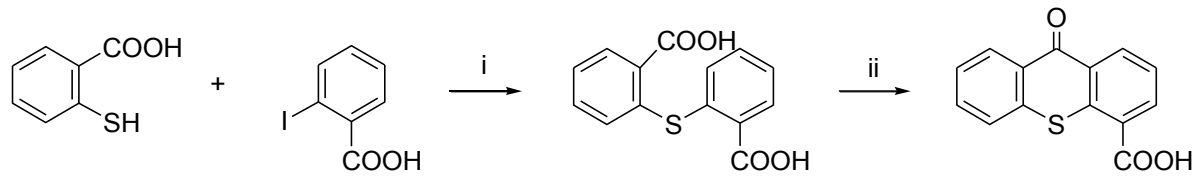

Scheme 2. Synthesis of thioxanthone-4-carboxylic acid. (i). K_2CO_3, DMF, 60 °C, 4 h; (ii). conc. H_2SO_4, 100 °C, 2.5-3 h, 79%.

(Scheme 1). Their amide groups were functionalized with *N,N*-dimethylamino and isomeric pyridyl groups attached via the short (1-3 carbon atoms) alkyl linkers [38]. Taking into account the above considerations, we have decided to prepare cationic derivatives of tricyclic heterocycles. One of the possible ways to obtain compounds of this type would be a quaternization of nitrogen atoms of basic aliphatic and aromatic substituents present in the already prepared carboxamides **1,2a-e**. We have also decided to extend the range of tricyclic heteroaromatic systems by adding their structural analogue, thioxanthone.

Carboxamides **1,2a-e** have been previously synthesized from carboxylic acids [38]. To obtain analogues based on thioxanthone, first of all, we have elaborated an efficient procedure for the synthesis of thioxanthone-4-carbocylic acid (TCA). This procedure is similar to that commonly used for the synthesis of acridone-4-carboxylic acid [44] and is based on intramolecular cyclization of *bis*-dicarboxyphenyl sulfide formed in the reaction of 2-mercaptobenzoic and 2-iodobenzoic acids.

We have modified a published protocol [45] using potassium carbonate as a base instead of NaOH, and 2-iodobenzoic acid in place of 2-chlorobenzoic acid. The condensation of two acids at 60 °C followed by the intermediate cyclization by heating in conc. sulfuric acid afforded TCA in 79% yield (Scheme 2). The use of less reactive bromobenzoic acid in the condensation required heating at a higher temperature (100 °C) and resulted in a significantly lower total yield of target tricyclic carboxylic acid (below 50%).

The synthesis of new *N*-substituted carboxamides of thioxanthone was based on our previous approach developed for phenazine and acridone series [38]. This convenient one-flask process consisted in the formation of acyl chloride followed by its reaction with amine. Target neutral amides **3a-e** were obtained by the reaction of TCA chloride with corresponding amines in the presence of TEA (Scheme 1).

The neutral compounds **1-3a-e** were found to easily react with methyl iodide, and the quaternization of nitrogen atoms in amide substituents allowed obtaining a series of novel cationic derivatives **1-3f-j**. *N*-Alkylation reaction was carried out in polar solvent (methanol, acetonitrile) at room temperature or with some heating (up to 50 °C). Since salt-type products precipitated from the reaction mixture, the use of crude amides instead of analytically pure samples did not significantly affect the total yield of iodides from starting carboxylic acids.

The primary centres of *N*-methylation are obviously tertiary aliphatic ($AlkNMe_2$) and pyridine nitrogen atoms in carboxamide fragments. Only one additional methyl group signal appeared in ^{1}H NMR spectra of all cationic derivatives. It is known that the quaternization of phenazine under the applied conditions does not occur, but possible alkylation of endocyclic nitrogen or exocyclic oxygen atom of the acridone ring could not be excluded. However, NMR spectra of the obtained derivatives and their comparison with the spectral data of reference compounds confirmed that compounds **1f-j** do not contain *N*-methyl group located at acridine ring, as one-proton low-field signals at $\delta \geq 12$ ppm characteristic of the 10-NH ring proton of neutral carboxamides of acridone carboxylic acid [44] are observed in the spectra. NMR spectra of cationic TCA carboxamides also contain the signals of methyl groups only from trimethylammonium or *N*-methylpyridinium residues.

Cationic aliphatic trimethylammonium group of compounds **1-3f-g** is represented by singlets at 3.1-3.4 ppm, whereas the spectra of pyridinium derivatives **1h-j**, **2i**, and **3i** contain the signals of cationic *N*-methyl group located at 4.2-4.4 ppm. Low-field shift of signals of the cationic fragments is observed in NMR spectra of the salts, as compared to corresponding neutral carboxamides. In general, the deshielding effect of cationic structures results in the shift of CONH and methylene protons (low-field shift for 0.1-0.5 and 0.15-0.25 ppm, respectively) in comparison with neutral precursors.

Thus, we have prepared a series of 11 new compounds containing trimethylammonium group attached via the ethyl or propyl linker, and compounds with isomeric *N*-methylpyridinium fragments. This small library would allow analyzing the structure-activity relationship among the derivatives of three tricyclic systems – phenazine, acridone, and thioxanthone.

Investigation of antitumor activity of compounds in vitro

Preliminary evaluation of the antiproliferative activity of some new compounds was performed *in vitro* in the culture of U87MG tumor cells (human malignant glioma). To determine the effect of quaternization on biological activity, the representative pairs of the derivatives of two different heterocycles, acridone and phenazine, containing the same pyridyl and *N*-metyylpyridinium fragments (**1d, i** and **2d, i**) were tested. The cells were cultured in 24-well plates and treated for 3 days by drugs added at concentrations ranging from 20 to 0.5 μM.

In vitro cytostatic activity of compounds towards cancer cell line was determined using the classic MTT assay [46]. MTT test is based on the transformation of MTT reagent (3-(4,5-dimethylthiazol-2-yl)-2,5-diphenyltetrazolium bromide) by the mitochondrial dehydrogenase of viable cells into the blue formazan which can then be measured spectrophotometrically. The optical density of the probe is proportional to the number of live cells. From the obtained data, the plots of the number of live cells in the probe as compared to a control (cell growth inhibition level) *vs*. drug concentration were built, from which the GI_{50} value was obtained for each tested carboxamide. GI_{50} was determined as a concentration of drug required for 50% of maximal inhibition of cell proliferation (decreasing cell vitality by 50%) as compared to the non-treated control.

Tested carboxamides demonstrated a significant dose-dependent antiproliferative activity towards U87MG cells at low micromolar concentrations, with GI_{50} below 10 μM for three of four compounds (Table 1).

Table 1. Antiproliferative activity of compounds in the culture of U87MG cells (M ± SD).

Compound	GI_{50}, μM
1d	11 ± 2
1i	7.2 ± 1.4
2d	1.7 ± 0.3
2i	5.5 ± 0.9

It is interesting to note that the cationic acridone derivative **1i** (GI_{50} 7.2 μM) was more active than its neutral analogue **1d** (GI_{50} 11 μM), whereas for the pair of phenazine carboxamides the cationic compound **2i** was three times less efficient as compared to its non-charged counterpart **2d** (GI_{50} 5.5 and 1.7 μM, respectively).

The opposite effects of quaternization on the biological activity of acridone and phenazine carboxamides may be due to different molecular targets of the studied compounds and/or different modes of inhibitor-target interaction. However, at this moment we have only limited information on biological properties of a small set of derivatives, and molecular mechanisms of bioactivity of new compounds require further investigation. In particular, it will include the studies on the inhibition of the enzymes of nucleic acid biosynthesis and ligand interactions with nucleic acids. It would be also interesting to access the antibacterial activity of these derivatives.

Conclusions

A convenient protocol was proposed for the synthesis of cationic *N*-functionalized carboxamide derivatives of acridone, phenazine, and thioxanthone, the tricyclic systems with DNA-intercalating properties. A series of compounds with aliphatic and aromatic cationic substituents were obtained. Their heteroaromatic cores contained the carboxamide functions modified with *N*-methylpyridiniumyl and *N,N,N*-trimethylammonium groups. Preliminary evaluation of the antiproliferative activity of several compounds in tumor cell culture *in vitro* demonstrated that cationic tricyclic carboxamides could be suitable scaffolds for the development of new efficient antitumor agents.

Experimental section

Reagents and solvents for synthesis were purchased from UkrOrgSynthez (Ukraine), Fluka (Switzerland), and Sigma-Aldrich (Germany). Solvents were purified and dried by standard methods. DMSO for molecular biology and MTT reagent (3-(4,5-dimethylthiazol-2-yl)-2,5-diphenyltetrazolium bromide) were obtained from Sigma (USA). ^{1}H NMR spectra were recorded on a Mercury-400 instrument (400 MHz, Varian, USA) in DMSO-d_6 with tetramethylsilane as an internal standard; chemical shifts are given in ppm. Thin-layer chromatography (TLC) was performed on Silica gel $60F_{254}$ plates (Merck, Germany) in following solvent systems: $CHCl_3$/MeOH 9:1 (A); $CHCl_3$/MeOH 1:1 (B); $CHCl_3$/HOAc/acetone 10:0.125:0.125 (C); *i*-PrOH/NH_4OH/H_2O 7:1:2 (D), $CHCl_3$/HOAc/acetone (E). Melting points were determined using a Boethius PNMK 05 apparatus (Nagema, Germany).

Chemistry

Acridone and phenazine carboxamide derivatives **1,2a-e** were obtained as previously reported [38].

9-Oxo-9H-thioxanthene-4-carboxylic acid (TCA).

The mixture of 2-mercaptobenzoic acid (1.16 g, 7.53 mmol), 2-iodobenzoic acid (1.89 g, 7 mmol) and powdered K_2CO_3 (2.09 g, 15.2 mmol) in 10 ml of dry DMF was stirred at 60 °C for 7.5 h. After cooling, 60 ml of water was added and insoluble material was filtered off. The filtrate was neutralized with 10% HCl, the precipitate was collected by filtration, washed with water and dried. The obtained crude 2-(2-carboxyphenylthio)benzoic acid (1.94 g) was kept in 7.5 ml of conc. sulfuric acid for 2.5-3 h at 100 °C (control TLC in system E). The reaction mixture was cooled and poured into ice-cold water, and the precipitate was filtered and extensively washed with water. After its re-precipitation from 20 ml of 10% NaOH with 10% HCl the crude product (1.52 g) was crystallized from DMF. Yield of yellow crystals 79%, mp 332-335 °C. ^{1}H NMR (400 MHz, DMSO-d_6) δ 8.78 (d, 1H, *J* 8.0 Hz, Ar), 8.49 (d, 1H, *J* 7.6 Hz, Ar), 8.43 (d, 1H, *J* 8.0 Hz, Ar), 7.92 (d, 1H, *J* 8.0 Hz, Ar), 7.81 (t, 1H, *J* 7.2 Hz, Ar), 7.70 (t, 1H, *J* 7.6 Hz, Ar), 7.61 (t, 1H, *J* 7.6 Hz, Ar).

*General procedure for the synthesis of N-substituted amides of thioxanthone-4-carboxylic acid (**3a-e**).*

0.5 Mmol (128 mg) of TCA was suspended in 3 ml of dry toluene, and 50 μl of thionyl chloride and 60 μl of dry pyridine (0.7 mmol each) were added with stirring and the mixture was heated at 90 °C for 1.5-2 h. After cooling to room temperature corresponding amine (1.25 mmol) and triethylamine (1.25 mmol) were added, and the mixture was

stirred at ambient temperature until the reaction was complete (control TLC). The mixture was evaporated, the residue was treated with 10 ml of chloroform and washed with saturated $NaHCO_3$ (3×5 ml). The organic phase was dried over Na_2SO_4 and evaporated to dryness. The product was crystallized from the appropriate solvent.

*9-Oxo-9H-thioxanthene-4-carboxylic acid (2-dimethylaminoethyl)-amide (**3a**)*

was obtained from 146 mg (0.57 mmol) TCA and 138 μl (1.26 mmol) *N,N*-dimethylaminoethylene diamine. Yield 26%, mp 160-163 °C (acetonitrile). ^{1}H NMR (400 MHz, DMSO-d_6) δ 8.72 (br t, 1H, CONH), 8.63 (d, 1H, *J* 8.0 Hz, Ar), 8.42 (dd, 1H, *J* 8.0 Hz, 0.8 Hz, Ar), 7.98 (d, 1H, *J* 6.4 Hz, Ar), 7.85 (m, 1H, Ar), 7.79 (t, 1H, *J* 7.6 Hz, Ar), 7.66 (t, 1H, *J* 8.4 Hz, Ar), 7.58 (t, 1H, *J* 7.6 Hz, Ar), 3.44 (m, 2H, NH*CH*$_2$), 2.40 (t, 2H, *J* 6.4 Hz, CH_2N), 2.21 (s, 6H, NMe_2).

*9-Oxo-9H-thioxanthene-4-carboxylic acid (3-dimethyl-aminopropyl)-amide (**3b**)*

was obtained from 128 mg (0.5 mmol) of TCA and 120 μl (1.25 mmol) of *N,N*-dimetylaminopropylene-1,3-diamine. Yield 58 mg (34%), mp 162-165 °C (acetonitrile). ^{1}H NMR (400 MHz, DMSO-d_6) δ 8.80 (br t, 1H, *J* 5.6 Hz, CONH), 8.62 (dd, 1H, *J* 8.4 Hz, 1.2 Hz, Ar), 8.43 (dd, 1H, *J* 8.0 Hz, 0.8 Hz, Ar), 7.99 (dd, 1H, *J* 7.4 Hz, 1.2 Hz, Ar), 7.88-7.84 (m, 1H, Ar), 7.80-7.76 (m, 1H, Ar), 7.66 (t, 1H, *J* 7.6 Hz, Ar), 7.59 (t, 1H, *J* 7.6 Hz, Ar), 3.35 (m, 2H, NH*CH*$_2$), 2.34 (t, 2H, *J* 7.2 Hz, CH_2N), 2.17 (s, 6H, NMe_2), 1.70 (t, 2H, *J* 7.2 Hz, CH_2).

*9-Oxo-9H-thioxanthene-4-carboxylic acid (pyridin-2-ylmethyl)-amide (**3c**)*

was obtained from *o*-aminomethylpyridine. Yield 19%, mp 192-194 °C (EtOH). ^{1}H NMR (400 MHz, DMSO-d_6) δ 9.45 (t, 1H, *J* 6.0 Hz, CONH), 8.65 (dd, 1H, *J* 8.4 Hz, 1.2 Hz, Ar), 8.55 (d, 1H, *J* 4.8 Hz, Ar), 8.43 (dd, 1H, *J* 8.4 Hz, 1.2 Hz, Ar), 8.16 (dd, 1H, *J* 7.6 Hz, 1.6 Hz, Ar), 7.87-7.78 (m, 3H, Ar), 7.70 (t, 1H, *J* 7.6 Hz, Ar), 7.59 (dt, 1H, *J* 8.0 Hz, 1.2 Hz, Ar), 7.43 (d, 1H, *J* 7.6 Hz, Ar), 7.31 (dd, 1H, *J* 7.6 Hz, 6.8 Hz, Ar), 4.57 (d, 2H, *J* 6.0 Hz, CH_2).

*9-Oxo-9H-thioxanthene-4-carboxylic acid (pyridin-3-yl-methyl)-amide (**3d**)*

was obtained from 207 mg (0.81 mmol) of TCA and 147 μl (1.45 mmol) of *m*-aminomethylpyridine. Yield 152 mg (54%), mp 194-198 °C (acetonitrile/i-PrOH). ^{1}H NMR (400 MHz, DMSO-d_6) δ 9.41 (br t, 1H, *J* 4.4 Hz, CONH), 8.65 (m, 2H, Ar), 8.51 (d, 1H, *J* 3.2 Hz, Ar), 8.43 (d, 1H, *J* 6.4 Hz, Ar), 8.11 (d, 1H, *J* 6.0 Hz, Ar), 7.88-7.75 (m, 3H, Ar), 7.67 (t, 1H, *J* 6.4 Hz, Ar), 7.57 (t, 1H, *J* 6.0 Hz, Ar), 7.44-7.40 (m, 1H, Ar), 4.57 (d, 2H, *J* 4.8 Hz, CH_2).

*9-Oxo-9H-thioxanthene-4-carboxylic acid (pyridin-4-ylmethyl)-amide (**3e**)*

was obtained from *p*-aminomethylpyridine. Yield 30%, mp 194-197 °C (EtOH). ^{1}H NMR (400 MHz, DMSO-d_6) δ 9.45 (t, 1H, *J* 6.0 Hz, CONH), 8.66 (dd, 1H, *J* 7.6 Hz, 1.2 Hz, Ar), 8.55 (m, 2H, Ar), 8.43 (dd, 1H, *J* 8.0 Hz, 0.8 Hz, Ar), 8.15 (dd, 1H, *J* 7.6 Hz, 1.6 Hz, Ar), 7.88-7.85 (m, 1H, Ar), 7.78 (dt, 1H, *J* 7.6 Hz, 1.2 Hz, Ar), 7.71 (t, 1H, *J* 7.6 Hz, Ar), 7.60 (dt, 1H, *J* 7.6 Hz, 1.2 Hz, Ar), 7.40 (dd, 2H, *J* 4.4 Hz, 1.6 Hz, Ar), 4.57 (d, 2H, *J* 6.0 Hz, CH_2).

General procedure for the quaternization of carboxamides.

Neutral heterocyclic *N*-substituted carboxamide **1-3a-e** (0.1 mmol) and 150 μl of methyl iodide in 2 ml of methanol or acetonitrile were kept at room temperature or with weak heating (up to 50 °C) until the reaction was complete (control TLC). The precipitated product (**1-3f-j**) was collected by filtration and crystallized from the appropriate solvent.

*Trimethyl-{2-[(9-oxo-9,10-dihydroacridine-4-carbonyl)-amino]-ethyl}-ammonium iodide (**1f**).*

Yield 75%, mp 260-263 °C (EtOH). ^{1}H NMR (400 MHz, DMSO-d_6) δ 12.26 (s, 1H, NH (Ar)), 9.28 (br t, 1H, CONH), 8.48 (d, 1H, *J* 7.6 Hz, Ar), 8.24 (m, 2H, Ar), 7.78-7.70 (m, 2H, Ar), 7.40 (t, 1H, *J* 7.6 Hz, Ar), 7.34 (t, 1H, *J* 7.2 Hz, Ar), 3.80 (m, 2H, NH*CH*$_2$), 3.61 (br t, 2H, CH_2N), 3.19 (s, 9H, N^+Me_3).

*Trimethyl-{3-[(9-oxo-9,10-dihydroacridine-4-carbonyl)-amino]-propyl}-ammonium iodide (**1g**).*

Yield 64%, mp 262-264 °C (acetonitrile). ^{1}H NMR (400 MHz, DMSO-d_6) δ 12.40 (s, 1H, NH (Ar)), 9.10 (br t, 1H, CONH), 8.46 (d, 1H, *J* 8.0 Hz, Ar), 8.27 (m, 1H, Ar), 7.79-7.71 (m, 2H, Ar), 7.39-7.31 (m, 2H, Ar), 3.45-3.39 (m, 4H, NH*CH*$_2$, CH_2N), 3.19 (s, 9H, N^+Me_3), 2.05 (br t, 2H, CH_2).

*1-Methyl-2-{[(9-oxo-9,10-dihydroacridine-4-carbonyl)-amino]-methyl}-pyridinium iodide (**1h**).*

Yield 37%, mp 269-273 °C (DMF). ^{1}H NMR (400 MHz, DMSO-d_6) δ 12.10 (s, 1H, NH (Ar)), 9.86 (t, 1H, *J* 4.8 Hz, CONH), 9.06 (d, 1H, *J* 4.8 Hz, Ar), 8.58-8.52 (m, 2H, Ar), 8.44 (d, 1H, *J* 7.6 Hz, Ar), 8.24 (d, 1H, *J* 8.4 Hz, Ar), 8.17 (d, 1H, *J* 8.4 Hz, Ar), 8.06 (m, 1H, Ar), 7.78-7.74 (m, 1H, Ar), 7.68 (d, 1H, *J* 8.4 Hz, Ar), 7.43 (m, 1H, Hz, Ar), 7.32 (m, 1H, Ar), 5.0 (d, 2H, *J* 4.8 Hz, CH_2), 4.44 (s, 3H, N^+Me).

*1-Methyl-3-{[(9-oxo-9,10-dihydroacridine-4-carbonyl)-amino]-methyl}-pyridinium iodide (**1i**).*

Yield 75%, mp 240-244 °C (acetonitrile). ^{1}H NMR (400 MHz, DMSO-d_6) δ 12.27 (s, 1H, NH (Ar)), 9.73 (br t, 1H, CONH), 9.06 (s, 1H, Ar), 8.92 (s, 1H, Ar), 8.61 (d, 1H, *J* 8.8 Hz, Ar), 8.50 (d, 1H, *J* 7.2 Hz, Ar), 8.39 (d, 1H, *J* 8.4 Hz, Ar), 8.46 (d,1H, *J* 8.4 Hz, Ar), 8.13 (s, 1H, Ar), 7.79-7.77 (m, 2H, Ar), 7.45-7.29 (m, 2H, Ar), 4.78 (d, 2H, *J* 5.6 Hz, CH_2), 4.37 (s, 3H, N^+Me).

*1-Methyl-4-{[(9-oxo-9,10-dihydroacridine-4-carbonyl)-amino]-methyl}-pyridinium iodide (**1j**).*

Yield 66%, mp 206-209 °C (acetonitrile). ^{1}H NMR (400 MHz, DMSO-d_6) δ 12.29 (br s, 1H, NH (Ar)), 9.83 (br s, 1H, CONH), 8.95 (m, 2H, Ar), 8.45-8.55 (m, 2H, Ar), 8.30-

8.12 (m, 3H, Ar), 7.80-7.65 (m, 2H, Ar), 7.45-7.25 (m, 2H, Ar), 4.86 (br t, 2H, CH_2), 4.31 (s, 3H, N^+Me).

*Trimethyl-{2-[(phenazine-1-carbonyl)-amino]-ethyl}-ammonium iodide (**2f**).*

Yield 42%, mp 272-276 °C (EtOH/DMF). ^{1}H NMR (400 MHz, DMSO-d_6) δ 10.55 (br t, 1H, CONH), 8.67 (d, 1H, *J* 7.2 Hz, Ar), 8.45-8.52 (m, 2H, Ar), 8.32 (d, 1H, *J* 8.0 Hz, Ar), 8.16-8.05 (m, 3H, Ar), 4.02 (d, 2H, *J* 6.0 Hz, NHCH_2), 3.70 (br t, 2H, CH_2N), 3.25 (s, 9H, N^+Me_3).

*Trimethyl-{3-[(phenazine-1-carbonyl)-amino]-propyl}-ammonium iodide (**2g**).*

Yield 76%, mp 277-280 °C (butanol/DMF). ^{1}H NMR (400 MHz, DMSO-d_6) δ 10.42 (s, 1H, CONH), 8.67 (d, 1H, *J* 6.0 Hz, Ar), 8.48 (m, 2H, Ar), 8.32 (d, 1H, *J* 6.8 Hz, Ar), 8.14-8.01 (m, 3H, Ar), 3.62 (br s, 2H, NHCH_2), 3.47 (br t, 2H, CH_2 N), 2.17 (s, 9H, N^+Me_3), 2.15 (br t, 2H, CH_2).

*1-Methyl-3-{[(phenazine-1-carbonyl)-amino]-methyl}-pyridinium iodide (**2i**).*

Yield 81%, mp 236-238 °C (EtOAc). ^{1}H NMR (400 MHz, DMSO-d_6) δ 10.94 (br t, 1H, CONH), 9.11 (s, 1H, Ar), 8.92 (d, 1H, *J* 6.0 Hz, Ar), 8.73 (d, 1H, *J* 8.4 Hz, Ar), 8.66 (d, 1H, *J* 6.8 Hz, Ar), 8.54 (d, 1H, *J* 8.0 Hz, Ar), 8.48 (d, 1H, *J* 8.4 Hz, Ar), 8.34 (d, 1H, *J* 7.6 Hz, Ar), 8.19 (dd, 1H, *J* 7.2, 6.0 Hz, Ar), 8.12-8.02 (m, 3H, Ar), 4.97 (d, 2H, *J* 6.0 Hz, CH_2), 4.37 (s, 3H, N^+Me).

*Trimethyl-{2-[(9-oxo-9H-thioxanthene-4-carbonyl)-amino]-ethyl}-ammonium iodide (**3f**).*

Yield 39%, mp 267-270 °C (butanol/DMF). ^{1}H NMR (400 MHz, DMSO-d_6) δ 9.12 (br.t, 1H, CONH), 8.67 (d, 1H, *J* 7.6 Hz, Ar), 8.44 (d, 1H, *J* 7.2 Hz, Ar), 8.06 (d, 1H, *J* 6.0 Hz, Ar), 7.85-7.78 (m, 2H, Ar), 7.73-7.69 (m, 1H, Ar), 7.61 (m, 1H, Ar), 3.75 (d, 2H, *J* 6.0 Hz, NHCH_2), 3.60 (br t, 2H, CH_2N), 3.24 (s, 9H, N^+Me_3).

*Trimethyl-{3-[(9-oxo-9H-thioxanthene-4-carbonyl)-amino]-propyl}-ammonium iodide (**3g**).*

Yield 52%, mp 263-265 °C (EtOH). ^{1}H NMR (400 MHz, DMSO-d_6) δ 8.90 (br.s, 1H, CONH), 8.66 (br s, 1H, Ar), 8.43 (br s, 1H, Ar), 8.11 (br s, 1H, Ar), 7.85-7.60 (m, 4H, Ar), 3.52-3.33 (m, 4H, NHCH_2, CH_2N), 3.09 (s, 9H, N^+Me_3), 2.05 (br t, 2H, CH_2)

*1-Methyl-3-{[(9-oxo-9H-thioxanthene-4-carbonyl)-amino]-methyl}-pyridinium iodide (**3i**).*

Yield 81%, mp 228-231 °C (MeOH/DMF). ^{1}H NMR (400 MHz, DMSO-d_6) δ 9.57 (br t, 1H, CONH), 9.06 (s, 1H, Ar), 8.93 (d, 1H, *J* 5.6 Hz, Ar), 8.68 (d, 1H, *J* 8.0 Hz, Ar), 8.61 (d, 1H, *J* 8.4 Hz, Ar), 8.43 (d, 1H, *J* 8.0 Hz, Ar), 8.23 (d, 1H, *J* 7.6 Hz, Ar), 8.16 (m, 1H, Ar), 7.85-7.81 (m, 2H, Ar), 7.73 (m, 1H, Ar), 7.62 (m, 1H, Ar), 4.73 (d, 2H, *J* 5.6 Hz, CH_2), 4.39 (s, 3H, N^+Me).

In vitro antitumor assay.

Antiproliferative activity of compounds was evaluated in the culture of human malignant glioma cells (U87MG line). The cells were grown in 24-well plastic plates (TTP, Switzerland) in CO_2-incubator at 37 °C, 5% CO_2. The cells ($2x10^3$ per well) were cultured in Dulbecco's modified Eagle's medium (DMEM, Sigma, USA) supplemented with 2.5% fetal bovine serum (Sigma, USA). In 24 h after cell seeding, tested compounds in DMSO were added to the culture at concentrations 20, 10, 5, 2, 1 and 0.5 μM (final drug concentration in the medium) using a serial dilution approach, and then cells were incubated for 72 h. In all cases, DMSO content in the medium was 0.2%. Preliminary experiments confirmed that DMSO at this concentration did not affect cell growth. The cells cultured in the presence of 0.2% DMSO without drugs were used as a control. After the incubation of cells with or without drugs, the number of viable cells in each well was determined using a standard MTT colorimetric assay [46]. After the treatment wit MTT reagent, optical density in the wells was measured at 570 nm using BioTek ELx800 plate reader (BioTek, USA). Using the absorbance measurements, the percent of growth inhibition as compared with a non-treated control was calculated for each drug concentration. Growth inhibition levels were plotted against inhibitor concentrations, and GI_{50} parameter (drug concentration giving a 50% growth inhibition in comparison with a control culture) was determined for each compound. Each experiment was performed in triplicate. The data are presented as the mean (M) ± standard deviation (SD).

Notes

Acknowledgments. The authors are grateful to Dr. O. Balynska for assistance with biological testing of compounds.

The authors declare no conflict of interest.

Author contributions. **V. G. K.**: synthesis of compounds, investigation. **I. V. A.**: investigation, NMR spectra analysis, writing the experimental part (chemistry). **N. A. L.**: synthesis of compounds. **V. V. N.**: biological experiments, writing the experimental part (biology). **I. Y. D.**: supervision, data analysis, writing, and editing the manuscript.

References

1. Gensicka-Kowalewska, M.; Cholewiński, G.; Dzierzbicka, K. Recent developments in the synthesis and biological activity of acridine/acridone analogues. *RSC Adv*. **2017**, *7*, 15776-15804.
2. Prasher, P.; Sharma, M. Medicinal chemistry of acridine and its analogues. *Medchemcomm*. 2018, *9*, 1589-1618.
3. Buus, J.; Nielsen, J. Phenazine natural products: biosynthesis, synthetic analogues, and biological activity. *Chem. Rev.* **2004**, *104*, 1663-1686.
4. Guttenberger, N.; Blankenfeldt, W.; Breinbauer, R. Recent developments in the isolation, biological function, biosynthesis, and synthesis of phenazine natural products. *Bioorg. Med. Chem*. **2017**, *25*, 6149-6166.
5. Paiva, A. M.; Pinto, M. N.; Sousa, F. A century of thioxanthones: through synthesis and biological applications. *Curr. Med. Chem*. **2013**, *20*, 2438-2457.
6. Piestrzeniewicz, M. K.; Wilmańska, D.; Studzian, K.; Szemraj, J.; Czyż, M.; Denny, W. A.; Gniazdowski, M. Inhibition of RNA synthesis in vitro by acridines – relation between structure and activity. *Z. Naturforsch., C, J. Biosci.* **1998**, *53*, 359-368.

7. Rewcastle, G. W.; Atwell, G. J.; Chambers, D.; Baguley, B. C.; Denny, W. A. Potential antitumor agents. 46. Structure-activity relationships for acridine monosubstituted derivatives of the antitumor agent *N*-[2-(dimethylamino)ethyl]-9-aminoacridine-4-carboxamide. *J. Med. Chem*. **1986**, *29*, 472-477.
8. Atwell, G. J.; Rewcastle, G. W.; Baguley, B. C.; Denny, W. A. Potential antitumor agents. 50. *In vivo* solid-tumor activity of derivatives of *N*-[2-(dimethylamino)ethyl]acridine-4-carboxamide. *J. Med. Chem*. **1987**, *30*, 664-669.
9. Wakelin, L. P. G.; Adams, A.; Denny, W. A. Kinetic studies of the binding of acridine carboxamide topoisomerase poisons to DNA: implications for mode of binding of ligands with uncharged chromophores. *J. Med. Chem*. **2002**, *45*, 894-901.
10. Goodell, J. R.; Madhok, A. A.; Hiasa, H.; Ferguson, D. M. Synthesis and evaluation of acridine- and acridone-based anti-herpes agents with topoisomerase activity. *Bioorg. Med. Chem*. **2006**, *14*, 5467-5480.
11. Ferreira, R.; Aviño, A.; Mazzini, S.; Eritja, R. Synthesis, DNA-binding and antiproliferative properties of acridine and 5-methylacridine derivatives. *Molecules* **2012**, *17*, 7067-7082.
12. Lafayette, E. A.; Vitalino de Almeida, S. M. Synthesis, DNA binding and topoisomerase I inhibition activity of thiazacridine and imidazacridine derivatives. *Molecules* **2013**, *18*, 15035-15050.
13. Janočková, J.; Plšiková, J.; Kova', J.; Jendželovský, R.; Mikeš, J.; Kašpárková, J.; Brabec, V.; Hamulaková, S.; Fedoročko, P.; Kožurková, M. Tacrine derivatives as dual topoisomerase I and II catalytic inhibitors. *Bioorg. Chem*., **2015**, *59*, 168-176.
14. Krokidis, M. G.; Molphy, Z.; Efthimiadou, E. K.; Kokoli, M.; Argyri, S.-M.; Dousi, I.; Masi, A.; Papadopoulos, K.; Kellett, A.; Chatgilialoglu, C. Assessment of DNA topoisomerase I unwinding activity, radical scavenging capacity, and inhibition of breast cancer cell viability of *N*-alkyl-acridones and N,N′-dialkyl-9,9′-biacridylidenes. *Biomolecules* **2019**, *9*, 177-191.
15. Nunhart, P.; Konko'ová, E.; Janovec, L.; Jendželovský, R.; Vargová, J.; Ševc, J.; Matejová, M.; Miltáková, B.; Fedoročko, P.; Kozurkova, M. Fluorinated 3,6,9-trisubstituted acridine derivatives as DNA interacting agents and topoisomerase inhibitors with A549 antiproliferative activity. *Bioorg. Chem*. **2020**, *94*, 103393.
16. Gamage, S. A.; Spicer, J. A.; Rewcastle, G. W.; Milton, J.; Sohal, S.; Dangerfield, W.; Mistry, P.; Vicker, N.; Charlton, P. A.; Denny, W. A. Structure-activity relationships for pyrido-, imidazo-, pyrazolo-, pyrazino- and pyrrolophenazine carboxamides as topoisomerase-targeted anticancer agents. *J. Med. Chem*. **2002**, *45*, 740-743.
17. Yang, P.; Yang, Q.; Qian, X.; Cui, J. Novel synthetic isoquinolino[5,4-ab]phenazines: Inhibition toward topoisomerase I, antitumor and DNA photo-cleaving activities. *Bioorg. Med. Chem*. **2005**, *13*, 5909-5914.
18. Gamage, S. A.; Rewcastle, G. W.; Baguley, B. C.; Charlton, P. A.; Denny, W. A. Phenazine-1-carboxamides: Structure-cytotoxicity relationships for 9-substituents and changes in the H-boding pattern of the cationic side chain. *Bioorg. Med. Chem*. **2006**, *16*, 1160-1168.
19. Zhuo, S.-T.; Li, C.-Y.; Hu, M.-H.; Chen, S.-B.; Yao, P.-F.; Huang, S.-L.; Ou, T.-M.; Tan, J.-H.; An, L.-K.; Li, D.; Gu, L.-Q.; Huang, Z.-S. Synthesis and biological evaluation of benzo[a]phenazine derivatives as a dual inhibitor of topoisomerase I and II. *Org. Biomol. Chem*. **2013**, *11*, 3989-4005.
20. Cuenca, F.; Moore, M. J. B.; Johnson, K.; Guyen, B.; De Cian, A.; Neidle, S. Design, synthesis and evaluation of 4,5-di-substituted acridone ligands with high G-quadruplex affinity and selectivity, together with low toxicity to normal cells. *Bioorg. Med. Chem. Lett*. **2009**, *19*, 5109-5113.
21. Sparapani, S.; Haider, S. M.; Doria, F.; Gunaratnam, M.; Neidle, S. Rational design of acridine-based ligands with selectivity for human telomeric quadruplexes. *J. Am. Chem. Soc*. **2010**, *132*, 12263-12272.
22. Ungvarsky, J.; Plsikova, J.; Janovec, L.; Koval, J.; Mikes, J.; Mikesová, L.; Harvanova, D.; Fedorocko, P.; Kristian, P.; Kasparkova, J.; Brabec, V.; Vojtickova, M.; Sabolova, D.; Stramova, Z.; Rosocha, J.; Imrich, J.; Kozurkova, M. Novel trisubstituted acridines as human telomeric quadruplex binding ligands. *Bioorg. Chem*. **2014**, *57*, 13-29.
23. Gao, C.; Zhang, W.; He, S.; Li, S.; Liu, F.; Jiang, Y. Synthesis and antiproliferative activity of 2,7-diamino l0-(3,5-dimethoxy)benzyl-9(10H)-acridone derivatives as potent telomeric G-quadruplex DNA ligands. *Bioorg. Chem*. **2015**, *60*, 30-36.
24. Negrutska, V. V.; Saraieva, I. V.; Kostina, V. G.; Alexeeva, I. V.; Lysenko, N. A.; Dubey, I. Ya. Telomerase inhibition by new di- and trisubstituted acridine derivatives. *Biopolym. Cell* **2016**, *32*, 468-471.
25. Si, M. K.; Pramanik, S. K.; Ganguly, B. Tuning the ring strain effect in acridine derivatives on binding affinity with G-quadruplex-DNA: A computational and experimental study. *Int. J. Biol. Macromol*. **2019**, *124*, 1177-1185.
26. Bischoff, G.; Hoffmann, S. DNA-binding of drugs used in medicinal therapies. *Curr. Med. Chem*. **2002**, *9*, 321-348.
27. Martinez, R.; Chacon-Garcia, L. The search of DNA-intercalators as antitumoral drugs: what it worked and what did not work. *Curr. Med. Chem*. **2005**, *12*, 127-151.
28. Pindur, U.; Jansen, M.; Lemster, T. Advances in DNA-ligands with groove binding, intercalating and/or alkylating activity: chemistry, DNA-binding and biology. *Curr. Med. Chem*. **2005**, *12*, 2805-2847.
29. Paul, A.; Bhattacharya, S. Chemistry and biology of DNA-binding small molecules. *Curr. Sci*. **2012**, *102*, 212-231.
30. Neidle, S. Quadruplex nucleic acids as novel therapeutic targets. *J. Med. Chem*. **2016**, *59*, 5987-6011.
31. Spiegel, J.; Adhikari, S.; Balasubramanian, S. The structure and function of DNA G-quadruplexes. *Trends Chem*. **2020**, *2*, 123-136.
32. Gatasheh, M.K.; Kannan, S.; Hemalatha, K.; Imrana, N. Proflavine an acridine DNA intercalating agent and strong antimicrobial possessing potential properties of carcinogen. *Karbala Int. J. Mod. Sci*. **2017**, *3*, 272-278.
33. Zozulya, V.; Blagoi, Yu.; Löber, G.; Voloshin, I.; Winter, S.; Makitruk, V.; Shalamay, A. Fluorescence and binding properties of phenazine derivatives in complexes with polynucleotides of various base composition and secondary structure. *Biophys. Chem*. **1997**, *65*, 55-63.
34. Cimmino, A.; Evidente, A.; Mathieu, V.; Andolfi, A.; Lefranc, F.; Kornienko, A.; Kiss, R. Phenazines and cancer. *Nat. Prod. Rep*. **2012**, *29*, 487-501.
35. Atwell, G. J.; Cain, B. F.; Baguley, B. C.; Finlay, G. J.; Denny, W. A. Potential antitumor agents. Part 43. Synthesis and biological activity of dibasic 9-aminoacridine-4-carboxamides, a new class of antitumor agent. *J. Med. Chem*. **1984**, *27*, 1481-1486.
36. Stankiewicz-Drogon, A.; Palchykovska, L. G.; Kostina, V. G.; Alexeeva, I. V.; Shved, A. D.; Boguszewska-Chachulska, A. M. New acridone-4-carboxylic acid derivatives as potential inhibitors of *Hepatitis C* virus infection. *Bioorg. Med. Chem*. **2008**, *16*, 8846-8852.
37. Stankiewicz-Drogon, A.; Dörner, B.; Erker, T.; Boguszewska-Chachulska, A.M. Synthesis of new acridone derivatives, inhibitors of NS3 helicase, which efficiently and specifically inhibit subgenomic HCV replication. *J. Med. Chem*. **2010**, *53*, 3117-3126.
38. Kostina, V. G.; Alexeeva, I. V.; Lysenko, N. A.; Negrutska, V. V.; Dubey, I. Ya. Synthesis and biological evaluation of new derivatives of tricyclic heteroaromatic carboxamides as potential topoisomerase I inhibitors. *Ukr. Bioorg. Acta*. **2016**, *14*, 3-8.
39. Palchykovska, L. G.; Alexeeva, I. V.; Kostina, V. G.; Platonov, M. O.; Negrutska, V. V.; Deriabin, O. M.; Tarasov, O. A.; Shved, A. D. New amides of phenazine-1-carboxylic acid: antimicrobial activity and structure-activity relationship. *Ukr. Biokhim. Zh*. **2008**, *80*, 140-147 (in Ukr.).
40. De Logu, A.; Palchykovska, L. H.; Kostina, V. H.; Sanna, A.; Meleddu, R.; Chisu, L.; Alexeeva, I. V.; Shved, A. D. Novel *N*-aryl- and *N*-heteryl phenazine-1-carboxamides as potential agents for the treatment of infections sustained by drug-resistand and multidrug-resistand *Mycobacterium tuberculosis*. *Int. J. Antimicrob. Agents* **2009**, *33*, 223-229.
41. US Patent No 5380749. Thioxanthenone antitumor agents / Miller, T. C.; Collins, J. C.; Mattes, K. C.; Wentland, M. P.; Perni, R. B.; Corbett, T. H.; Guiles, J. W. Patent appl. No 8/216989 23.03.1994. Publ. 10.01.1995.
42. Palmeira, A.; Vasconcelos, M. H.; Paiva, A.; Fernandes, M. X.; Pinto, M.; Sousa, E. Dual inhibitors of P-glycoprotein and tumor cell growth: (re)discovering thioxanthones. *Biochem. Pharmacol*. **2012**, *83*, 57-68.
43. Lima, R. T.; Sousa, D.; Paiva, A. M.; Palmeira, A.; Barbosa, J.; Pedro, M.; Pinto, M. M.; Sousa, E.; Vasconcelos, M.H. Modulation of autophagy by a thioxanthone decreases the viability of melanoma cells. *Molecules* **2016**, *21*, 1343-1357.
44. Rewcastle, G. W.; Denny, W. A. The synthesis of substituted 9-oxoacridan-4-carboxylic acids. Part 2. The use of 2-iodoisophthalic acid in the Jourdan-Ullmann reaction. *Synthesis* **1985**, *1985*, 217-220.
45. Zhu, X.; Yang, J.; Zhao, G.; Luo, X.; Zhang, Q.; Mao, G.; Nie, J. Synthesis and characterization of highly efficient thioxanthone-based macrophotoinitiator. *Sci. J. Mater. Sci*. **2012**, *2*, 1-8.
46. Carmichael, J.; DeGraff, W. G.; Gazdar, A. F.; Minna, J. D.; Mitchell, J. B. Evaluation of a tetrazolium-based semiautomated colorimetric assay: assessment of chemosensitivity testing. *Cancer Res*. **1987**, *47*, 936-942.

Катіонні карбоксамідні похідні трициклічних гетероароматичних сполук: синтез та попередня оцінка антипроліферативної активності

В. Г. Костіна, І. В. Алексєєва, Н. А. Лисенко, В. В. Негруцька, І. Я. Дубей*

Інститут молекулярної біології і генетики НАН України, вул. Заболотного, 150, Київ, 03680, Україна

Резюме: Метою роботи був синтез і вивчення біологічної активності карбоксамідів трициклічних гетероароматичних систем акридону, феназину та тіоксантону, що містять катіонні замісники в амідній функції. Вказані гетероциклічні ядра є ДНК-інтеркаляторами, а введення в них катіонних груп може забезпечити додаткові йонні взаємодії лігандів з їхніми біологічними мішенями, зокрема, ДНК й ферментативними комплексами системи біосинтезу нуклеїнових кислот. Модифікацію вказаних гетероциклів такими групами зручно здійснювати через карбоксамідні похідні. Виходячи з цього, було отримано невелику бібліотеку *N*-заміщених аліфатичних і ароматичних катіонних похідних амідів акридон-4-, феназин-1- та тіоксантон-4-карбонових кислот. Їх синтезували з виходом 37-81% з використанням м'якої селективної реакції кватернізації йодистим метилом атомів азоту в *N,N*-диметиламіноалкільних (алкіл = етил, пропіл) і піридилметильних фрагментах нейтральних *N*-функціоналізованих карбоксамідів. При цьому трициклічні ядра не реагують. Розроблено зручний протокол синтезу тіоксантон-4-карбонової кислоти (ТСА), що ґрунтується на реакції 2-меркаптобензойної та 2-йодбензойної кислот із наступною циклізацією інтермедіату (вихід 79%). Отримано також серію нових нейтральних *N*-функціоналізованих амідів ТСА, які є прекурсорами відповідних катіонних карбоксамідів, взаємодією її хлорангідриду з амінами. Попереднє тестування чотирьох карбоксамідів *in vitro* як потенційних протипухлинних засобів проводили в культурі клітин U87MG (злоякісна гліома людини). Сполуки виявили значну антипроліферативну активність у низьких мікромолярних концентраціях; їхні показники інгібування клітинного росту GI_{50} знаходяться в межах 1.7-11 мкМ. Отримані дані свідчать про те, що катіонні карбоксаміди трициклічних гетероароматичних систем є перспективними скафолдами для дизайну нових протипухлинних препаратів.

Ключові слова: акридон; феназин; тіоксантон; карбоксаміди; протипухлинні засоби.

ISSN 1814-9758. Ukr. Bioorg. Acta, 2020, Vol. 15, N 1
UDC 615.322
DOI: hpps://doi.org/10.15407/bioorganica2020.01.042

Ukrainica Bioorganica Acta
www.bioorganica.org.ua

UBA

RESEARCH ARTICLE

Investigation of the extract's composition of Viper's bugloss *(Echium vulgare)*

Anna R. Kapusterynska, Vira R. Hamada, Anna S. Krvavych, Roksolana T. Konechna, Maria S. Kurka, Volodymyr P. Novikov*

Lviv Polytechnic National University, 3/4 St. Yura Sq., Lviv, 79013, Ukraine.

Abstract: The characteristics of Viper's bugloss (*Echium vulgare*) plant, its pharmacological properties, and extracts' composition are presented in this study. Results of the literature analysis, data on the biologically active compounds and areas of use of this medicinal plant are summarized. Viper's bugloss (*E. vulgare*) is a species of flowering plant in the borage family *Boraginaceae*. It is native to most of Europe as well as western and central Asia. Viper's bugloss (*E. vulgare*) is a plant that has been utilized as food (honey), medicine, a poison, an oil, and as a dye and tannin-producing ornamental plant. Viper's bugloss (*E. vulgare*) is especially rich in pyrrolizidine alkaloids, flavonoids, phenolcarboxylic acids, sterones and naphthoquinones. In traditional medicine, Viper's bugloss (*E. vulgare*) is utilized as exhilarant and a mood stimulant. That is why one of the possible uses of this plant is considered to be treatment of depressive states. Like most representatives of *Boraginaceae* family, it has been insufficiently studied. No previous work quantifying flavonoids content of aerial parts of Viper's bugloss (*E. vulgare*) growing in Ukraine has been presented. Continuing the studies of this species, the aqueous and ethanolic extracts from Viper's bugloss (*E. vulgare*) aerial parts were obtained and their phytochemical composition was investigated. For the first time, the qualitative analysis of biologically active compounds in Viper's bugloss's extract as well as the quantitative analysis of flavonoids by aluminum chloride spectrophotometric method are reported. The experimental results showed that the total concentration of flavonoids was 2.59% in the extract. The maximum yield of extractives was found to be 16%. The obtained research data will be used in future investigations.

Keywords: Viper's bugloss (*Echium vulgare*); biologically active substances; flavonoids; depression.

Introduction

Depressive disorders, including major depression and dysthymia, are serious, disabling, and often difficult-to-treat illnesses. A promising direction in the treatment of depressive disorders is the study of existing and creation of new effective herbal remedies. A large number of herbal antidepressants on the Ukrainian market, such as "Life 900", "Sedariston", "Neuroplant", "Deprivit" and others, based on the extract of St. John's wort (*Hypericum perforatum*).

Among these objects of research, the well-known honeysuckle Viper's bugloss (*Echium vulgare*) attracts special attention as a promising source of biologically active substances (BAS) for the treatment of depression [1]. This paper analyzes the literature sources that contain information on the chemical composition of the plant, its application in folk and traditional medicine and prospects for its use. We also presented our studies of the quantitative content of extractive substances, flavonoids, and qualitative determination of various BAS groups in the plant raw materials [2].

Results and Discussion

Viper's bugloss (*E. vulgare*), or Blueweed, is a species of flowering plant in the borage family of *Boraginaceae*. Viper's bugloss (*E. vulgare*) can be biennial or short-lived perennial. The stems of mature plants are straight and reaching over 70 cm in height. Stem leaves are alternate, linear-lanceolate, sessile, basal leaves narrowed to a petiole,

Received: 20.05.2020
Revised: 03.06.2020
Accepted: 10.06.2020
Published online: 30.06.2020

* Corresponding author. Tel.: +380-32-258-2478;
e-mail: tbsfb.dept@lpnu.ua (V.P. Novicov)
ORCID: 0000-0002-0485-8720

dry up during the flowering stage. Both stems and leaves are covered with stout. The stem terminates in a panicle inflorescence, and each branch of the panicle forms a short helicoid cyme subtended by an upper foliage leaf. There can be as many as 50 cymes per stem, and each cyme bears up to 20 flowers on the top. The showy flowers range in size from 1 to 2 cm. The funnel-shaped, five-lobed flowers are typically bright blue, but may also be purple, pink or rarely, white (Figure 1). The seeds of Viper's bugloss (*E. vulgare*) are called nutlets. They are brown or gray with a rounded pyramid shape and are quite small. [3].

Figure 1. Viper's bugloss (*E. Vulgare*).

Viper's bugloss (*E. vulgare*) grows throughout Ukraine. It grows best in sunny areas, such as meadows, overgrazed pastures, poorly drained slopes and roadsides. It usually will not do well in cultivated ground. [4].

E. vulgare belongs to dye and tannin producing, medicinal, ornamental, and bee plants since it is a source of nectar and pollen forage. The flowers of *E. vulgare* are frequently visited by bumblebees and honey bees. Nectar contains 30-40% sugars and is mostly sucrose-dominated. Honey productivity is 300-400 kg/ha. Honey from *E. vulgar*e has a light color, a pleasant smell, and a delicate taste. It contains a number of components that act as conservatives, such as vitamin C, flavonoids, and other phenols, as well as enzymes like glucose oxidase, catalase, and peroxidase, so it can remain preserved in a completely edible form for a long time. Basal leaves and young shoots of *E. vulgare* can be eaten in salads or stirfried.

The decoction of the Blueweed is used in folk medicine as an expectorant and soothing remedy for common or whooping cough, and as anticonvulsant and sedative for epilepsy. It is also used externally against rheumatic pains in joints, tendon sprains etc. [5]. *E. vulgare* contains hepatotoxic pyrrolizidine alkaloids such as cynoglossin and consolidin, which can be toxic to horses and cattle when consumed in large amounts. Its roots yield a water-insoluble carmine-red dye alkannin for wool, and its flowers contain anthocyanin, which appears as a red pigment in acidic and blue in alkaline conditions. Viper's bugloss (*E. vulgare*) has been planted as an ornamental plant. It also has the fatty acid composition of the seed oil (28-32%) and is grown as an oilseed crop. The seed oil from *E. vulgare* contains significant amounts of omega-3 and omega-6 polyunsaturated fatty acids (PUFA) such as g-linolenic acid (GLA) and rare stearidonic acid (SDA) [3].

Based on literature reports on the chemical composition of the Viper's bugloss (*E. vulgare*), we can identify the following groups of BAS (Figure 2):

• flavonoids (derivatives of kaempferol, quercetin, quercitrin, hesperidin, hesperetin, rutin, naringenin, naringin, apigenin);

• alkaloids (echimidine, acetylechimidine, uplandicine, 9-*O*-angelylretronecine, echiuplatine, leptanthine, echimiplatine, echivulgarine, vulgarine, and 7-*O*-acetylvulgarine);

• tannins (in the roots (1.59%), leaves, flowers (0.98%), stems (0.58%));

• dyes (alkannin in the roots and anthocyanin in the flowers);

• fatty acids (saturated palmitic (5.65-17.81%), stearic (1.49-5.08%) fatty acids, mono-unsaturated oleic (8.83-55.32%), eicosenoic (0.22-6.21%), erucic (0.04-8.94%), nervonic (0.08-2.71%) fatty acids, and PUFAs such as linoleic (between 1.41 and 68.44%) and stearidonic acids (between 0.02 and 14.59%);

• polysaccharides (D-galactose, D-glucose, L-arabinose, and L-rhamnose);

• amino acids (16 amino acids, including 7 essential: lysine (247.10 µg/100 mg), tyrosine (236.20 µg/100 mg), glutamic (184.95 µg/kg) and aspartic acids (186.35 µg/100 mg) in the roots; phenylalanine (244.53 µg/100 mg), glutamic acid (488.20 µg/kg), and glycine (283.54 µg/100 mg) in the shoots;

• phenolic acids (gallic, benzoic, isopherulic, chlorogenic, vanillic, salicylic, ferulic, p-hydroxybenzoic, protocatechuic, alpha-coumaric and p-coumaric acids, catechol, catechin);

• microelements (potassium (9.660 µg/kg in the roots, 9.170 µg/kg in the shoots), calcium (2.710 µg/kg in the roots, 2.220 µg/kg in the shoots); the content of silicon in the shoots is 2.580 µg/kg, which is 1.7 times higher than in the roots) [5-7].

The major phytochemicals that were recognized in *E. vulgare* extract are kaempferol 3-*O*-neohesperidoside **1**, which is a derivative of kaempferol **2**, uridine **3**, 3-(3,4-dihydroxyphenyl)lactic acid **4**, and rosmarinic acid **5** (Figure 2) [8].

Iranian scientists at Mashhad University of Medical Sciences have found that the aqueous and ethanolic flavonoids-containing extracts of *E. vulgare* inhibit mono-amino oxidase enzyme (MAO) that can leads to a significant antidepressant effect [9]. The potential antidepressant effects of extracts of *E. vulgare* were investigated on mice using a forced swimming test. This

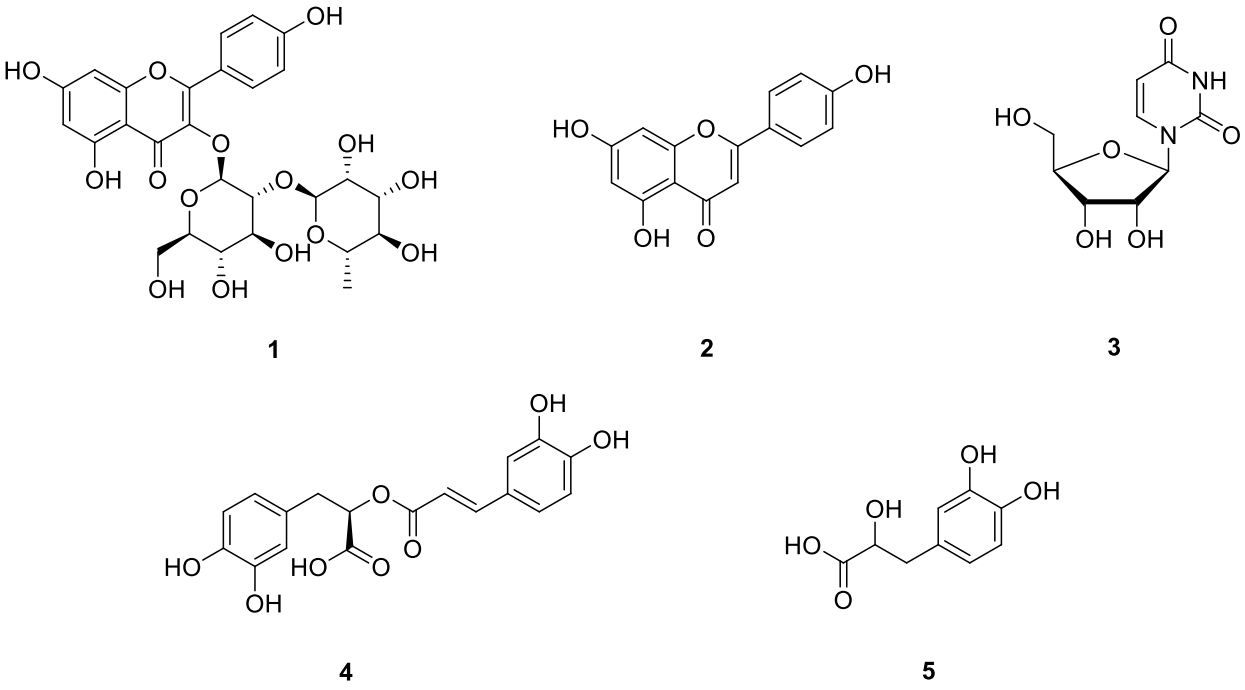

Figure 2. The major components of the Viper's bugloss (*E. vulgare*) alcoholic extract: kaempferol 3-*O*-neohesperidoside **1**, kaempferol **2**, uridine **3**, 3-(3,4-dihydroxyphenyl)lactic acid **4** and rosmarinic acid **5**.

test was performed in two sessions. In the pretest session (24 hours before the main session), each mouse (BALB/c male, weight 25-30 g) was forced to swim in a cylindrical-shaped container (diameter 10 cm, height 25 cm, water height 11 cm, temperature 25±1 °C). This preliminary test is stress-inducing and mice gradually lose their movement behavior. After 15 minutes, animals were removed and dried. Then, 23.5 hours later the relevant extract sample was injected intraperitoneally (IP) into mice. The main test was performed 30 minutes later. In this test, each mouse was left in the same container for 6 minutes and the following behaviors were recorded:

1. Immobility: floating in the water without swimming.
2. Swimming: active movement of extremities and circling in the container.
3. Climbing: active movement of forelimbs on the container wall.

The tests were performed on three groups of mice, eight mice in each. The first group received the drug imipramine, which is a selective inhibitor of monoamine reuptake (antidepressant). Group 2 received aqueous and alcoholic extracts of Viper's bugloss (*E. vulgare*) in various concentrations. The results showed that the extracts have a clear antidepressant activity that is comparable to imipramine. [9].

The pyrrolizidine alkaloids previously identified in floral honey attributed to *E. vulgare* were detected by Boppre *et al.* in Germany. Pyrrolizidine alkaloids were isolated from the aqueous acid extracts of pollen by use of strong cation-exchange, solid-phase extraction and identified by liquid chromatographic/mass spectrometric (LCMS) analysis. The pyrrolizidine alkaloids in the pollen are present mainly as the *N*-oxides. In addition to the previously described pyrrolizidine alkaloids and/or their *N*-oxides (echimidine, acetylechimidine, uplandicine, 9-*O*-angelylretronecine, echiuplatine, leptanthine, and echimiplatine), one unidentified (echivulgarine), but previously found in honey, and two previously undescribed (vulgarine and 7-*O*-acetylvulgarine) pyrrolizidine alkloids and/or their *N*-oxides were identified in the pollen [10]. Pyrrolizidine alkaloid-containing plants are widely distributed throughout the world. The structural types and concentrations of the alkaloids vary among plant species. In addition, within a species of plant, concentrations vary with environment and location. Many pyrrolizidine alkaloids are toxic and cause poisoning in livestock and humans [11-13]. That is why to detect and determine the content of alkaloids in specific plants it is necessary to develop a rapid, sensitive, and specific method, which will be one of our goals of future research.

Experimental section

The source material for phytochemical studies was the stems of Viper's bugloss (*E. vulgare*), which was collected in the Mykolaiv region during the period of maximum accumulation BAR (July 2019). The procurement of raw materials was carried out according to regulatory and analytical documentation [2]. Air-dried raw materials were prepared in an Excelsior-shredding Machine. Studies of the

extracts were performed according to standard methods using reagents that were supplied by Sigma-Aldrich Corp. and Merk. Analytical scales AS 220 from RADWAG, Poland was used to weigh samples.

The amount of extractives was measured by the gravimetric method [2]. The maximum yield of extractives was 16%.

The method of UV spectroscopy (Hitachi U-2810 spectrophotometer) was used to detect the quantitative content of flavonoids. The aluminum chloride method was used to determine the total flavonoid compounds [3]. The content of flavonoids in terms of avicularin and absolutely dry raw material in percent (X) was calculated by the formula:

$$x = \frac{D \times 100 \times 100 \times 25}{330 \times m \times (100 - W)}$$

where D is the optical density of the test solution; 330 – specific absorption rate of avicularin complex with aluminum chloride at 410 nm; m – weight of sample in grams; W – weight loss during drying of raw materials, %.

The powdered plant materials in the amount of 1 g was loaded into a 150 ml flask, 30 ml of 70% alcohol was added and refluxed in a water bath for 30 minutes. The flask was cooled to room temperature, and the mixture were passed through filter paper into a 100 ml volumetric flask. The extraction protocol was repeated 2 times as described above. The combined extracts were filtered, the solids were washed with 70% alcohol and the volume of the filtrate was adjusted to the mark (solution A).

Solution A (4 ml) was loaded into a 25 ml volumetric flask, 2 ml of a 2% solution of aluminum chloride in 95% ethanol was added and brought the volume with a 95% ethanol to the mark; after 20 min, the optical density of the solution was determined using spectrophotometer at a wavelength of 410 nm in a cuvette with a layer thickness of 10 mm. For comparison, the following solution was used: 4 ml of solution A was loaded into a 25 ml volumetric flask, a 1 drop of a dilute hydrochloric acid was added and the volume of the solution was adjusted to the mark with 95% ethanol. The flavonoid content was calculated based on dry raw material and found to be 2.59%.

With the help of qualitative reactions, the analysis for the presence of certain groups of BAS of medicinal plant raw materials was performed. The results of the identified substances are presented in Table 1.

Therefore, the obtained data demonstrated the presence of BAS in the object under study and provide insentives for further study.

It should be noted that the presence echimidine in the extract of the Viper's bugloss (*E. vulgare*) requires additional studies on the toxicity of extracts from this plant. Because this plant is widely used as a honey plant and contains alkaloids, there are several studies on their presence in honey.

Table 1. The results of the qualitative analysis of the Viper's bugloss (*E. vulgare*) shoot extract.

BAS	Reagents	Results
Alkaloids	50% C_2H_5OH, 95% C_2H_5OH, Mg (dust), conc. HCl	+ (red solution)
	Bouchard-Wagner $K[I_3]$	+ (red-brown precipitate)
	Sonnenschein 1% $H_3PO_4 \cdot 12MoO_3 \cdot 2H_2O$	+ (amorphous precipitates with yellowish color)
	0,1% tannic acid soluton	+ (colorless)
Tannins	1% gelatin solution	+ (precipitate → dissolves in excess of reagent)
	$NH_4Fe(SO_4)_2 \cdot 12\ H_2O$	+ (dirty green)
	10% CH_3COOH, 10% $Pb(CH_3COO)_2$	+ (precipitate)
	1% $NH_4Fe(SO_4)_2 \cdot 12\ H_2O$, solid CH_3COONa	+ (dirty green precipitate)
Saponins	Foaming	+
	Salkowsky $CHCl_3$, conc. H_2SO_4	+ (dirty orange solution)
	$FeCl_3$, $K_4[Fe(CN)_6]$	+ (blue solution)
	$CuSO_4$, 1% NH_4SCN	+ (white precipitate)
	$NaHCO_3$, $FeSO_4$, H_2SO_4 aq. sol.	+ (purple → colorless)
Polysaccharides	95% C_2H_5OH	+ (precipitate)

Conclusions

The literature review has shown that Viper's bugloss (*E. vulgare*) as a study object has several advantages and

disadvantages. The positive characteristics of the raw material include its availability and high prevalence. Viper's bugloss (*E. vulgare*) grows throughout Ukraine (rocky slopes, steppes, dry meadows, crops, fields). Significant antidepressant effect is equal in power to the official drugs and confirmed by foreign preclinical studies as well as public sector research of this raw material. The negative characteristics include the presence of pyrolyzidine alkaloids among the plant's secondary metabolites, which are dangerous to human health due to their hepatotoxic effect. On the other hand, this opens new horizons in the study of the psychotropic activity of the Viper's bugloss (*E. vulgare*) along with the development of methods to diagnose the toxicity of raw materials. Studies of Viper's bugloss (*E. vulgare*) indicate the relevance and prospects for further pharmacognostic and pharmacological studies of the plant.

Notes

Author contributions. **A. R. K., A. S. K.**: performed the spectrophotometric analysis. **V. R. H., R. T. K.**: a qualitative and quantitative analysis. **A. S. K.**: wrote the manuscript. **M. S. K.**: writing review. **V. P. N.**: conceptualization, supervision.

References

1. Kapusterynska A. R., Hamada V. R., Krvavych A. S., Konechna R. T., Novikov V. P. Perspektyva vykorystannia dosvidu narodnoi medytsyny dlia likuvannia depresyvnykh ta tryvozhnykh staniv, 6th International Scientific and Practical Internet Conference "Modern Movement of Science", Dnipro, Ukraine, **2019**, 418-423 (In Ukrainian).
2. State Pharmacopoeia of Ukraine. State Enterprise "Scientific-Expert Pharmacopoeia Center", 1st ed., RIREG: Kharkiv, 2001; p 376 (In Ukrainian).
3. Wikipedia contributors. Echium vulgare [Internet]. Wikipedia, The Free Encyclopedia; 2020 Jan 9, 19:38 UTC. Available from: https://en.wikipedia.org/w/index.php?title=Echium_vulgare&oldid=93499075. (accessed on June 10, 2020).
4. Medicinal plants: Encyclopedic Reference book, Grodzinsky, A. M., Ed., UVKTS "Olimp": Kyiv, 1992; p 397 (In Ukrainian).
5. Gontova, T. M. Study of blueweed polysaccharides. Problems of ecological and medical genetics and clinical immunology **2013**, *116*, 132-137 (In Ukrainian).
6. Ozcan, T. Analysis of the total oil and fatty acid composition of seeds of some Boraginaceae taxa from Turkey. Plant Systematics and Evolution **2008**, *274*. 143-153.
7. Alsanie, W. F. et al. Viper's Bugloss (Echium Vulgare L) Extract as A Natural Antioxidant and Its Effect on Hyperlipidemia. International Journal of Pharmaceutical and Phytopharmacological Research (eIJPPR) **2018**, *8*, 81-89.
8. Kuruuzum-Uz, A. et al. Phytochemical and antimicrobial investigation of Echium vulgare growing in Turkey. Biochemical systematics and ecology **2004**, *32*, 833-836.
9. Moalem, S. A.; Hosseinzadeh, H.; GhonchehIranian, F. Evaluation of Antidepressant Effects of Aerial Parts of Echium vulgare on Mice. Iran J. Basic Med. Sci. **2007**, *10*, 189-196.
10. Boppre, M.; Colegate, S. M.; Edgar, J. A. Pyrrolizidine alkaloids of Echium vulgare honey found in pure pollen. J. Agric. Food Chem. **2005**, *53*, 594-600.
11. Lee, S. T.; Schoch, T. K.; Stegelmeier, B. L.; Gardner, D. R. et al. Development of enzyme-linked immunosorbent assays for the hepatotoxic alkaloids riddelliine and riddelliine N-oxide. J. Agric. Food Chem. **2001**, *49*, 4144-4151.
12. Mashtaler, L. V. V. Content of amino acids in dense extracts from raw material of Echium vulgare L. Zaporozhye medical journal. **2013**, *79*, 43-44 (In Ukrainian).
13. Gontova, T.M.; Mashtaler, V.V.; Mishneva, K.D. Investigations organic acids and vitamins in raw materials of the Symphytum and the Echium genus. Phytochemical researches **2013**, *25*, 44-46 (In Ukrainian).

Дослідження компонентного складу екстрактів синяка звичайного (*Echium vulgare*)

А. Р. Капустеринська, В. Р. Гамада, А. С. Крвавич, Р. Т. Конечна, М. С. Курка, В. П. Новіков*

Національний університет «Львівська політехніка», пл. Св. Юра, 3/4, Львів, 79013, Україна

Резюме: Об`єктом наших досліджень було обрано траву синяка звичайного *(Echium vulgare)*. В цій статті надається узагальнена характеристика лікарської рослини синяка звичайного *(E. vulgare)*, його фармакологічних властивостей, вмісту біологічно активних речовин. Синяк звичайний *(E. vulgare)* - це вид квітучої рослини сімейства шорсткolистих *(Boraginaceae)*. Поширений синяк по всій Україні. Заготовляють його у районах поширення. Синяк звичайний *(E. vulgare)* - медоносна, харчова, лікарська, отруйна, танідоносна, фарбувальна, олійна і декоративна рослина. Синяк звичайний *(E. vulgare)* особливо багатий алкалоїдами піролізидину, флавоноїдами, фенолкарбоновими кислотами, фітостеронами та нафтохінонами. Ця лікарська рослина, як і більшість представників *Boraginaceae*, недостатньо вивчена. Продовжуючи працювати з дослідженням цього виду, отримали водні та етанольні екстракти з надземної частини синяка звичайного *(E. vulgare)* та визначали їх фітохімічний склад. Вперше наводиться аналіз якісного складу синяка звичайного *(E. vulgare)*, що росте в Україні, щодо вмісту біологічно активних речовин та визначений кількісний вміст флавоноїдів за допомогою спектрофотометричного методу. Експериментальні результати показали, що загальний вміст флавоноїдів становить 2,59%. Максимальний вихід екстрактивних речовин становив 16%. У традиційній медицині синяк звичайний *(E. vulgare)* використовується як кровоочисний та протисудомний засіб,а також як стимулятор настрою. Ось чому рослина розглядається з точки зору можливого використання при лікуванні депресивних станів. Не було зафіксовано жодної попередньої роботи щодо кількісного вмісту флавоноїдів у надземній частині синяка звичайного *(E. vulgare)*, що росте в Україні. Отримані дані будуть використані у майбутніх дослідженнях.

Ключові слова: синяк звичайний *(Echium vulgare)*; біологічно активні речовини; флавоноїди; депресія.

ISSN 1814-9758. Ukr. Bioorg. Acta, 2020, Vol. 15, N 1
UDC 544.6 + 541.138.3: 539.2: 539.216
DOI: hpps://doi.org/10.15407/bioorganica2020.01.047

UBA
Ukrainica Bioorganica Acta
www.bioorganica.org.ua

RESEARCH ARTICLE

The mathematical description of dopamine electrochemical oxidation, accompanied by its chemical and electrochemical polymerization

Volodymyr V. Tkach[1,2]*, Marta V. Kushnir[1], Yana G. Ivanushko[3], Svitlana M. Lukanova[1], Silvio C. de Oliveira[2], Petro I. Yagodynets[1]

[1] *Yuriy Fedkovich Chernivtsi National University, 2 Kotsiubynsky St., Chernivtsi, 58012, Ukraine*
[2] *Universidade Federal de Mato Grosso do Sul, Ave. Sen. Felinto. Müller, 1555, C/P. 549, 79074-460, Campo Grande, MS, Brazil*
[3] *Bukovinian State Medical University, 9 Teatralna Sq., Chernivtsi, 58000, Ukraine*

Abstract: The electrooxidation of dopamine is accompanied by its chemical and electrochemical polymerization, and in which either the monomer or the polymer may be oxidized to the respective quinonic form, was investigated from the theoretical point of view. Dopamine is one of the important neurotransmitters in human and mammal organisms. It is a precursor to epinephrine, which influences the cardiovascular, hormonal and renal functions. Its lack causes diseases like Parkinson, therefore, dopamine has been used as a drug for their treatment. On the other hand, its excess stimulates the sympatic nervous system yielding the metabolic disorders and even schizophrenia. Thus, the development of the rapid and accurate method for its concentration measurement is very important. Dopamine is very popular analyte in electroanalytical systems. The modified electrodes for its determinations have been developed by many researchers. Dopamine is widely used as a monomer for synthesis of a conducting polymer – polydopamine, whis is used as electrodes' modifier in capacitors and in anticorrosive coatings. The electropolymerization of dopamine into polydopamine proceeds along with its traditional quinone-hydroquinonic oxidation. Both processes give their impact to the electrochemical behavior of dopamine during its electropolymerization. The mechanism's complexity is also responsible for the electrochemical instabilities during electro-oxidation. In order to understand these instabilities it's necessary to develop the mathematical model that is capable to describe the behavior of the system. It also helps us to esteem the influence of the electrochemical instabilities, by which it may be accompanied. The goal of this work is to describe an electrochemical oxidation and polymerization of dopamine that will provide an important connection between the electrochemical detection of biologically active compounds and their electropolymerization for electrode modification.

Keywords: dopamine; polydopamine; electrooxidation; electropolymerization; mathematical model.

Introduction

Dopamine is a hormone and one of the major neurotransmitters in human and mammalian organisms [1-4] that is synthesized in the body. It is a member of the catecholamine family of neurotransmitters in the brain and is a precursor to epinephrine (adrenaline) and norepinephrine (noradrenaline) hormons [5]. Its lack causes illnesses like Parkinson disease [6], therefore it can be used as a drug in medical protocols [7]. Its excess can cause different effects on sympathic segment of neurosystem, methabolic disturbance and even schizophrenia [8]. Therefore, the development of a novel method that is capable to detect its concentration in a rapid, precise, accurate and sensitive way is very important task.

Chemically modified electrodes have various advantages, the main of which is the affinity between the modifier and the analyte, reason why they are one of the modern, cheap and tunable electroanalytic tools. For example, for detection of hydroquinonic compounds, various electrode modifiers of a different nature and composition were developed [9-15]. Some hydroquinonic and quinonic compounds may also serve as electrode

Received: 03.04.2020
Revised: 10.04.2020
Accepted: 14.05.2020
Published online: 30.06.2020

* Corresponding author. Tel.: +380-50-640-0359;
e-mail: nightwatcher2401@gmail.com (V. V. Tkach)
ORCID: 0000-0001-7696-0954

modifiers [16-17]. Dopamine is a polymerizable compound [18] and its polymer can be used as an electrode modifier similarly as of polyalizarine [19]. Moreover, if the supporting electrolyte contains oxidizing ions, they can promote chemical polymerization of dopamine. In order to evaluate the effect of polymerization by the electrochemical (electroanalytical) process it´s necessary to investigate the system with polymerization-accompanied electrochemical oxidation of dopamine from mechanistic point of view.

Therefore, it's important to develop and analyze the mathematical model that is capable to describe the behavior of the system. It will be useful us to evalate the influence of the electrochemical instabilities that can be occurred [20-21].

The goal of this work is to evaluate by mechanistic way the influence of chemical and electrochemical polymerization of dopamine and introduce an important connection between the electrochemical detection of biologically active compounds and their electropolymerization.

System and its modeling

The dopamine polymerization is occured in electrode potential lower than for benzolic compounds. It is due to the presence of donor groups (two hydroxyls and an ethylamine group) in the benzene ring, therefore, the number of chemical oxidants that is capable to promote polymerization, has to be higher compared to benzene. The bond between monomer units is formed either by participation of oxygen, or by creating C-C bond between positions 3 and 6 of the ring.

While the hydroquinonic structure is present (at least in part) in the polymer backbone, the polymer can be also oxidized further to its quinonic form. The oxidation of hydroquinonic monomer units makes the system similar to so called "polythiophene paradox" [22]. The electrochemical oxidation of the dopamine polymer is reversable in nature while overoxidation of the same polymer is irreversible. Therefore we can safely assume that these processes are different.

Taking in account the described assumptions, we are introducing three variables:

c – the dopamine concentration in the pre-surface layer;

θ – dopamine coverage degree;

θ_p – polydopamine (chemically, or electrochemically obtained) coverage degree.

In order to simplify the mathematical model, we introduce several assumptions:

• the background electrolyte is present in an excess, therefore we can disregard the migration flow and the oxidizing dopant concentration change;

• the reactor is intensively stirred, so we can disregard the influence of convection flow;

• the concentration profile of dopamine in the pre-surface layer is linear;

• the thickness of pre-surface layer is constant and equal to δ.

It is possible to demonstrate that the differential equations' set that are describing the electrochemical oxidation system can be defined as following:

$$\begin{cases} \dfrac{dc}{dt} = \dfrac{2}{\delta}\left(\Delta/\delta\,(c_0 - c) + r_{-1} - r_1\right) \\ \dfrac{d\theta}{dt} = \dfrac{1}{G}\left(r_1 - r_{-1} - r_2 - r_{p1} - r_{p2}\right) \\ \dfrac{d\theta_p}{dt} = \dfrac{1}{J}\left(r_{p1} + r_{p2} - r_3\right) \end{cases} \quad (1)$$

where Δ is the dopamine diffusion coefficient to from electrolite to the surface, c_0 is its concentration in the solution, G and J are the maximal surface concentration of the dopamine and its polymer correspondengly, and the parameters r are the dopamine rates of adsorption (r_1), desorption (r_{-1}), electrooxidation (r_2), chemical (r_{p1}) and electrochemical (r_{p2}) polymerization, and the rate of polydopamine oxidation (r_3). These rates can be express as following:

$$r_1 = k_1 c(1 - \theta - \theta_p)\exp(\alpha\theta); \quad (2)$$

$$r_{-1} = k_{-1}\theta\exp(-\alpha\theta); \quad (3)$$

$$r_2 = k_2\theta\exp\left(\frac{2F\gamma\theta}{RT}\right); \quad (4)$$

$$r_{p1} = k_p\theta^n\exp\left(\frac{zF\gamma\theta}{RT}\right)f(\theta_p); \quad (5)$$

$$r_{p2} = k_p\theta^m f(\theta_p); \quad (6)$$

$$r_3 = k_3\theta_p\exp\left(\frac{jF\xi\theta_p}{RT}\right) \quad (7)$$

where the parameters k are the correspondent reaction rate constants, parameter α is a variable, which describes the interaction between the dopamine adsorbed molecules, F is the Faraday number, z and j are the numbers of transferred electrons during the polymer formation and oxidation correspondingly, γ and ξ are parameters that describes the influences of the electrochemical processes on the double electric layer (DEL) capacitances, R is the universal gas constant, T is the absolute temperature of the solution, f is the function that describes the autocatalytic reaction of the dopamine polymerization and relates to the polymerization's reaction order.

The electrochemical dopamine polimerization system is similar to "the polythiophene paradox" that combines nearly all variables. Its behavior, however, is slightly different, and will be discussed in the next section.

Results and discussion

In order to understand and investigate the behavior of the electrochemical system that includes dopamine's electrooxidation and polymerization we apply a linear stability theory to equation set (1). Its steady-state Jacobian matrix members can be described as :

$$\begin{pmatrix} a_{11} & a_{12} & a_{13} \\ a_{21} & a_{22} & a_{23} \\ a_{31} & a_{32} & a_{33} \end{pmatrix} \tag{8}$$

where variables can be described by Equations 9-17 (Figure 1).

$$a_{11} = \frac{2}{\delta}\left(-\Lambda/\delta - k_1(1-\theta-\theta_p)\exp(\alpha\theta)\right) \tag{9}$$

$$a_{12} = \frac{2}{\delta}\left(k_1 c\exp(\alpha\theta) - \alpha k_1 c(1-\theta-\theta_p)\exp(\alpha\theta) + k_{-1}\exp(-\alpha\theta) - \alpha k_{-1}\theta\exp(-\alpha\theta)\right) \tag{10}$$

$$a_{13} = \frac{2}{\delta}\left(k_1 c\exp(\alpha\theta)\right) \tag{11}$$

$$a_{21} = \frac{1}{G}\left(k_1(1-\theta-\theta_p)\exp(\alpha\theta)\right) \tag{12}$$

$$a_{22} = \frac{1}{G}\begin{pmatrix} -k_1 c\exp(\alpha\theta) + \alpha k_1 c(1-\theta-\theta_p)\exp(\alpha\theta) - k_{-1}\exp(-\alpha\theta) + \alpha k_{-1}\theta\exp(-\alpha\theta) - \\ -k_2\exp\left(\frac{2F\gamma\theta}{RT}\right) - \gamma k_2\theta\exp\left(\frac{2F\gamma\theta}{RT}\right) - nk_p\theta^{n-1}\exp\left(\frac{zF\gamma\theta}{RT}\right)f(\theta_p) - \gamma k_p\theta^n\exp\left(\frac{zF\gamma\theta}{RT}\right)f(\theta_p) \end{pmatrix} \tag{13}$$

$$a_{23} = \frac{1}{G}\left(-k_1 c\exp(\alpha\theta) - f'(\theta_p)(k_p\theta^n\exp\left(\frac{zF\gamma\theta}{RT}\right) + k_p\theta^m)\right) \tag{14}$$

$$a_{31} = 0 \tag{15}$$

$$a_{32} = \frac{1}{J}\left(nk_p\theta^{n-1}\exp\left(\frac{zF\gamma\theta}{RT}\right)f(\theta_p) + \gamma k_p\theta^n\exp\left(\frac{zF\gamma\theta}{RT}\right)f(\theta_p)\right) \tag{16}$$

$$a_{33} = \frac{1}{J}\left(f'(\theta_p)(k_p\theta^n\exp\left(\frac{zF\gamma\theta}{RT}\right) + k_p\theta^m) - k_3\exp\left(\frac{jF\xi\theta_p}{RT}\right) - \xi k_3\theta_p\exp\left(\frac{jF\xi\theta_p}{RT}\right)\right) \tag{17}$$

$$(-\xi-\Xi)(\Lambda\Sigma+\Omega\Sigma+\mathrm{P}\Sigma+\mathrm{PY}+\mathrm{PK}-\mathrm{K}\Lambda-\mathrm{K}\Omega-\mathrm{KP}) + \Xi(\mathrm{PY}-\Lambda\mathrm{K}+\Lambda\Sigma) < 0 \tag{30}$$

$$(-\xi-\Xi)(\Lambda\Sigma+\Omega\Sigma+\mathrm{P}\Sigma+\mathrm{PY}+\mathrm{PK}-\mathrm{K}\Lambda-\mathrm{K}\Omega-\mathrm{KP}) + \Xi(\mathrm{PY}-\Lambda\mathrm{K}+\Lambda\Sigma) = 0 \tag{31}$$

Figure 1. The series of Equations 9-17 and 30-31.

Observing the expressions (8), (12) and (15), it's possible to demonstrate the *oscillatory behavior* of the system. Moreover, it is even more likely occurance compare to similar systems [20-21]. It happens because the main matrix diagonal contains more positive elements compare to mathematical models for similar systems [20-21, 23-24].

The oscillatory behavior will be observed under following conditions:

• attraction between the adsorbed molecules that are represented by the positivity of the element $+\alpha k_1 c(1-\theta-\theta_p)\exp(\alpha\theta)$ and of $+\alpha k_{-1}\theta\exp(-\alpha\theta)$.

This influence factor is common to all similar systems and represents the surface instability that was described experimentally [20-21] and theoretically [23-24];

• strong influence of electrochemical processes on DEL capacitances. This cause is common to all similar systems and represent the electrochemical instability the oscillation amplitudes and electrolyte's composition [20]. In the case of dopamine three electrochemical processes are taking place that can cause changes to electrolyte's conductivity (increases or decreases). Therefore, the DEL capacitance will have its value altered, which will cause the electrochemical oscillations. Mathematically, they are described by the positivity of the elements

$$-\xi k_3\theta_p \exp\left(\frac{jF\xi\theta_p}{RT}\right), \quad (18)$$

$$-\gamma k_2\theta \exp\left(\frac{2F\gamma\theta}{RT}\right) \quad (19)$$

and

$$-\gamma k_p\theta^n \exp\left(\frac{zF\gamma\theta}{RT}\right) f(\theta_p) \quad (20)$$

which make part of the main diagonal elements a_{22} and a_{33}.

• the autocatalysis during polymer formation can occur because of rapid transference of an olygomer and a polymer compare to a monomer. This factor as a cause of the oscillatory behavior occures during the "polythiophene paradox". Mathematically it can be described by the positivity of the element

$$f'(\theta_p)(k_p\theta^n \exp\left(\frac{zF\gamma\theta}{RT}\right)+k_p\theta^m) \quad (21)$$

The oscillatory behavior has three possible causing factors compare to the two factors that are existing in the general [23]. Ther factors are being similar to the polythiophene paradox [24].

In order to evaluate the steady-state stability we apply the Routh-Hurwitz stability criterion to the differential equations' set (1). To avoid the appearance of the cumbersome expressions we introduce new variables:

$$\Delta/\delta = \kappa \quad (22)$$

$$k_1(1-\theta-\theta_p)\exp(\alpha\theta) = \Xi \quad (23)$$

$$k_1 c\exp(\alpha\theta) - \alpha k_1 c(1-\theta-\theta_p)\exp(\alpha\theta) + k_{-1}\exp(-\alpha\theta) - \alpha k_{-1}\theta\exp(-\alpha\theta) = \Lambda \quad (24)$$

$$k_1 c\exp(\alpha\theta) = \mathrm{Y} \quad (25)$$

$$k_2\exp\left(\frac{2F\gamma\theta}{RT}\right)+\gamma k_2\theta\exp\left(\frac{2F\gamma\theta}{RT}\right) = \Omega \quad (26)$$

$$nk_p\theta^{n-1}\exp\left(\frac{zF\gamma\theta}{RT}\right)f(\theta_p)+\gamma k_p\theta^n\exp\left(\frac{zF\gamma\theta}{RT}\right)f(\theta_p) = \mathrm{P} \quad (27)$$

$$k_3\exp\left(\frac{jF\xi\theta_p}{RT}\right)-\xi k_3\theta_p\exp\left(\frac{jF\xi\theta_p}{RT}\right) = \Sigma \quad (28)$$

so the Jacobian determinant can be described as following:

$$\frac{2}{\delta GJ}\begin{vmatrix} -\kappa-\Xi & \Lambda & \mathrm{Y} \\ \Xi & -\Lambda-\Omega-\mathrm{P} & -\mathrm{Y}-\mathrm{K} \\ 0 & \mathrm{P} & \mathrm{K}-\Sigma \end{vmatrix} \quad (29)$$

Opening the brackets and applying to the determinant the requirement Det $J < 0$ that is derived from the criterion we can obtain the steady-state stability condition that is described in Equation 30 (Figure 1).

The topological area of satisfaction of the inequation (30) is less than in the similar cases, including even the case of the polythiophene paradox [20-24]. Nevertheless, the steady-state stability is easy to maintain as it will be warranted to be stable if:

• the repulsion between the adsorbed particles that is described by the positivity of the parameter Λ when the parameter α is negative. Together with the satisfaction of the conditions exposed below, the element $\Lambda\Sigma$ is maintained positive, and the left-side expression of the inequation is more negative;

• the influence of the electrochemical processes to the DEL capacitances that is described by the positivities of the parameters Ω, P and Σ. Each parameter corresponds to the certain electrochemical process – electrooxidation (Ω), electropolymerization (P) and the polymer electrooxidation (Σ). In the case of the positivity of the these parameters the expression $\Lambda\Sigma+\Omega\Sigma+\mathrm{P}\Sigma+\mathrm{P}\mathrm{Y}$ will have the a positive value, and it will "push" the left-side expression of the

inequation (30) to more negative values, resulting in its satisfaction;

• the absence or fragility of autocatalytic effect during electropolymerization. If the autocatalysis isn't realized, f(θ)=const and f´(θ)=0, which anihilates the elements containing the parameter K, the nulity or negativity of which "pushes" the left-side expression of the inequation (30) to more negative values, satisfying the steady-state stability condition.

Depending on dopamine concentration and on electrode's shape the electrochemical process can be diffusion-controlled or adsorption-controlled.

It will correspond to a linear dependence between an electrochemical parameter and a dopamine concentration from the electroanalytical point of view. It will correspond to a polymer formation from electrosynthetic point of view.

The monotonic instability is also probable if the destabilizing and stabilizing influences are equal and it relates to a detection limit from the electroanalytical point of view. It will be caused by an autocatalysis and its conditions can be described by Equation 31 (Figure 2).

Not only dopamine, but also other compounds that are having a hydroquinonic structural characteristics and active sites for electropolymerization can undergo the process that is described in this work. For example, acetaminophen (paracetamole) can be also polymerized [25]. Its electrochemical detection on poly- (aniline blue) electrodes was reported [26] and described theoretically [27]. The section 2 reported electropolymerization that was accompanied by electrochemical detection of paracetamol over polymeric surface. Our model can be used to described polyacetaminophen electrooxidation.

Conclusions

The analysis of dopamine electrooxidation that is accompanied by chemical and electrochemical polymerization allow us to conclude that:

• the stable steady-state, despite to the narrower parameter topological zone, can be easily maintain. The factors, which are warranting the steady-state stability, are repulsion between particles, fragility of DEL influences of electrochemical processes and the absence or fragility of autocatalysis

• depending on dopamine concentration, the electrode area and the presence of active sites, the process will be controlled by diffusion or by adsorption;

• the oscillatory behavior in this case is more probable than in the cases of electropolymerization. It caused by a surface, an electrochemical and an autocatalytical factors;

• the monotonic instability of this system can appear and can be caused by autocatalysis in electropolymerization.

Notes

The authors declare no conflict of interest.

Author contributions. The manuscript was written through contributions of all authors. All authors have given approval to the final version of the manuscript.

References

1. Fellous, J-M.; Suri, R. E. The Roles of Dopamine. In *The Handbook of Brain Theory and Neural Networks*, 2nd Ed.; Arbib, M. A., Ed.; MIT Press: Cambridge, MA, 2003; pp 361-365.
2. Benes, F. M. Carlsson and the discovery of dopamine. *Trends in Pharmacol. Sci*. **2001**, *22*, 46-47.
3. Dopamine, CID=681. In PubChem Database. National Center for Biotechnology Information [Internet]. Available from: https://pubchem.ncbi.nlm.nih.gov/compound/dopamine#section=Use-and-Manufacturing (accessed on April 03, 2020).
4. Dopamine, GtoPdb Ligand ID: 940. In IUPHAR Database (IUPHAR-DB) via the Guide to PHARMACOLOGY website [Internet]. Available from: http://www.guidetopharmacology.org/GRAC/LigandDisplayForward?tab=biology&ligandId=940 (accessed on April 03, 2020).
5. Kirshner, N.; Goodall, Mc. C. The formation of adrenaline from noradrenaline. *Biochim. Biophys. Acta* **1957**, *24*, 658-659.
6. Triarhou, L. C. Dopamine and Parkinson's Disease. In Madame Curie Bioscience Database [Internet]. (Austin, TX: Landes Bioscience;) 2000-2013. Available from: https://www.ncbi.nlm.nih.gov/books/NBK6271/ (accessed on April 03, 2020).
7. Seeman, P. Glutamate and dopamine components in schizophrenia. *J. Psychiatry Neurosci*. **2009**, *34*, 143-149.
8. Costa, M. de L.; Loria, A.; Marchetti, M.; Balaszczuk, A. M.; Arranz, C. T. Effects of dopamine and nitric oxide on arterial pressure and renal function in volume expansion. *Clin. Exp. Pharmacol. Physiol.* **2002**, *29*, 772-776.
9. Sasso, L.; Heiskanen, A.; Diazzi, F.; Dimaki, M.; Castillo, J.; Vergani, M.; Landini, E.; Raiteri, R.; Ferrari, G.; Carminati, M.; Sampietro, M.; Svendsen, W. E.; Emnéus, J. Doped Overoxidized Polypyrrole Microelectrodes as Sensors for the Detection of Dopamine Released from Cell Populations. *Analyst* **2013**, *138*, 3651-3659.
10. Scarpetta, A.; Mariño, K.; Bolaños et al. Determination of hydroquinone using a glassy carbon electrode modified with chitosan, multi-wall carbon nano-tubes and ionic liquid. Possible use as sensor. *Rev. Colomb. Cienc. Quim. Farm.* **2015**, *44*, 311-321. (In Spanish).
11. Ankireddy, R.; Kim, J. Selective detection of dopamine in the presence of ascorbic aced via fluorescence quenching of InP/ZnS quantum dots. *Int. J. Nanomed.* **2015**, 10, 113-119.
12. Fayemi, O. F., Adekunle, A. S., Ebenso, E. E. Metal oxide nanoparticles/multi-walled carbon nanotube nanocomposite modified electrode for the detection of dopamine: comparative electrochemical study. *J. Biosens. Bioelectr.* **2015**, *6*, 190-204.
13. Peik-See, T.; Pandikumar, A.; Nay-Ming, H.; Hong-Ngee, L.; Sulaiman, Y. Simultaneous electrochemical detection of dopamine and ascorbic acid using an iron oxide/reduced grapheme oxide modified glassy carbon electrode. *Sensors* **2014**, *14*, 15227-15243.
14. Vishwanatha, C. C.; Swamy, B. E. K.; Pai, K. V. Electrochemical Studies of Dopamine, Ascorbic Acid and Uric Acid at Lignin Modified Carbon Paste Electrode by Cyclic Voltammetric. *J. Anal. Bioanal. Tech*. **2015**, *6*, 237-242.
15. Raoof, J. B.; Kiani, A.; Ojani, R.; Valliolahi, R. Electrochemical determination of dopamine using banana-MWCNTs modified carbon paste electrode. *Anal. Bioanal. Electrochem*. **2011**, *3*, 59-66.
16. Ojani, R.; Rahimi, V.; Raoof, J. A new voltammetric sensor for hydrazine based on michael addition reaction using 1-amino-2-naphtol-4-sulfonic acid. *J. Chin. Chem. Soc*. **2015**, *62*, 90-96.
17. Khajvand, T.; Ojani, R.; Raoof, J. B. Tetrachloro-ortho-Benzoquinone as Catalyst for Electrocatalytic Oxidation of Sulfite in Acidic Media and its Analytical Application. *Anal. Bioanal. Electrochem*. **2014**, *6*, 501-514.
18. Wang, J. L.; Li, B. C.; Li, Z. J. *et. al.* Electropolymerization of dopamine for surface modification of complex-shaped cardiovascular stents. *Biomaterials* **2014**, *35*, 7679-7689.

19. Mahantesha, K. R.; Swamy, B. E. K.; Pai, K. V. Poly (alizarin) Modified glassy carbon electrode for the electrochemical investigation of omeprazole: A voltammetric study. *Anal. Bioanal. Electrochem.* **2014**, *6*, 234-244.
20. Das, I., Agrawal, N.R.; Ansari, S. A.; Gupta, S. K. Pattern formation and oscillatory polymerization of thiophene. *Ind. J. Chem.* **2008**, *47A*, 1798-1803.
21. Tkach, V.; Nechyporuk, V.; Yagodynets, P. Electropolymerization of heterocyclic compounds. Mathematical models. *Ciên. Tecn. Mat.* **2012**, *24*, 54-58 (In Portuguese).
22. Krische, B.; Zagorska, M. The polythiophene paradox. *Synth. Met.* **1989**, *28*, 263-268.
23. Tkach, V.; Nechyporuk, V.; Yagodynets, P. Description matematica de la sintesis electroquimica de polimeros conductors en la presencia de surfactants. *Avances en. Quimica*. **2013**, *8*, 9-15 (In Spanish).
24. Tkach, V.; Ojani, R., Nechyporuk, V.; Yagodynets, P. The mathematical description for the sensor of dopamine, based on carbon paste electrode, modified by nanotubes and banana tissues. *Rev. Colomb. Cien. Quim. Farm.* **2015**, *44*, 58-71 (In Portuguese).
25. Li, Y.; Chen, Sh. M. The Electrochemical Properties of Acetaminophen on Bare Glassy Carbon Electrode. *Int. J. Electrochem. Sci.* **2012**, *7*, 2175-2187.
26. Vishwanath, C. C.; Swamy, B. E. K. Electrochemical studies of paracetamol at Poly (Aniline Blue) modified carbon paste electrode: A voltammetric study. *Anal. Bioanal. Electrochem.* **2014**, *6*, 573-582.
27. Tkach, B. Kumara-Swamy, R. Ojani et al. Paracetamol behavior during the electrocatalytic oxidation of poly (aniline blue) and its mathematical description. *Rev. Colomb. Cienc. Quim. Farm.* **2015**, *44*, 148-161 (In Portuguese).

Математичний опис електроокиснення допаміну, що супроводжується його хімічною та електрохімічною полімеризацією

В. В. Ткач[1,2]*, М. В. Кушнір[1], Я. Г. Іванушко[3], С. М. Луканова[1], С. С. де Олівейра[2], П. І. Ягодинець[1]

[1] *Чернівецький національний університет імені Юрія Федьковича, вул. Коцюбинського, 2, Чернівці, 58012, Україна*

[2] *Федеральний університет штату Мату-Гросу-ду-Сул, просп. Сенадора Філінто Мюллера, 1555, Кампу-Гранді, Мату-Гросу-ду-Сул, 79074-460, Бразилія*

[3] *Буковинський державний медичний університет, пл. Театральна, 2, Чернівці, 58002, Україна*

Резюме: Цікавий випадок електроокиснення допаміну, що супроводжується його хімічною та електрохімічною полімеризацією, в умовах якої як мономер, так і полімер можуть електрохімічно окиснюватися, досліджено з теоретичної точки зору. Допамін – один із найважливіших нейротрансмітерів в людських організмах, а також в організмах інших ссавців. Він є прекурсором епінефрину – однієї із найважливіших молекул нейтротрансмітерів з важливими впливами на функції серцево-судинної системи, гормонального апарату, нирок тощо. Його нестача стає причиною ряду хвороб – таких, як хвороба Паркінсона. Відтак, допамін використовується як лікарський препарат при їх лікуванні. З іншого боку, надлишок допаміну призводить до стимулювання симпатичної нервової системи, метаболічних порушень і навіть шизофренії. Відтак, розробка методу його визначення точно і швидко – дійно актуальна задача. Сам по собі допамін є дуже популярним аналітом в електроаналітичних системах. Модифіковані електроди для його визначення були розроблені багатьма вченими. Допамін також широко використовується як мономер провідного полімеру – полідопаміну, який використовується як модифікатор електроду у конденсаторах та як протикорозійне покриття. Оскільки електрополімеризація допаміну іде паралельно з його традиційним окисненням за хінон-гідрохінонним механізмом, обидва процеси вносять свій вклад в електрохімічну поведінку допаміну під час його електрополімеризації. Відтак гібридність механізму теж стає відповідальною за появу електрохімічних нестійкостей при електроокисненні допаміну, що супроводжується його електрополімеризацією. Вони можуть призводити до ускладнення інтерпретації аналітичного сигналу, а також до поломки електрохімічного обладнання. Щоби з'ясувати імовірність появи цих нестійкостей, необхідно апріорно дослідити поведінку у даній системі з теоретичної точки зору, що і відбувається у цій роботі. Для цього поведінка в електроаналітичному процесі описується системою трьох балансових диференціальних рівнянь, аналіз якої показує, що: а). Стійкість стаціонарного стану, незважаючи на звуження топологічної області параметрів, яка їй відповідає, підтримується легко. Фактори, що забезпечують стійкість стаціонарного стану – відштовхуюча взаємодія адсорбованих молекул мономеру або полімеру, слабкість впливів електрохімічних процесів на подвійний електричний шар та відсутність або слабкість автокаталізу; б). В залежності від концентрації допаміну та активної площі електроду, електроаналітичний процес може бути дифузійно- або адсорбційно-контрольованим; в). Осциляторна поведінка в цьому випадку стає більш імовірною, ніж в загальних випадках електрополімеризації. Вона спричиняється поверхневими, електрохімічними та автокаталітичними факторами; - монотонна нестійкість в цій системі можлива. Вона спричиняється головно факторами автокаталітичного росту ланцюга.

Ключові слова: допамін; полідопамін; електроокиснення; електрополімерізація; математична модель.

ISSN 1814-9758. Ukr. Bioorg. Acta, 2020, Vol. 15, N 1
UDC 544.6 + 541.138.3: 539.2: 539.216
DOI: hpps://doi.org/10.15407/bioorganica2020.01.053

Ukrainica Bioorganica Acta
www.bioorganica.org.ua

RESEARCH ARTICLE

Theoretical evaluation of electroanalitical determination of diazoline (mebhydrolin) on a polymer electrode

Volodymyr V. Tkach[1,2]*, Marta V. Kushnir[1], Yana G. Ivanushko[1,3], Sílvio C. de Oliveira[2], Olga V. Luganska[4], Petro I. Yagodynets[1], Zholt O. Kormosh[5]

[1] *Yuriy Fedkovich Chernivtsi National University, 2 Kotsiubynsky St., Chernivtsi, 58012, Ukraine*
[2] *Universidade Federal de Mato Grosso do Sul, Ave. Sen. Felinto. Müller, 1555, C/P. 549, 79074-460, Campo Grande, MS, Brazil*
[3] *Bukovinian State Medical University, 9 Teatralna Sq., Chernivtsi, 58000, Ukraine*
[4] *Zaporizhzhya National University, 66 Zhukovskogo St., Zaporizhzhya, 69600, Ukraine*
[5] *Lesya Ukrainka Eastern European National University, 13 Volya Ave., Lutsk, 43025, Ukraine*

Abstract: Mebhydrolin, the active substance of diazoline, is a histamine H1-blocker that possesses the anti-allergic, anti-pruritic, antioxidative properties as well as weak sedative effect. It is used to treat diseases and pathological conditions. Its long-term and excessive use leads to different side effects and complications such as granulocytopenia, neutropenia, dyscrasia, and granulocytosis. That is why the development of effective methods for determining the concentration of this drug is vital. There are no reports to date available on the electrochemical determination of diazoline (mebhydrolin). Based on the structural characteristics of the molecule it can be concluded that it is an electroactive compound. Its oxidation can effectively occur on the conductive polymer layer. Moreover, the electrochemical behavior of the drug promises to be very interesting, as it is developed by a complicated mechanism. In this work, the electrochemical determination of a mebhydrolin concentration on the leading polymer was studied from a theoretical point of view. The polymerization and the reactions sequences was describe by a mathematical model, which was derived and analyzed using linear stability theory and bifurcation analysis. From the model analysis we concluded that: a). The polymer electrode promotes an electrooxidation of mebhydrolin and the system is electroanalytically effective. The relationship between the electrochemical parameter (the current) and the concentration of nitrite is described and it is linear in nature. Therefore, the analytical signal can be easily interpreted. b). The electroanalytical process occurs in the diffusion mode at low concentrations of the analyte and in the adsorption mode at high concentration. c). The oscillatory behavior of this system is possible. It is caused by the effects of the electrochemical stage on DEL as well as also by surface instabilities.

Keywords: chemically modified electrodes, mebhydrolin, conductive polymers, electrochemical sensors, steady stationary state.

Introduction

Diazoline (mebhydrolin) is an anti-allergic drug [1-6], a blocker of histamine H1-receptors, that possesses anti-allergic, anti-pruritic, antioxidative, and weak sedative effect. It is used to treat diseases and pathological conditions such as hay fever, urticaria, eczema, itchy skin, allergic rhinitis, allergic conjunctivitis, skin reaction after insect bites, bronchial asthma (as part of combination therapy).

Nevertheless, diazoline is a toxic drug, long-term and excessive use of which leads to side effects [7-12] and even complications such as granulocytopenia, neutropenia, dyscrasia, and agranulocytosis. Diazoline is contraindicated in cases of angle-closure glaucoma and prostate hypertrophy. The level of ecotoxicity of the drug is high, which includes aquatic organisms. Both the positive and negative effects of the drug are dose-dependent. Therefore, the development of effective methods for determining the concentration of this drug is without a doubt an urgent task [13-16].

Received: 24.04.2020
Revised: 13.05.2020
Accepted: 28.05.2020
Published online: 30.06.2020

* Corresponding author. Tel.: +380-50-640-0359;
e-mail: nightwatcher2401@gmail.com (V. V. Tkach)
ORCID: 0000-0001-7696-0954

There are no reports to date on the electrochemical determination of mebhydrolin. Base on the structural characteristics of the molecule it can be concluded that it is an electroactive substance that can be effectively oxidized on the conductive polymeric layer. However, the development of new electroanalytical systems is always associated with solving certain problems such as:

• uncertainty about the mechanism of electrochemical action of the electrode modifier with analyte and its role in the electroanalytical system;

• possibility of electrochemical instabilities (oscillatory and monotonic) characteristic of electrosynthesis and electrooxidation of small organic molecules (including electropolymerization of heterocyclic compounds, which produces polymer coatings) [17-22].

These problems can be solved at the stage of sensor development if the experimental tests are preceded by *a priori* theoretical mechanistic study of the electroanalytical system. It will include the development and analysis of a mathematical model that would adequately describe the electroanalytical system. Thus, the main purpose of this paper is a theoretical description of the electrochemical system for the determination of mebhydrolin at the polymer electrode. In order to achieve the goal, you need to achieve intermediate objectives, namely:

• to present the sequence of chemical and electrochemical transformations that leads to the appearance of the analytical signal and, therefore, form the basis of the electroanalytical process;

• to develop a mathematical model that would adequately describe the behavior of this system. A mathematical model should consider reaction sequences and physical processes that accompany them;

• to analyze model, and find the conditions of a steady-state stability (and, accordingly, the most efficient operation of the sensor and the best interpreted analytical signal), as well as oscillatory and monotonic instability;

• to compare the behavior of this system with similar ones [23–25].

The system and its model

Electrochemical oxidation of diazoline occurs via a radical mechanism with the expulsion of equal amounts of electrons and protons - either by the intramolecular mechanism, with the formation of a condensed indole derivative, or intermolecularly, forming a dimer; further polymerization, although theoretically possible, is hampered by the steric factor (although the polymer substrate on the surface, in general, promotes polymerization) [19]. In this case, the transfer of electrons and protons occurs through the polymer layer (Figure 1), with the radical centers of which (if any) can also recombine.

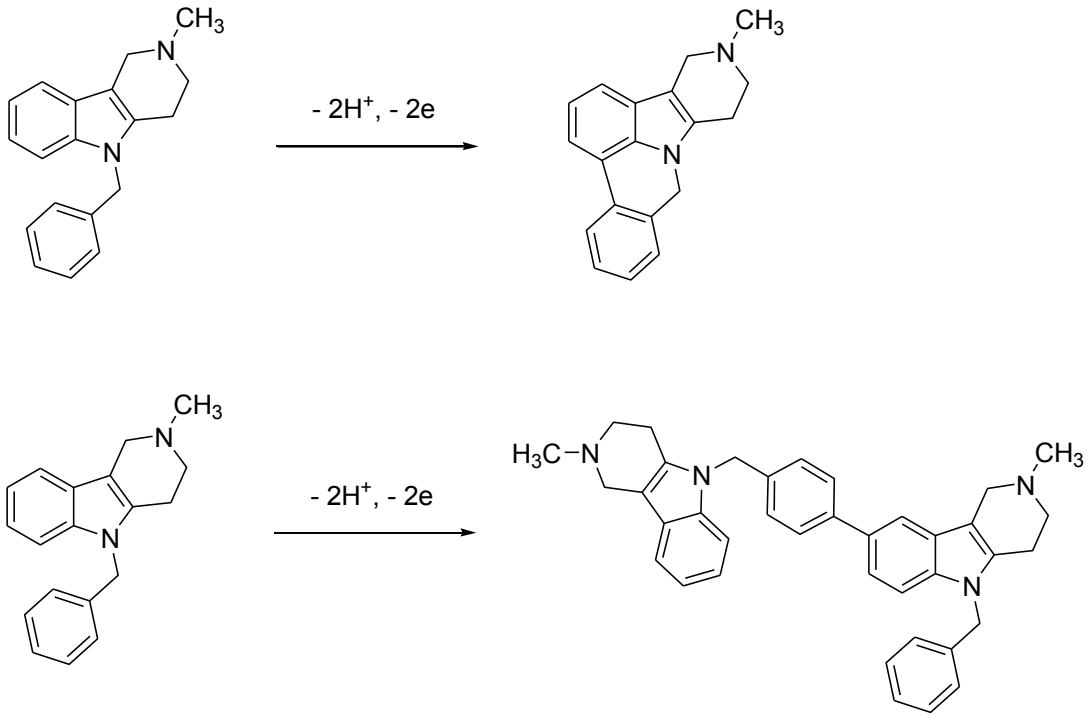

Figure 1. Possible ways of electrochemical oxidation of diazoline (mebhydrolin).

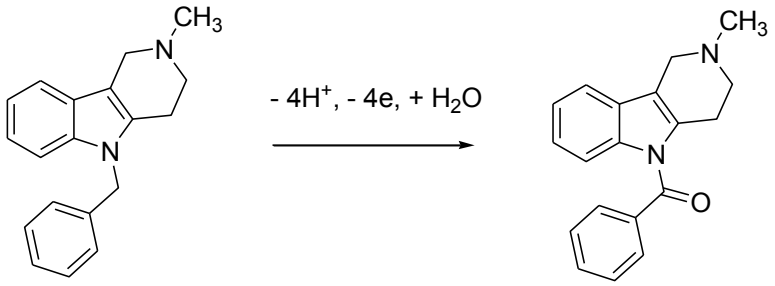

Figure 2. Oxidation of the methylene group to the carbonyl group in diazoline (mebhydrolin).

A slightly higher electrode potentials in aqueous solutions, alkaline environment, and the presence of electrode's modifiers might lead to the oxidation of the methylene group with the formation of the corresponding secondary alcohol and then ketone (Figure 2).

This paper presents electrochemical determination of diazoline at the polymer electrode and the method described in Figure 2 will not be considered (this will be the subject of one of our next works). We will limit ourselves to electrooxidation that is described in Figure 1.

In the simplest case an electroanalytical process in a neutral medium using a potentiostatic mode (amperometry) we consider three variables:

c – the concentration of diazoline in the near-surface layer;

θ – the degree of filling of the electrode's surface with diazoline;

p – the degree of filling of the electrode's surface with the polymer in a modified form.

To simplify the calculations, we assume that the reaction mixture is stirred vigorously (and we can neglect the convective flow) and the background electrolyte is in an excess (so that we can neglect the migration flow). We also assume that the concentration distribution of substances in the near-surface layer is linear, and the thickness of the layer itself is constant, equal to δ.

We can show that the behavior of this system is described by a system of differential equations (1):

$$\begin{cases} \frac{dc}{dt} = \frac{2}{\delta}\left(\frac{\Delta}{\delta}(c_0 - c) - r_{-1} - r_1\right) \\ \frac{d\theta}{dt} = \frac{1}{G}(r_1 - r_{-1} - r_{21} - r_{22} - r_{23}) \\ \frac{dp}{dt} = \frac{1}{P}(r_{21} + r_{22} + r_{23} - r_3) \end{cases} \quad (1)$$

wherein Δ is the diffusion coefficient, c_0 is its concentration in the thickness of the solution, G and P are the maximum surface concentrations of diazoline and modified polymer, respectively, and the parameters r are the rates of adsorption (r_1), desorption (r_{-1}) and chemical reactions, which can be calculated as:

$$r_1 = k_1 c(1-\theta)\exp(\alpha\theta) \quad (2)$$

$$r_{-1} = k_{-1}\theta\exp(-\alpha\theta) \quad (3)$$

$$r_{21} = k_{22}\theta(1-p)\exp(\beta\theta) \quad (4)$$

$$r_{22} = k_{22}\theta(1-p)\exp(\beta\theta) \quad (5)$$

$$r_{23} = k_{23}\theta(1-p)\exp(\beta\theta) \quad (6)$$

$$r_3 = k_3 p\exp\left(\frac{nF\varphi_0}{RT}\right) \quad (7)$$

wherein the parameters k are the specific rates of the corresponding processes, α is a variable describing the surface interaction of adsorbed diazoline particles, β is a variable describing the interaction of diazoline molecules with the surface layer, n is the number of electrons transferred at the electrochemical stage, F = N_A*e is the Faraday number, φ_0 - potential-jump relative to the potential of zero charges, R - universal gas constant, T - absolute temperature in the system.

Results and discussion

To study the behavior of electrochemical determination of diazoline at the polymer electrode, we analyze the system of differential equations (1) given the algebraic relations (2-7), by the methods of linear stability theory. Stationary elements of the Jacobi functional matrix would be written as:

$$\begin{pmatrix} a_{11} & a_{12} & a_{13} \\ a_{21} & a_{22} & a_{23} \\ a_{31} & a_{32} & a_{33} \end{pmatrix} \quad (8)$$

$$a_{11} = \frac{2}{\delta}\left(-\frac{\Delta}{\delta} - k_1(1-\theta)\exp(\alpha\theta)\right) \quad (9)$$

$$a_{12} = \frac{2}{\delta}\left(k_{-1}\exp(-\alpha\theta) - \alpha k_{-1}\theta\exp(-\alpha\theta) - k_1(1-\theta)\exp(\alpha\theta) + k_1 c\exp(\alpha\theta) - \alpha k_1(1-\theta)c\exp(\alpha\theta)\right) \quad (10)$$

$$a_{13} = 0 \quad (11)$$

$$a_{21} = \frac{1}{G}\left(k_1(1-\theta)\exp(\alpha\theta)\right) \quad (12)$$

$$a_{22} = \frac{1}{G}\begin{pmatrix} -k_{-1}\exp(-\alpha\theta) + \alpha k_{-1}\theta\exp(-\alpha\theta) - k_1(1-\theta)\exp(\alpha\theta) - k_1 c\exp(\alpha\theta) + \alpha k_1(1-\theta)c\exp(\alpha\theta) - \\ -k_{21}(1-p)\exp(\beta p) - k_{22}(1-p)\exp(\beta p) - k_{23}(1-p)\exp(\beta p) \end{pmatrix} \quad (13)$$

$$a_{23} = \frac{1}{G}\left(k_{21}\theta\exp(\beta p) - \beta k_{21}\theta(1-p)\exp(\beta p) + k_{22}\theta\exp(\beta p) - \beta k_{22}\theta(1-p)\exp(\beta p) + k_{23}\theta\exp(\beta p) - \beta k_{23}\theta(1-p)\exp(\beta p)\right) \quad (14)$$

$$a_{31} = 0 \quad (15)$$

$$a_{32} = \frac{1}{P}\left(k_{21}(1-p)\exp(\beta p) + k_{22}(1-p)\exp(\beta p) + k_{23}(1-p)\exp(\beta p)\right) \quad (16)$$

$$a_{33} = \frac{1}{P}\begin{pmatrix} -k_{21}\theta\exp(\beta p) + \beta k_{21}\theta(1-p)\exp(\beta p) - k_{22}\theta\exp(\beta p) + \beta k_{22}\theta(1-p)\exp(\beta p) \\ -k_{23}\theta\exp(\beta p) + \beta k_{23}\theta(1-p)\exp(\beta p) - k_3\exp\left(\frac{nF\varphi_0}{RT}\right) - \xi k_3 p\exp\left(\frac{nF\varphi_0}{RT}\right) \end{pmatrix} \quad (17)$$

Figure 3. The series of Equations 10-17.

wherein: (see Figure 3).

Considering the expressions (9), (13), and (17), we can see that in the main diagonal of the Jacobi matrix several elements can describe the positive feedback. Apart from the element $-\xi k_3 p\exp\left(\frac{nF\varphi_0}{RT}\right) > 0$, wherein if $\xi < 0$, which describes the effects on the DEL (double electric layer) capacity of the electrochemical oxidation of the modified polymer, the element can also be positive $\alpha k_{-1}\theta\exp(-\alpha\theta) > 0$ $\alpha k_1(1-\theta)c\exp(\alpha\theta) > 0$ i, if $\alpha > 0$, and also $\beta k_{21}\theta(1-p)\exp(\beta p)$, $\beta k_{22}\theta(1-p)\exp(\beta p)$, $\beta k_{23}\theta(1-p)\exp(\beta p)$, positive when $\beta > 0$, describing surface instabilities caused by the attraction of adsorbed diazoline molecules among themselves and with the polymer surface. This means that the Hopf bifurcation and the oscillatory behavior described by it are possible, and they are more probable than in similar systems [23-25]. As will be shown below, the oscillatory behavior will be observed outside of determination limit and will have little effect on the electroanalytical properties of the material.

To avoid the emergence of cumbersome expressions in the analysis of the determinant of Jacobian, we introduce new variables, so that the determinant would be written as:

$$\frac{2}{GP}\begin{vmatrix} -\kappa_1 - \Xi & \Lambda & 0 \\ \Xi & -\Lambda - \Omega & \mathrm{K} \\ 0 & \Omega & -\mathrm{K} - \Pi \end{vmatrix} \quad (18)$$

The criterion for the stability of the steady-state is the so-called Rauss-Hurwitz criterion. We can show that for trivariate systems it reduces to the inequality –Det J > 0, or, consequently, Det J < 0. By revealing the determinant of the matrix and applying to it the inequality that follows from the criterion, we can obtain the condition of stability of the steady-state, written as:

$$-\kappa_1(\Lambda\mathrm{K} + \Lambda\Pi + \Omega\Pi) - \Xi\Omega\Pi < 0 \quad (19)$$

This condition is guaranteed to be satisfied if the parameter j acquires positive values (which, in most cases, is observed). Thus, the steady-state is stable in a fairly wide

range of parameters, which from an electroanalytical point of view will mean that the system is electroanalytical efficient because in it the relationship between electrochemical parameter (in this case, current) and nitrite concentration is linear and the analytical signal is easily interpreted in a wide range of parameters. Also, the form of inequality (19) indicates that the electroanalytical process occurs in the diffusion mode at low concentrations of the analyte and the adsorption mode at large.

The limit of determination is determined by the implementation of monotonic instability, which corresponds to the implementation of the saddle-node bifurcation, the point of which separates stable steady states from unstable states. The condition for its occurrence for this system is as follows:

$$-\kappa_1(\Lambda K + \Lambda\Pi + \Omega\Pi) - \Xi\Omega\Pi = 0 \qquad (20)$$

In the case of a modification of the polymer surface with an inorganic material, the role of the active substance is assumed by this material. The polymer remains the mediator function of the electrochemical process, which changes the behavior of the system, expanding the range of electroanalytical efficiency of the process. This system will be considered by us in the following works.

Conclusions

Theoretical analysis of determining the concentration of diazoline at the polymer electrode demonstrates that:

• the polymer electrode promotes electrooxidation of diazoline, and the system is electroanalytical effective, because in it the relationship between the electrochemical parameter (in this case, the current) and the concentration of nitrite is linear, and the analytical signal is easily interpreted;

• the electroanalytical process occurs in the diffusion mode at low concentrations of the analyte and in the adsorption mode at large ones;

• oscillatory behavior in this system is possible and it is caused not only by the effects of the electrochemical stage on DEL but also by surface instabilities.

Notes

The authors declare no conflict of interest.

Author contributions. The manuscript was written through contributions of all authors. All authors have given approval to the final version of the manuscript.

References

1. Wu, B.; Wang, H. L.; Cee V. J., *et al*. Discovery of 5-(1H-indol-5-yl)-1,3,4-thiadiazol-2-amines as potent PIM inhibitors. *Bioorg. Med. Chem. Lett*. **2015**, *15*, 775-780.
2. Schoor, J. V. Antihistamines : a brief review : clinical. *Prof. Nurs. Today* **2012**, *16*, 16-21.
3. McKenna, K. E.; McMillan, J. C. Exacerbation of psoriasis, liver dysfunction and thrombocytopenia associated with mebhydrolin. *Clin. Exp. Dermatol*. **1993**, *18*, 131-132.
4. Waitzinger, J.; Lenders, H.; Pabst G., *et al*. Three explorative studies on the efficacy of the antihistamine mebhydroline (Omeril). *Int. J. Clin. Pharm. Ther*. **1995**, *33*, 373-383.
5. Croset, S. C. J. Drug repositioning and indication discovery using description logics. Ph.D. Thesis, Darwin College, University of Cambridge, 2004.
6. Möhrle, H.; Rohn, C.; Westle, G. Indole cleavage with mebhydroline by sodium periodate – Part 2. Mechanism of the dilactam formation. *Die Pharmazie, An Int. J. Pharm. Sci.* **2006**, *61*, 391-399 (in German).
7. Edoute, Y.; Nagler, A.; Brenner, B. Agranulocytosis Associated With Mebhydrolin Napadisylate (Incidal). *Harefuah* **1984**, *106*, 208-209 (in Hebrew).
8. Guzzetti, R.; Saggiorato, F. Studio dell'efficacia e tollerabilita della mebidrolina in confront a dimetindene maleate. *Clin. Ter*. **1986**, *116*, 109-114 (in Italian).
9. Hafeez, Z. H.; Antihistamines and Their Role in Dermatology. *J. Pak. Med. Assoc*. **1996**, *46*, 1-6.
10. Mebhydrolin napadisilate, CID=22529, In PubChem Database. National Center for Biotechnology Information. [Internet]. Available from: https://pubchem.ncbi.nlm.nih.gov/compound/Diazoline#section=Depositor-Provided-PubMed-Citations (accessed on April 24, 2020).
11. Mebhydrolin. EC nimber: 208-364-4, In ECHA Database. [Internet]. Available from: https://euon.echa.europa.eu/lt/web/guest/registration-dossier/-/registered-dossier/22142/11 (accessed on April 24, 2020).
12. Young, C. A. R.; Forrest, P.; Deveridge, S. F.; Gates, R. B.; Vincent, P.C. Abstract: Mebhydrolin induced agranulocytosis. *Aust. N. Z. J. Med*. **1982**, *12*, 173-176.
13. Nerdy, N. Development and validation of ultraviolet spectrophotometric method for determination of mebhydrolin napadisylate in tablet preparations. *Asian J. Pharm. Clin. Res*. **2017**, *10*, 367-372.
14. Wulandari, L. Determination and validation of mebhydroline napadisylate in tablets by HPLC. *Indo. J. Chem*. **2008**, *8*, 377-379.
15. Wulandari, L.; Evaluation of re-used HPTLC plate for qualitative abd quantitative analysis. *Indo. J. Chem*. **2006**, *6*, 338-340.
16. Suhadi, R.; Linawati, Y.; Wulandari, E. T.; Viriginia, D. M.; Setiawan, C. H. The metabolic disorders and cardiovascular risk among lower socioeconomic subjects in Yogyakarta-Indonesia. *Asian J. Pharm. Clin. Res*. **2017**, *10*, 367-372.
17. Pearlstein, A. J.; Johnson, J. A. Global and Conditional Stability of the Steady and Periodic Solutions of the Franck-FitzHugh Model of Electrodissolution of Fe in H_2SO_4. *J. Electrochem. Soc*. **1991**, *136*, 1290-1299.
18. Rahman, S. U.; Ba-Shammakh, M. S. Thermal effects on the process of electropolymerization of pyrrole on mild steel. *Synth. Met*. **2004**, *140*, 207-223.
19. de Andrade, V. M. *Confecção de biossensores através da imobilização de biocomponentes por eletropolimerização de pirrol*, M.S. Thesis, Universidade Federal de Mato Grosso do Sul, Porto Alegre, 2006 (In Portuguese).
20. Tosar Rovira, *J. P. Estudio de la inmovilización de oligonucleótidos a elétrodos modificados de oro:polipirrol, y detección electroquímica de secuencias complementarias,* M.S. Thesis, Universidad de la República, Montevideo, 2008 (In Spanish).
21. Das, I.; Goel, N.; Gupta, S. K.; Agrawal, N.R. Electropolymerization of pyrrole: Dendrimers, nano-sized patterns and oscillations in potential in presence of aromatic and aliphatic surfactants. *J. Electroanal. Chem*. **2012**, *670*, 1-10.
22. Singh, R. Prospects of Organic Conducting Polymer Modified Electrodes: Enzymosensors. *Int. J. Electrochem*. **2012**, N. 502707.
23. Tkach, V.; Swamy, B. K.; Ojani, R. *et. al*. El Mecanismo de la Oxidación de Omeprazol Sobre el Electrodo de Carbono Vitroso, Modificado por Polializarina, y Su Descripción Matemática. *Orbital Elec. J. Chem*. **2015**, *7*, 1-4 (In Spanish).
24. Tkach, V.; Swamy, B. K.; Ojani R. *et. al*. O comportamento de paracetamol durante a sua oxidação eletrocatalítica sobre poli(azul da anilina) e a sua descrição matemática. *Rev. Colomb. Cien. Quím. Farm*. **2015**, *44*, **148-161 (In Portuguese).**
25. Tkach, V.; Ojani, R.; Nechyporuk, V.; Yagodynets, P. The mathematical study of the electrochemical nitrite sensorbased on poly(p-aminoacetanilide). *Rev. Fac. Ing. UCV*. **2015**, *30*, 181-188 (In Portuguese).

Теоретична оцінка електроаналітичного визначення діазоліну (мебгідроліну) на полімерному електроді

В. В. Ткач[1,2]*, М. В. Кушнір[1], Я. Г. Іванушко[1,3], С. С. де Олівейра[2], О. В. Луганська[4], П. І. Ягодинець[1], Жолт О. Кормош[5]

[1] *Чернівецький національний університет імені Юрія Федьковича, вул. Коцюбинського, 2, Чернівці, 58012, Україна*

[2] *Федеральний університет штату Мату-Ґросу-ду-Сул, просп. Сенадора Філінто Мюллера, 1555, Кампу-Гранді, Мату-Ґросу-ду-Сул, 79074-460, Бразилія*

[3] *Буковинський державний медичний університет, пл. Театральна, 2, Чернівці, 58002, Україна*

[4] *Запорізький національний університет, вул. Жуковського, 66, Запоріжжя, 69600, Україна*

[5] *Східноєвропейський національний університет імені Лесі Українки, просп. Волі, 13, Луцьк, 43025,Україна*

Резюме: У даній роботі з теоретичної точки зору розглядається можливість електрохімічного визначення концентрації мебгідроліну (діюча речовина препарату діазоліну) на аноді, модифікованому провідним полімером . Мебгідролін є одним із широко застосованих антигістамінних препаратів. Його застосовують при таких патологічних станах як сінна лихоманка, кропив'янка, екзема, шкірний свербіж, алергічний риніт, алергічний кон'юнктивіт, шкірна реакція після укусу комахи, бронхіальна астма. Незважаючи на це, мебгідролін проявляє ряд побічних ефектів і протипоказаний до ряду категорій населення. В будь-якому разі, його дія є сильно залежною від дози. Тому його визначення є дійсно актуальним. Наразі не відомо жодної роботи, присвяченої електрохімічному визначенню мебгідроліну. Однак, з огляду на будову молекули, можна зробити висновок про те, що це електроактивна речовина, окиснення якої може ефективно відбутися на провідному полімерному шарі. Мало того, як похідне індолу, мебгідролін може бути підданим електрополімеризації, яка може супроводжуватися внутрішньомолекулярною циклізацією. Відтак, з огляду на «розгалуженість» механізму, а також можливість появи електрохімічних нестійкостей (осциляторна, монотонна), *a priori* теоретичне механістичне дослідження електроаналітичної системи, яке включатиме розробку та аналіз математичної моделі, що б адекватно описувала електроаналітичну систему є дійсно важливим. Для даного процесу було розроблено триваріантну математичну модель балансових диференціальних рівнянь, що включає обидва сценарії окиснення мебгідроліну з відщепленням протонів та електронів. Аналіз моделі показує, що: а). Полімерний електрод сприяє електроокисненню діазоліну, а система електроаналітично ефективна, оскільки в ній залежність між електрохімічним параметром (в даному випадку, струмом) і концентрацією нітриту є лінійною, а аналітичний сигнал легко інтерпретується. б). Електроаналітичний процес відбувається в дифузійному режимі за малих концентрацій аналіту і в адсорбційному за великих. в). Осциляторна поведінка в даній системі можлива і вона спричиняється не лишень впливами електрохімічної стадії на ПЕШ, а й поверхневими нестійкостями.

Ключові слова: хімічно модифікований електрод, мебгідролін, провідні полімери, електрохімічні сенсори, стійкий стаціонарний стан.

ТВОЯ УСПІШНА КАР'ЄРА В УКРАЇНІ

Науково-виробниче підприємство «Єнамін» (м. Київ) – найбільша українська організація, що займається дослідженням і синтезом сполук для потреб фарма- та агроіндустрії, а також надає послуги в сфері розробки новітніх лікарських засобів та ранніх доклінічних досліджень. За 29 років існування Єнамін став світовим лідером у своїй галузі, активно співпрацюючи з такими відомими фармацевтичними компаніями як Abbvie, Bayer, GlaxoSmithKline, Merck, Pfizer та інші. У компанії сформований злагоджений колектив науковців, до складу якого входять 140 докторів і кандидатів наук та понад 600 кваліфікованих спеціалістів – професіоналів у галузі органічної та медичної хімії, біохімії, клітинної біології, *in vitro* та *in vivo* фармакології. Щорічно науковий колектив Єнаміну публікує десятки статей у найпрестижніших фахових виданнях.

ДОЛУЧАЙСЯ ДО НАШОЇ КОМАНДИ!

Enamine

НАШІ ПЕРЕВАГИ:

- **Гідна заробітна платня**
- **Надання житла**
  Власні комфортабельні гуртожитки в м. Бровари (за 30 хвилин від місця роботи).
- **Кар'єрне зростання**
  Навіть, почавши простим лаборантом, маєте можливість вже за кілька років очолити лабораторію або відділ.
- **Навчання та наукова кар'єра**
  Завдяки гнучкому графіку легко поєднувати роботу в компанії з навчанням в університеті.

НАШІ РЕСУРСИ:

- **100 синтетичних лабораторій**
  оснащені найсучаснішим в Україні обладнанням
- **Найбільша у світі колекція реактивів**
  (понад 225 тисяч сполук)
- **4 власні ЯМР-спектрометри**
  (400 і 500 МГц)
- **40 препаративних та 20 аналітичних хроматографів**
- **Доступ до літературних баз даних**
  безпосередньо з робочих місць, що дозволяє оперативно отримувати посилання та статті з багатьох наукових періодичних видань
- **Власна складувна майстерня**
- **Власний Центр Фармакологічного Скринінгу**

КОНТАКТИ:

(044) 502-20-81
v.yanuta@mail.enamine.net
enamine.net